



Recent advances in the description of lepton-nucleus scattering

Noemi Rocco

QNP - The 10th International conference on Quark and Nuclear Physics

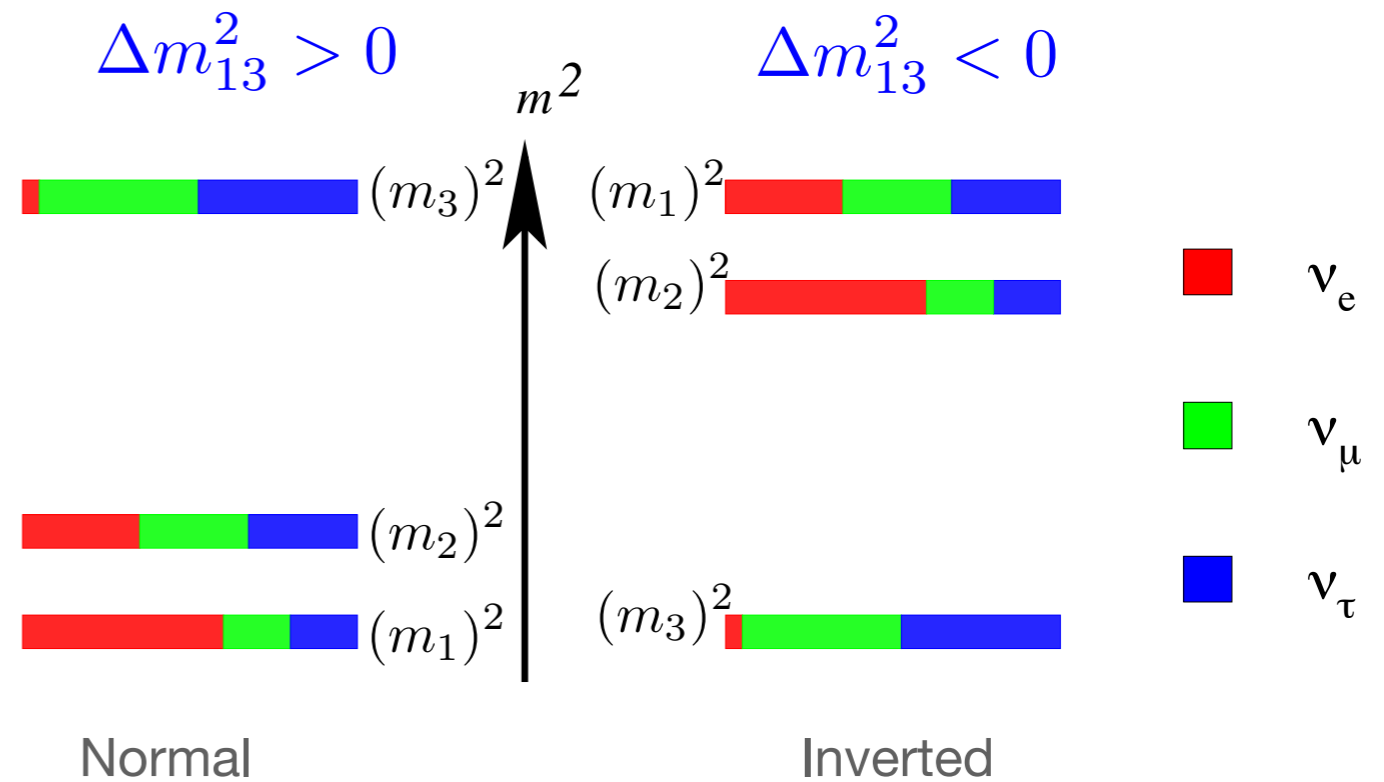
Universitat de Barcelona— July 8 - 12, 2024

Long baseline neutrino experiments

$$U_{\text{PMNS}} = \begin{pmatrix} 1 & 0 & 0 \\ 0 & c_{23} & s_{23} \\ 0 & -s_{23} & c_{23} \end{pmatrix} \begin{pmatrix} c_{13} & 0 & e^{-i\delta_{\text{CP}}} s_{13} \\ 0 & 1 & 0 \\ -e^{i\delta_{\text{CP}}} s_{13} & 0 & c_{13} \end{pmatrix} \begin{pmatrix} c_{12} & s_{12} & 0 \\ -s_{12} & c_{12} & 0 \\ 0 & 0 & 1 \end{pmatrix}$$

Many fundamental questions are still open:

- Correct mass ordering
- Are there CP violations in the lepton sector
 $P(\nu_\alpha \rightarrow \nu_\beta) \neq P(\bar{\nu}_\alpha \rightarrow \bar{\nu}_\beta)$
- Measure δ_{CP}
- What is the octant for θ_{23}

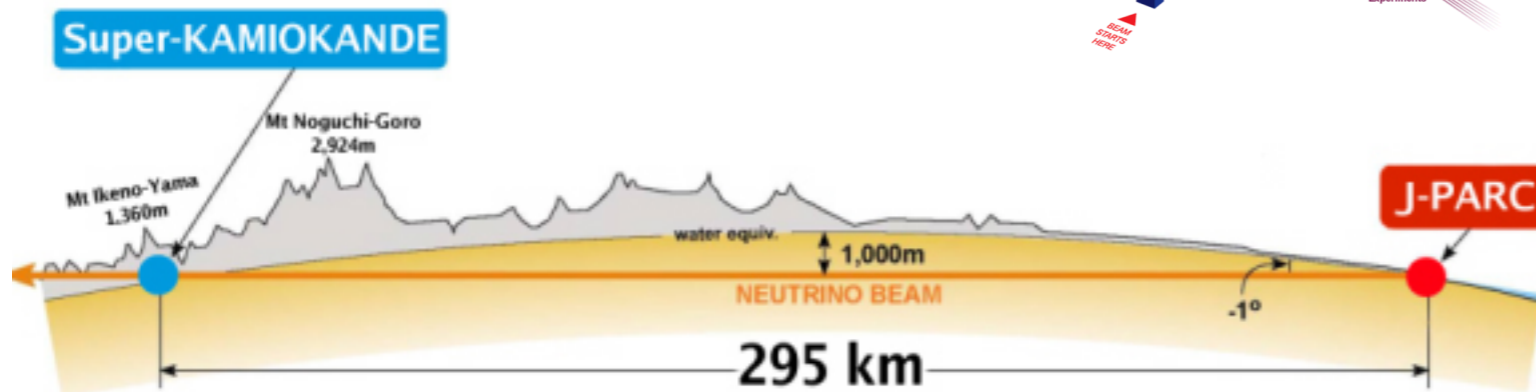


Long baseline neutrino experiments

These questions are addressed with **Long Baseline Neutrino Oscillation** experiments

T2K: Tokai to Kamioka

295 km



Currently measuring:

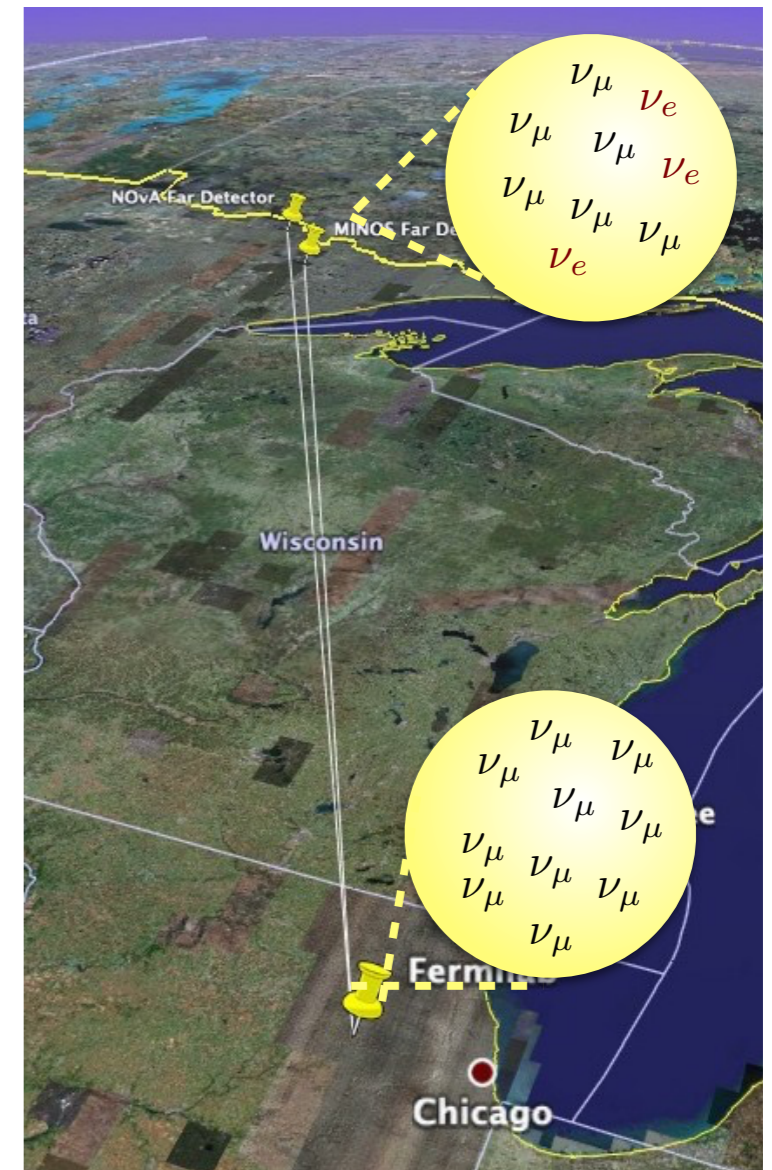
$$P(\nu_\mu \not\rightarrow \nu_\mu)$$

ν_μ disappearance

$$P(\nu_\mu \rightarrow \nu_e)$$

ν_e appearance

NOvA: Fermilab to Ash River
810 km



Why do we need more precision?

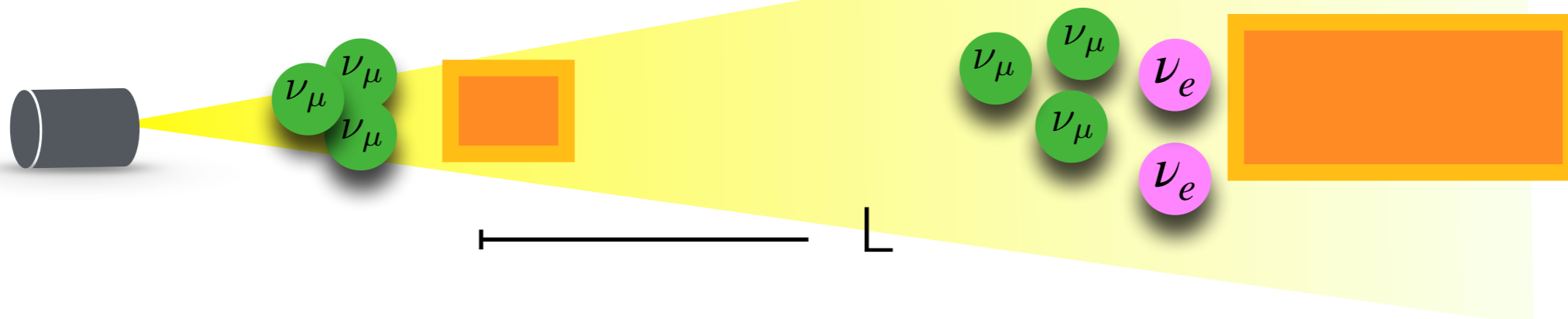
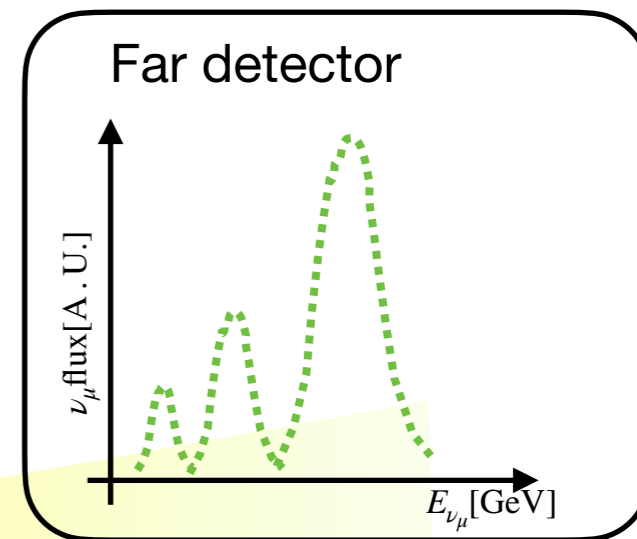
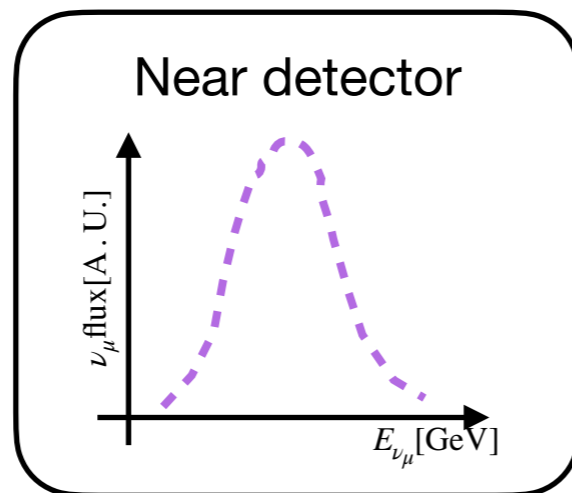


~ 2027



~ 2029

New generation of neutrino experiments will measure the unknown PMNS parameters with unprecedented accuracy



$$P(\nu_\mu \rightarrow \nu_e, E_\nu, L) = \frac{\Phi(E_\nu, L)}{\Phi_\mu(E_\nu, 0)} = \frac{N_e(E_\nu, L)/\sigma_e(E_\nu)}{N_\mu(E_\nu, L)/\sigma_\mu(E_\nu)}$$

Theory

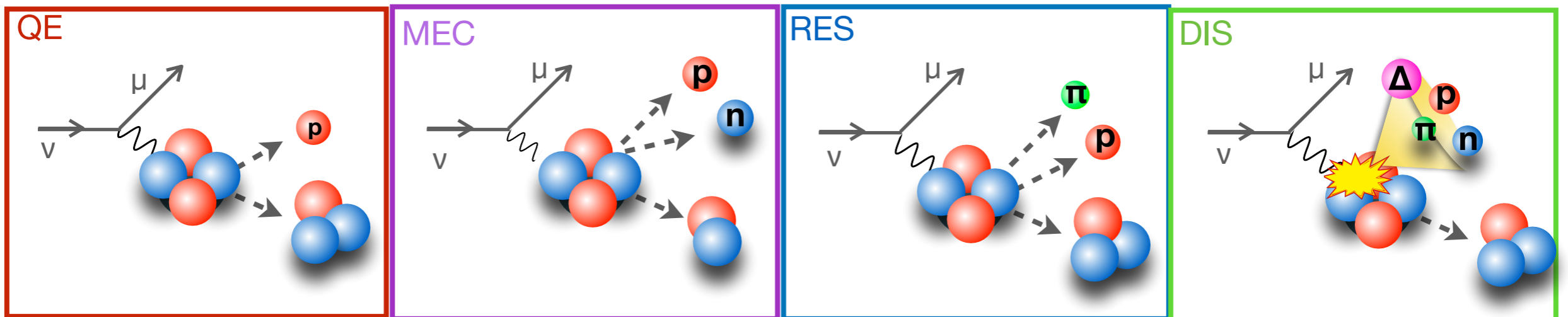
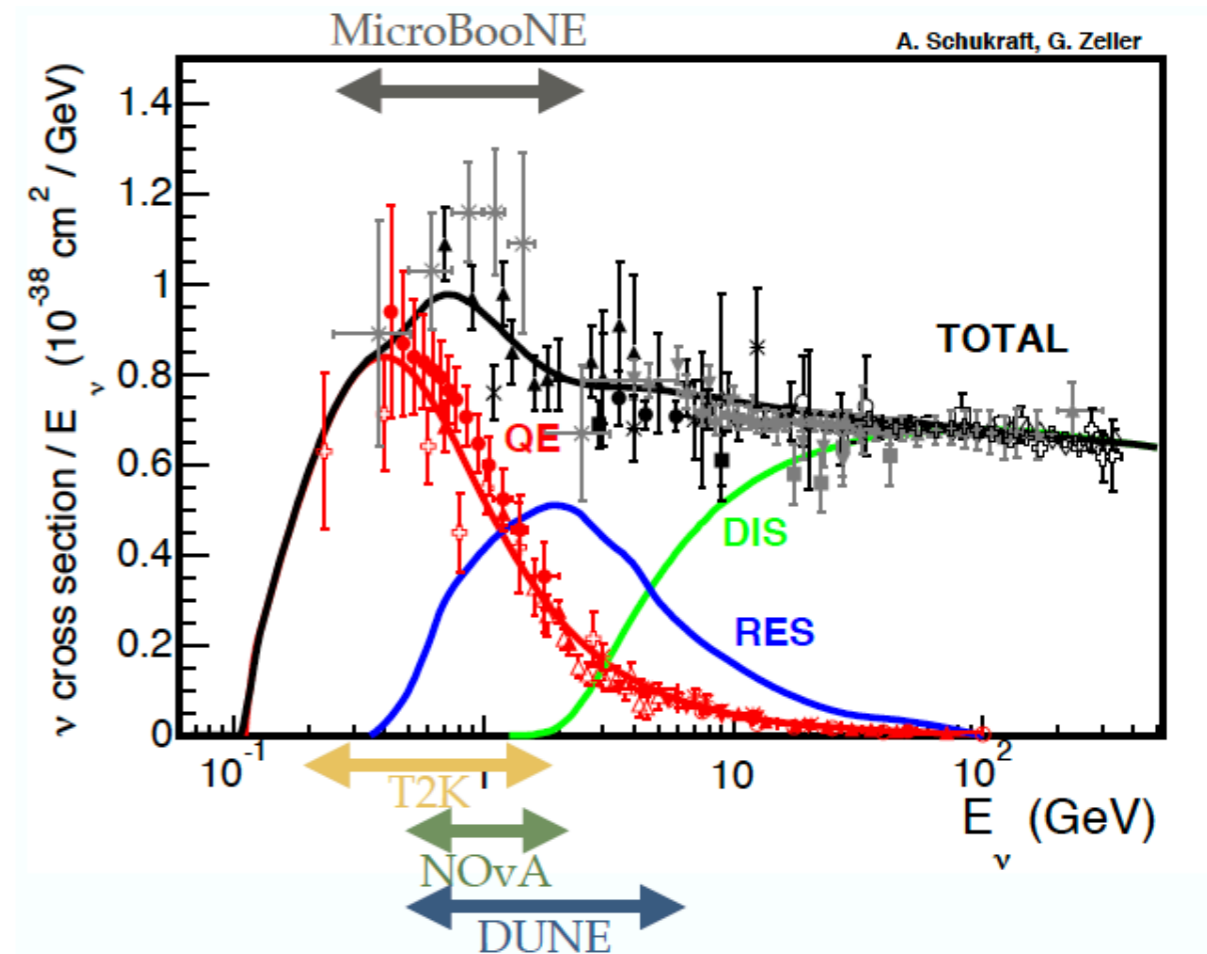
Experiment

Inputs for the nuclear model

More than 60% of the interactions at DUNE are non-quasielastic

Unprecedented accuracy in the determination of **neutrino-argon cross section** is required to achieve design sensitivity to CP violation at DUNE

Theoretical tools for neutrino scattering,
Contribution to: 2022 Snowmass Summer Study

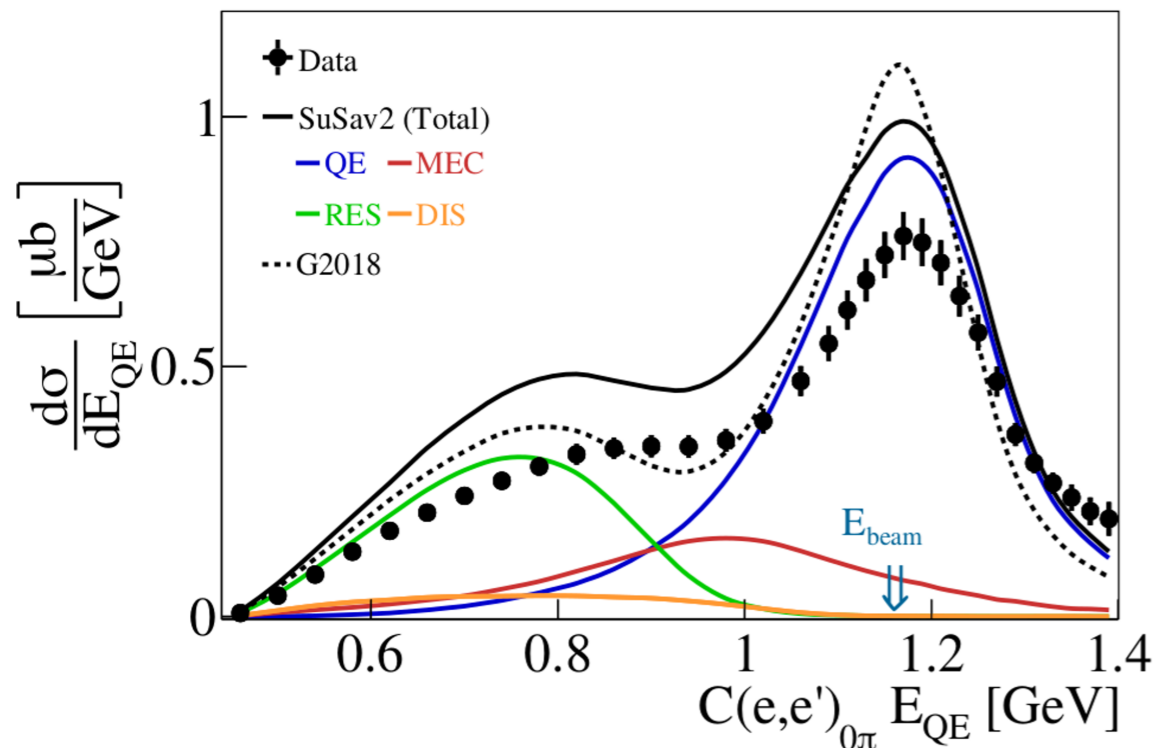


Why do we need more precision?

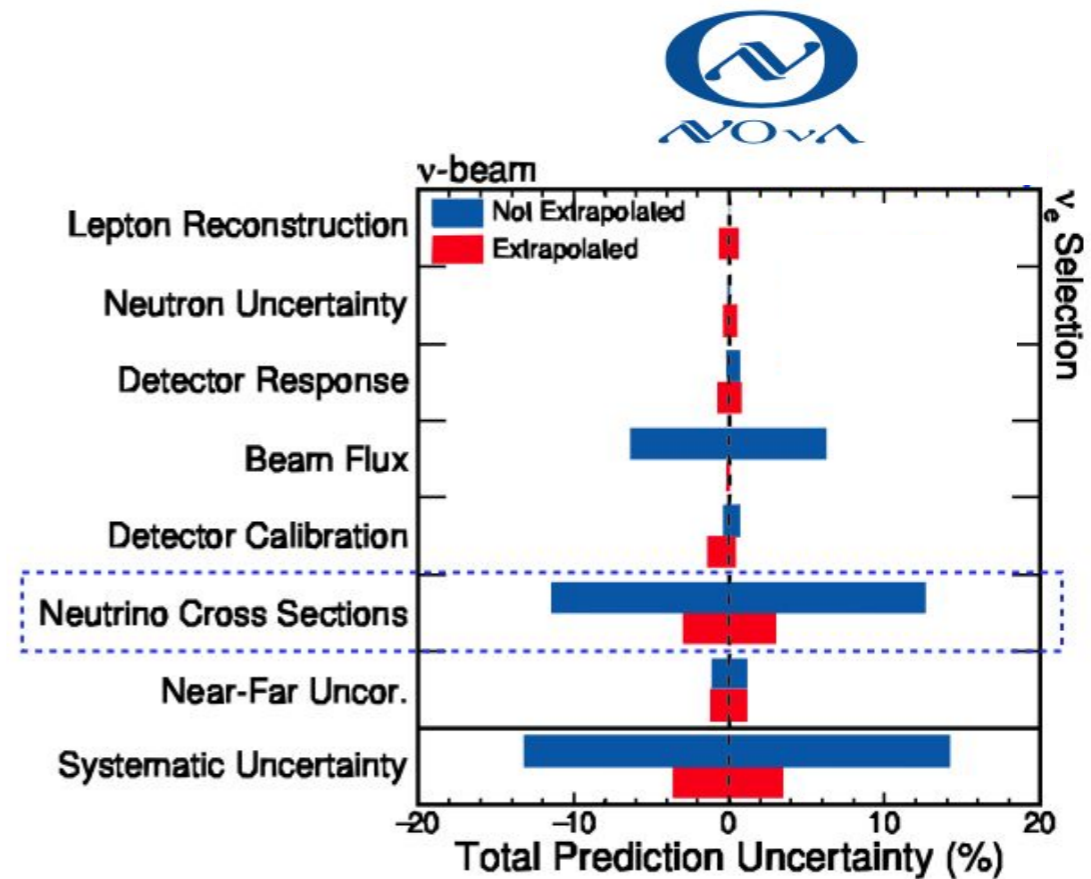
CLAS and e4v collaboration,
Nature 599 (2021) 7886, 565-570

Used semi-exclusive electron scattering data to test models and event generators used in oscillation analyses

The results indicate the **need for substantial improvement** in the **accuracy** of the neutrino interactions' models and simulations

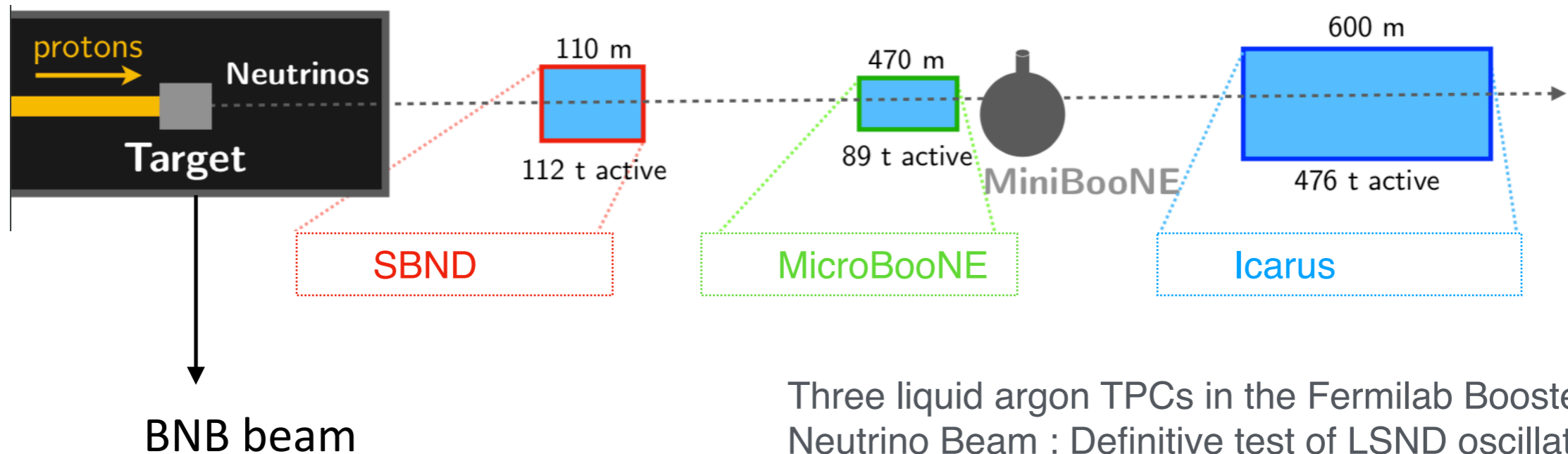


Current oscillation experiments report **large systematic uncertainties** associated with neutrino- nucleus interaction models.



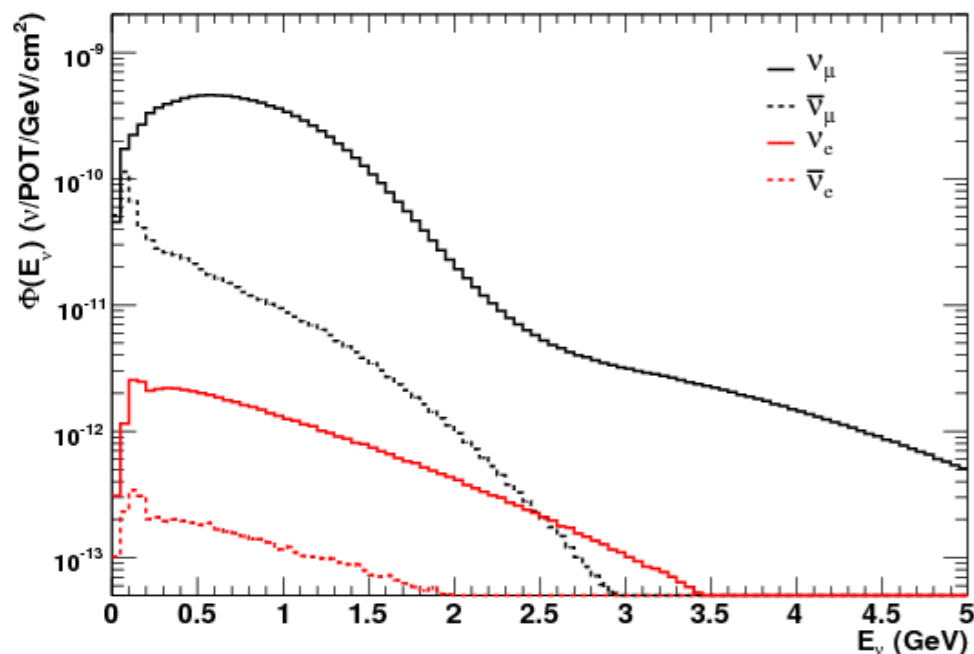
[Overview of neutrino cross section measurements, M. Buizza Avanzini, Neutrino 2024](#)

Short Baseline Neutrino program



Three liquid argon TPCs in the Fermilab Booster Neutrino Beam : Definitive test of LSND oscillations using three baselines

Neutrino flux @SBND



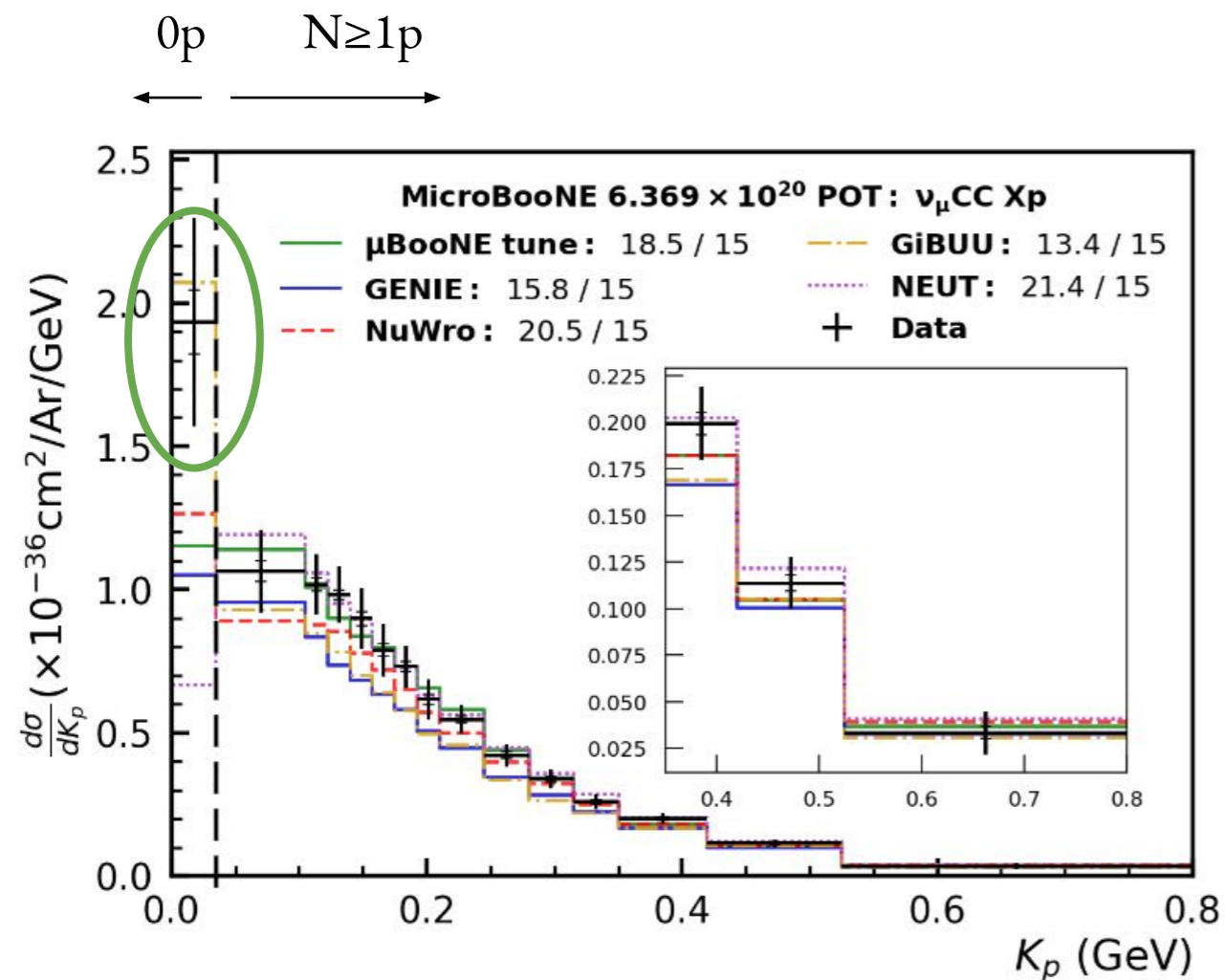
For BNB and T2K the dominant reaction mechanisms are quasi-elastic scattering

The contribution of π -production channels is $\sim 25\%$

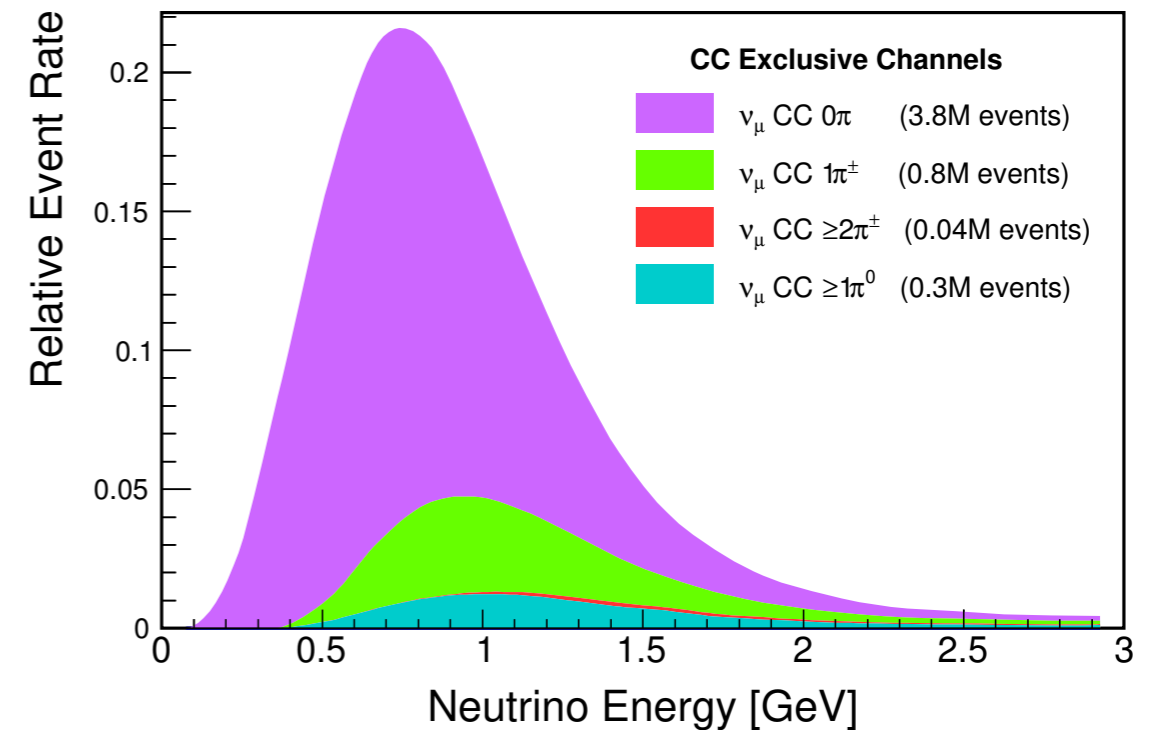
For the sub-GeV experiments the Delta is the only relevant resonance

Short Baseline Neutrino program

SBND will provide the world's highest statistics cross section measurements in LAr: 2 million events for ν_μ per year for the next 3 years



P. Machado et al, 1903.04608 (2019)



A. Papadopoulou Neutrino 2024

MicroBooNE provided the first simultaneous measurement of differential muon-neutrino CC cross sections on argon for final states with and without protons

D. Glibin, Neutrino 2024

ICARUS: new CC0 π analysis. Events with $1\mu + Np + 0\pi$

Theory of lepton-nucleus scattering

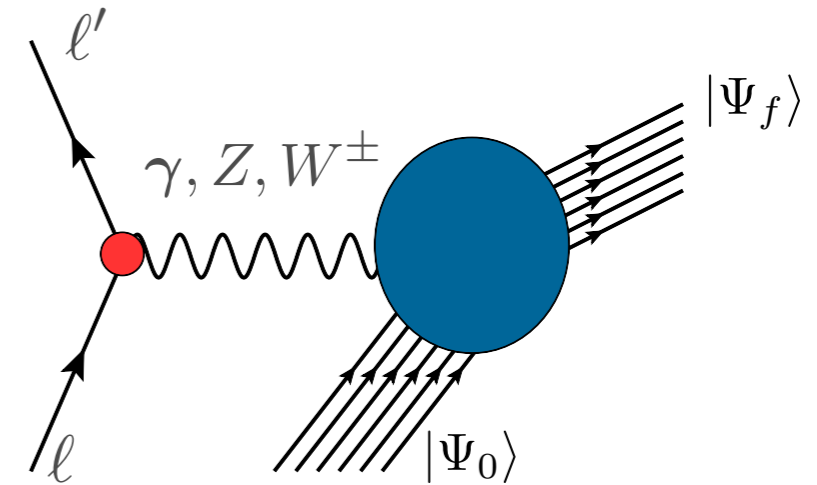
- The cross section of the process in which a lepton scatters off a nucleus is given by

$$d\sigma \propto L^{\alpha\beta} R_{\alpha\beta}$$

Leptonic Tensor: determined by lepton kinematics

Hadronic Tensor: nuclear response function

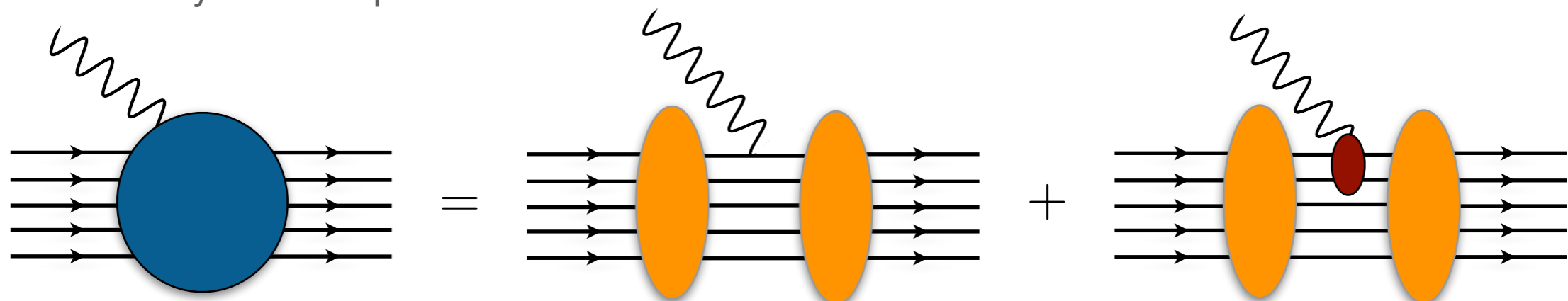
$$R_{\alpha\beta}(\omega, \mathbf{q}) = \sum_f \langle 0 | J_\alpha^\dagger(\mathbf{q}) | f \rangle \langle f | J_\beta(\mathbf{q}) | 0 \rangle \delta(\omega - E_f + E_0)$$



The initial and final wave functions describe many-body states:

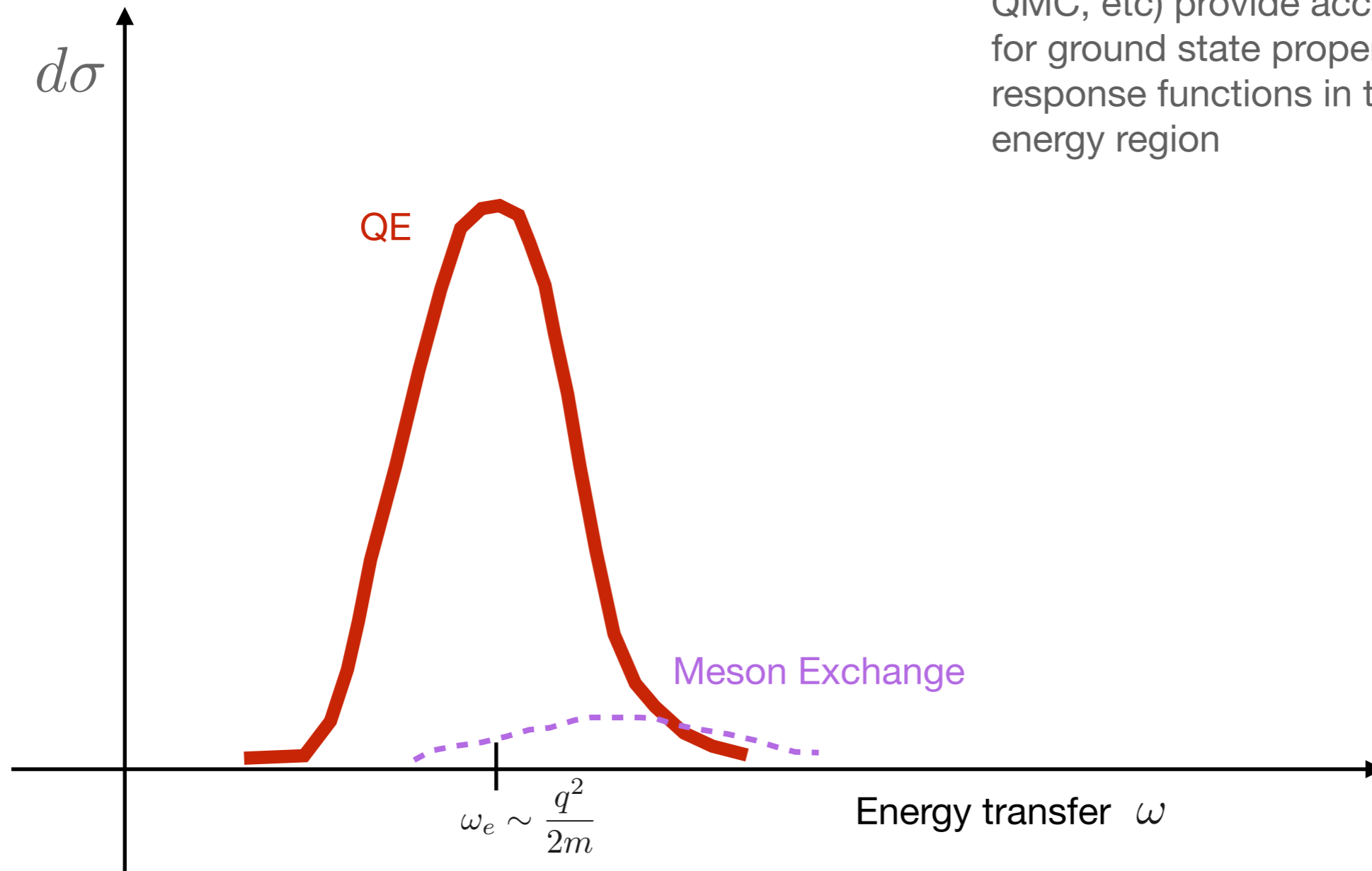
$$|0\rangle = |\Psi_0^A\rangle, |f\rangle = |\Psi_f^A\rangle, |\psi_p^N, \Psi_f^{A-1}\rangle, |\psi_k^\pi, \psi_p^N, \Psi_f^{A-1}\rangle \dots$$

One and two-body current operators



Ab initio Methods

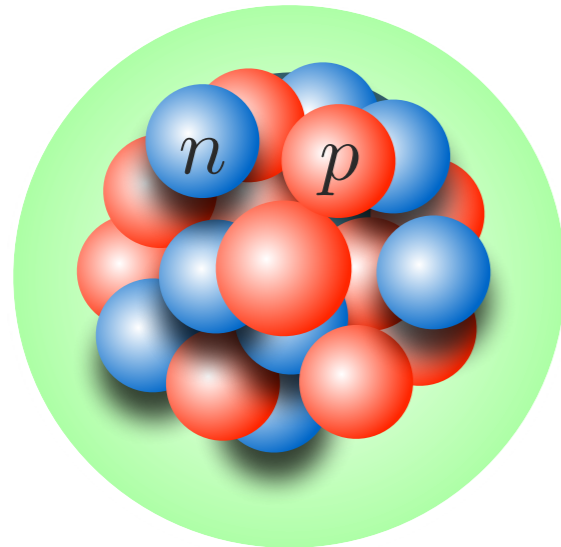
Ab-initio methods (CC, IMSRG, SCGF, QMC, etc) provide accurate predictions for ground state properties of nuclei + response functions in the low/moderate energy region



Hamiltonian and Currents

At low energy, the effective degrees of freedom are pions and nucleons:

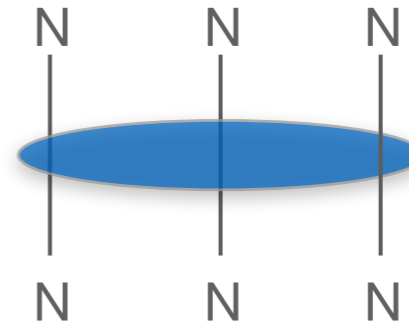
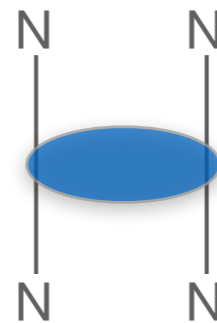
$$H = \sum_i \frac{\mathbf{p}_i^2}{2m} + \sum_{i < j} v_{ij} + \sum_{i < j < k} V_{ijk} + \dots$$



1-body

2-body

3-body



- AV18+IL7
- chiral interactions

The electromagnetic current is constrained by the Hamiltonian through the **continuity equation**

$$\nabla \cdot \mathbf{J}_{\text{EM}} + i[H, J_{\text{EM}}^0] = 0 \quad [v_{ij}, j_i^0] \neq 0$$

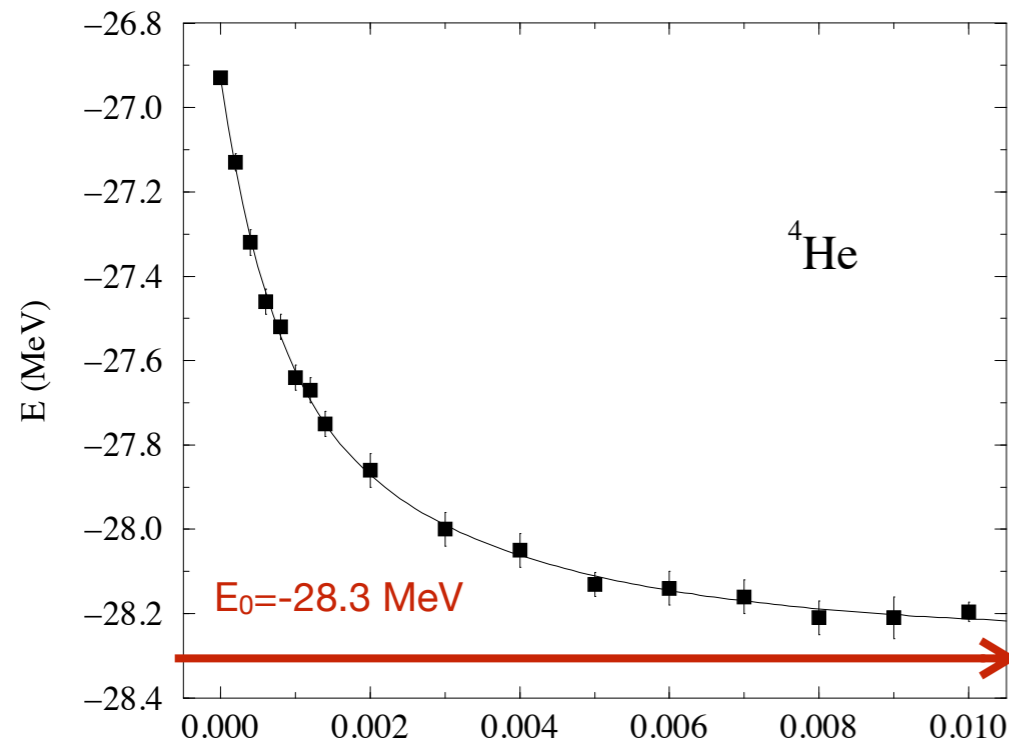
The above equation implies that the current operator includes one and two-body contributions

$$J^\mu(q) = \sum_i j_i^\mu + \sum_{i < j} j_{ij}^\mu + \dots$$

Many-Body method: GFMC

GFMC projects out the exact lowest-energy state:

$$e^{-(H-E_0)\tau} |\Psi_T\rangle \rightarrow |\Psi_0\rangle$$



The computational cost of the calculation is $2^A \times A! / (Z!(A-Z)!)$

$$|S\rangle = \begin{pmatrix} s \uparrow \uparrow \uparrow \\ s \uparrow \uparrow \downarrow \\ s \uparrow \downarrow \uparrow \\ s \uparrow \downarrow \downarrow \\ s \downarrow \uparrow \uparrow \\ s \downarrow \uparrow \downarrow \\ s \downarrow \downarrow \uparrow \\ s \downarrow \downarrow \downarrow \end{pmatrix}$$

Nuclear response function involves evaluating a number of transition amplitudes.

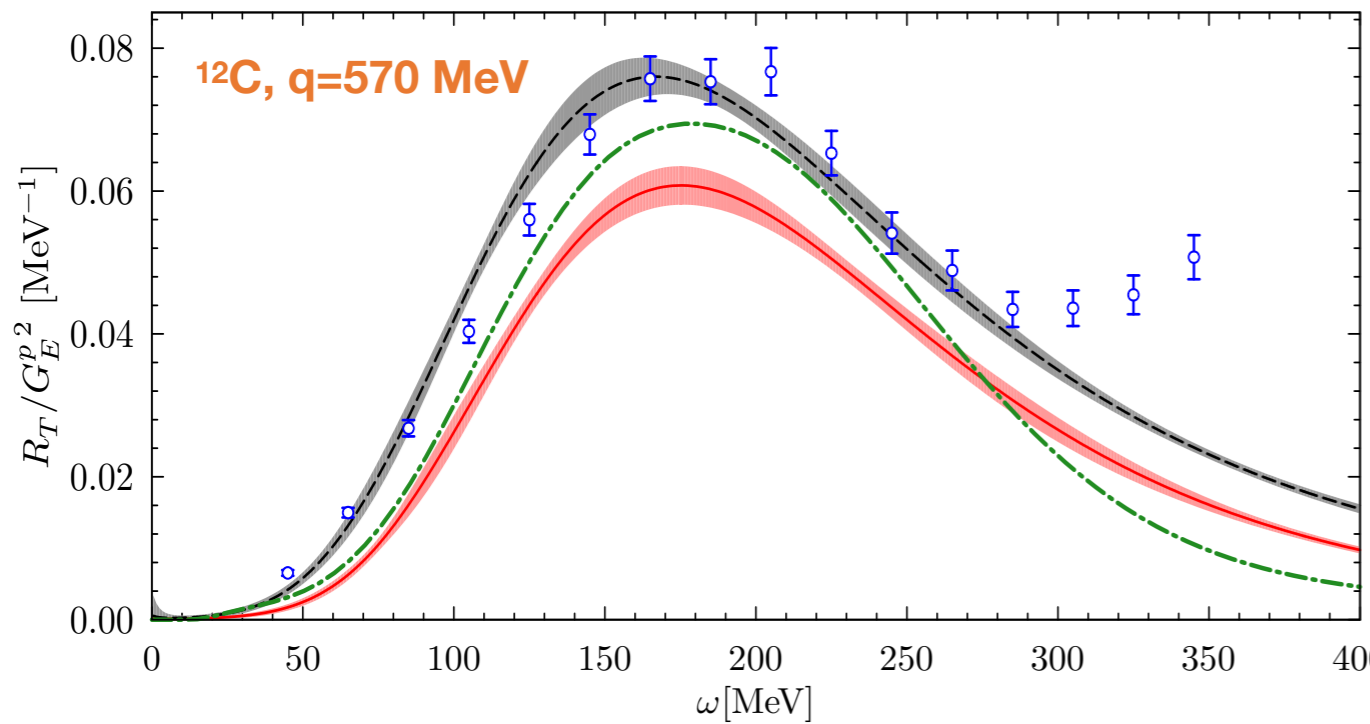
Valuable information can be obtained from the **integral transform of the response function**

$$E_{\alpha\beta}(\sigma, \mathbf{q}) = \int d\omega K(\sigma, \omega) R_{\alpha\beta}(\omega, \mathbf{q}) = \langle \psi_0 | J_{\alpha}^{\dagger}(\mathbf{q}) K(\sigma, H - E_0) J_{\beta}(\mathbf{q}) | \psi_0 \rangle$$

Inverting the Laplace transform is a complicated problem

A. Lovato et al, PRL117 (2016), 082501,
PRC97 (2018), 022502

Cross sections: Green's Function Monte Carlo



Legend for the top plot:

- GFMC O_{1b} (red dashed line)
- GFMC O_{1b+2b} (black solid line)
- PWIA (green dash-dotted line)
- World data (blue circles with error bars)

Alessandro Lovato et al. PRL 117 082501 (2016)

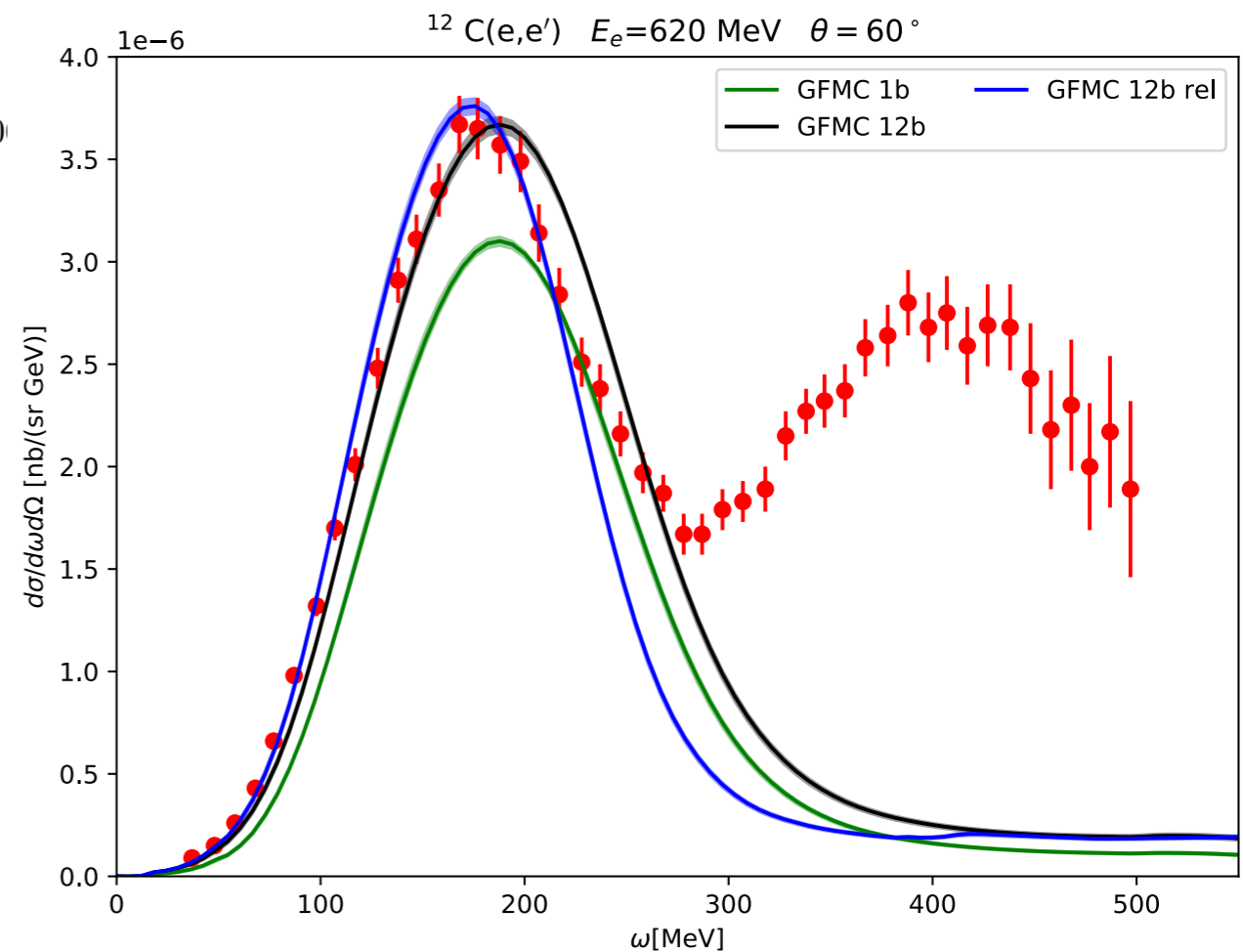
Limitations:

Medium mass nuclei $A < 13$

Inclusive results which are virtually correct in the QE

Relies on non-relativistic treatment of the kinematics

Can not handle explicit pion degrees of freedom



A.Lovato, NR, et al, submitted to Universe

Axial form factor determination

- The axial form-factor has been fit to the dipole form

$$F_A(q^2) = \frac{g_A}{(1 - q^2/m_A^2)^2}$$

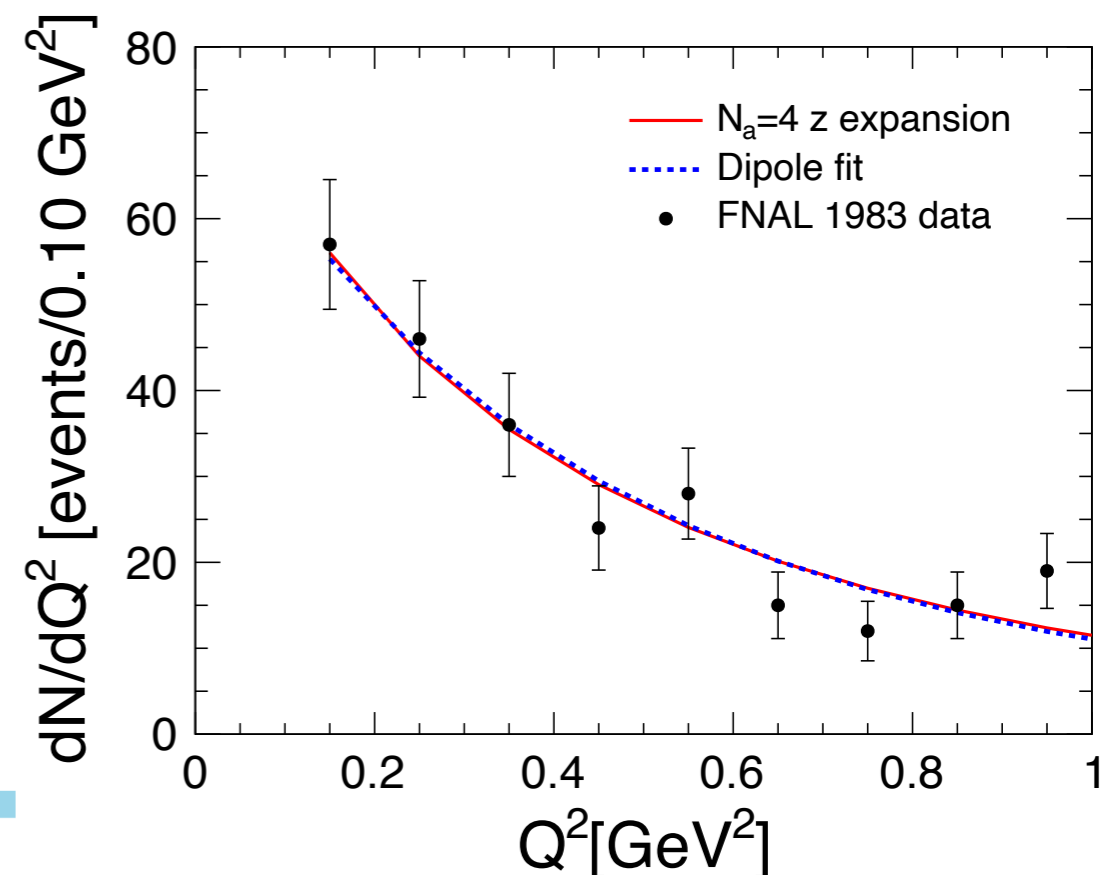
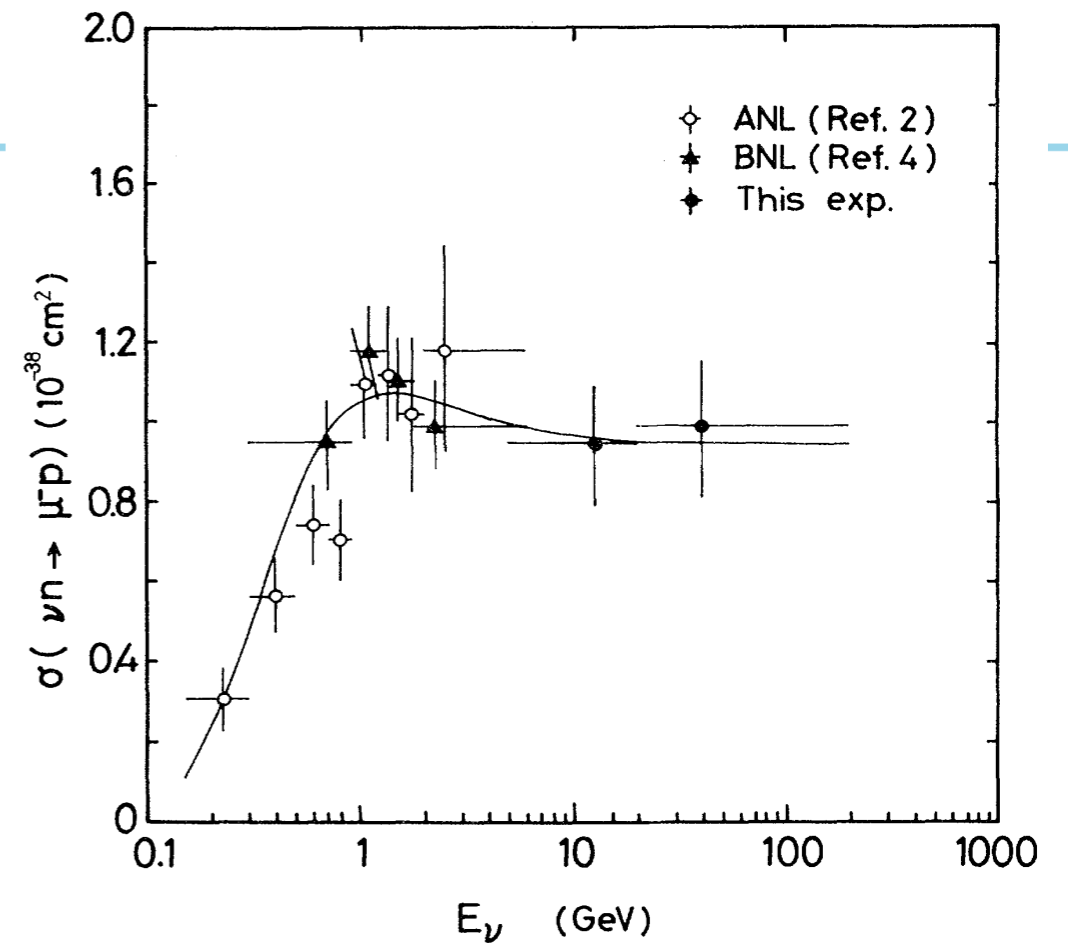
- The intercept $g_A = -1.2723$ is known from neutron β decay
- Different values of m_A from experiments
 - $m_A = 1.02$ GeV q.e. scattering from deuterium
 - $m_A = 1.35$ GeV @ MiniBooNE
- Alternative derivation based on **z-expansion**
 - model independent parametrization

$$F_A(q^2) = \sum_{k=0}^{k_{\max}} a_k z(q^2)^k,$$

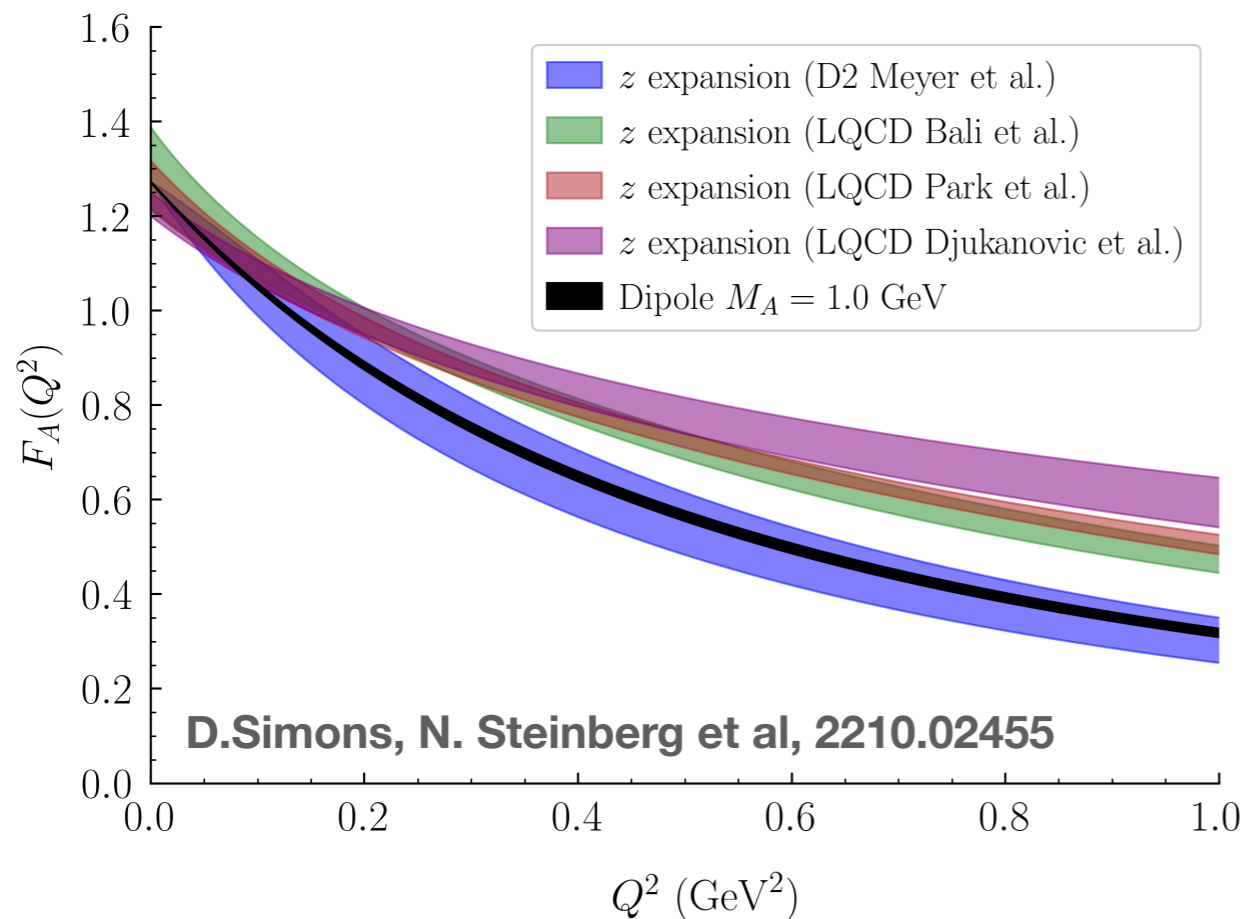
↑ known functions
↑ free parameters

Bhattacharya, Hill, and Paz PRD 84 (2011) 073006

A.S.Meyer et al, Phys.Rev.D 93 (2016) 11, 113015



Axial form factor determination



Comparison with recent MINERvA antineutrino-hydrogen charged-current measurements

Novel methods are needed to remove excited-state contributions and discretization errors

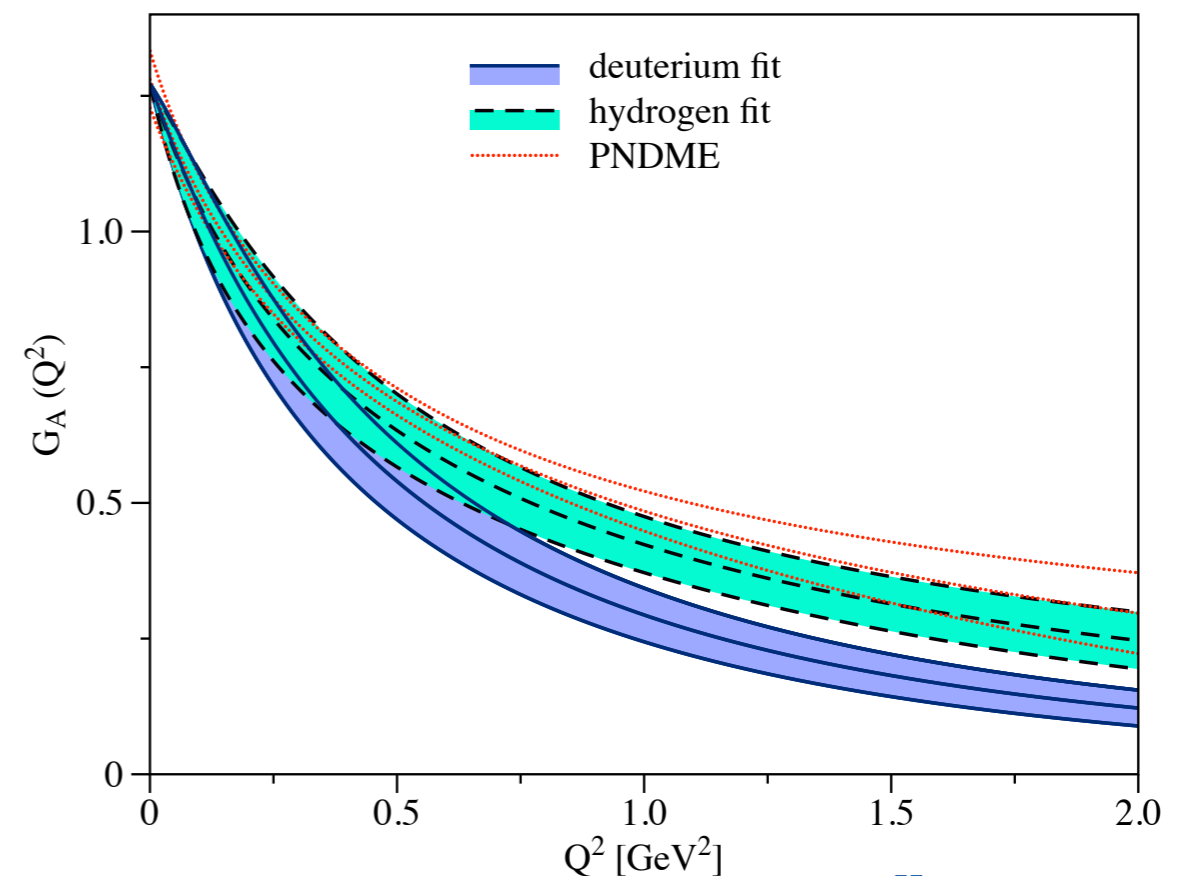
A. Meyer, A. Walker-Loud, C. Wilkinson, 2201.01839

D2 Meyer et al: fits to neutrino-deuteron scattering data

LQCD result: general agreement between the different calculations

LQCD results are 2-3 σ larger than D2 Meyer ones for $Q^2 > 0.3$ GeV²

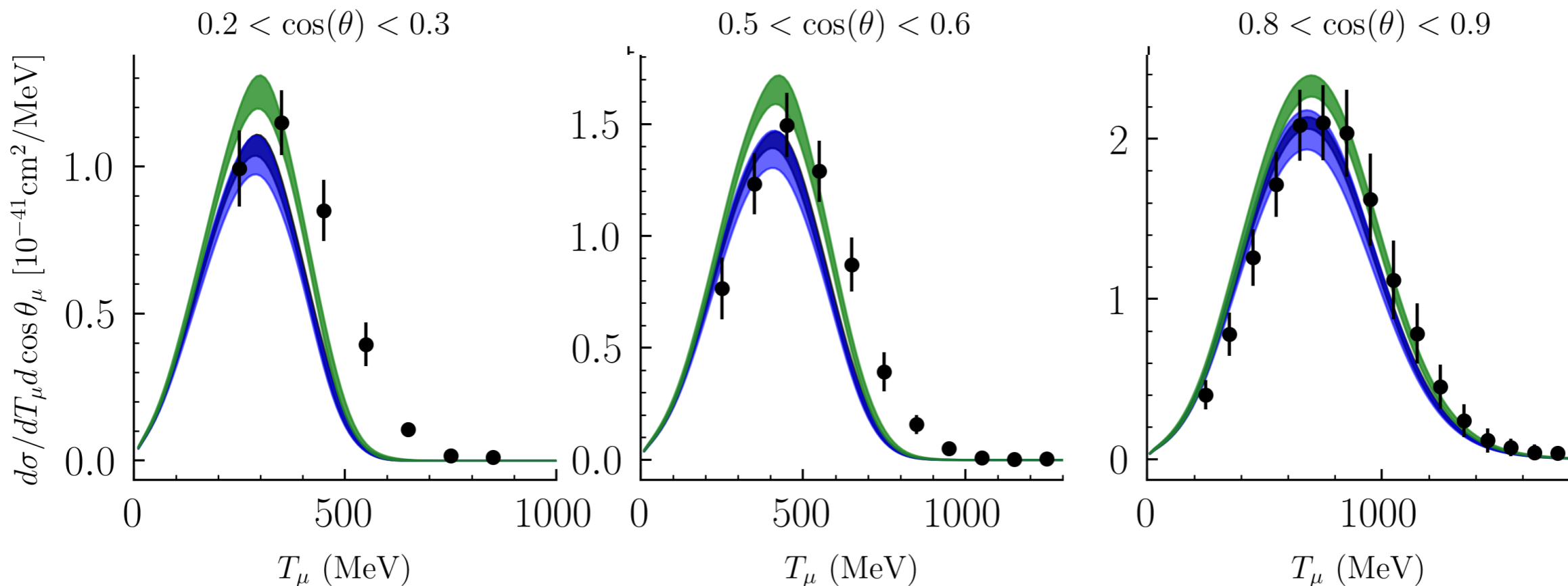
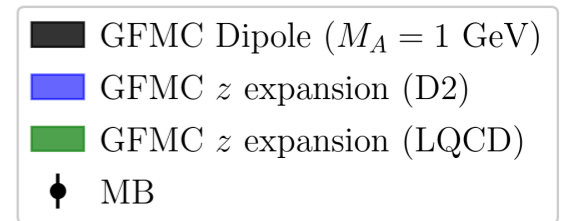
O. Tomalak, R. Gupta, T. Battacharaya, 2307.14920



Study of model dependence in neutrino predictions

MiniBooNE results; study of the dependence on the axial form factor:

D.Simons, N. Steinberg, NR, et al arXiv:2210.02455



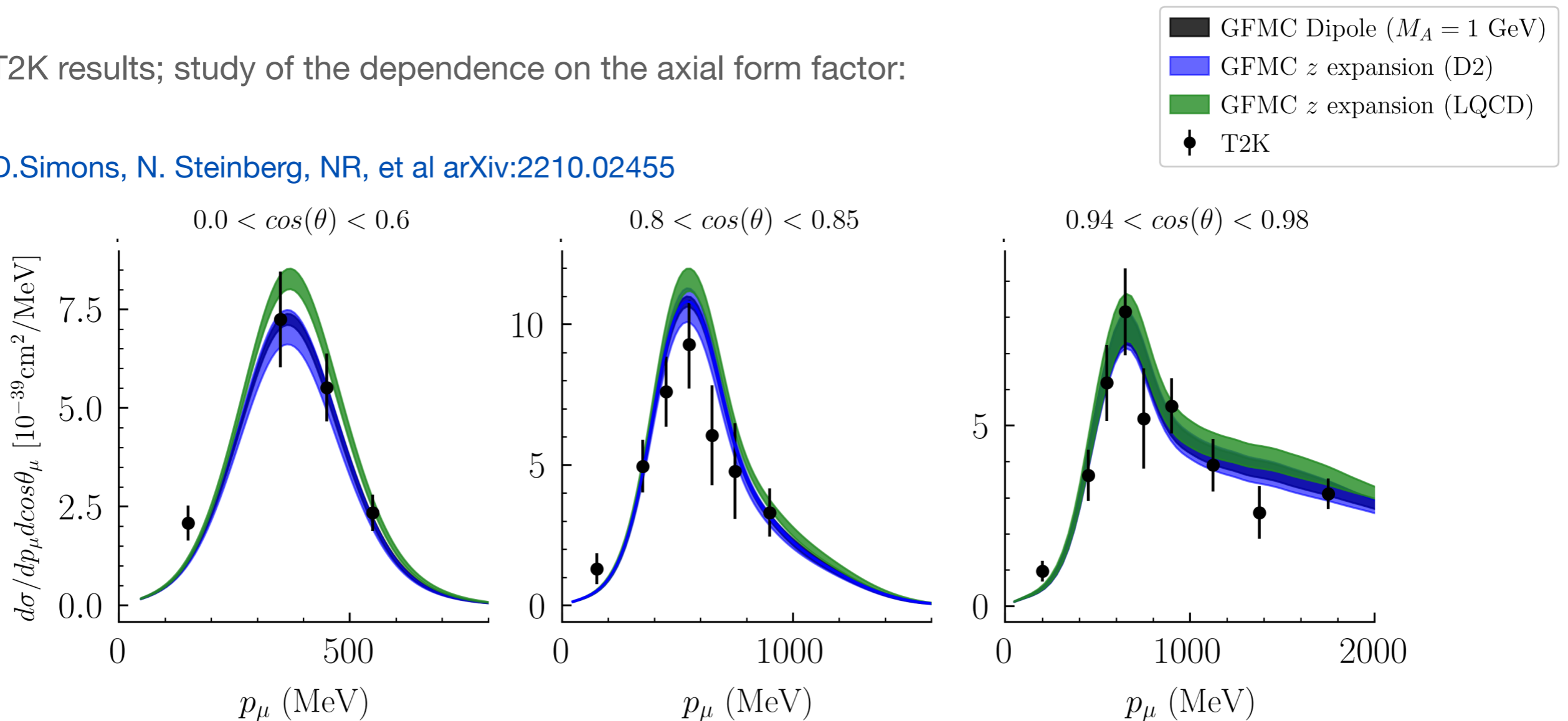
D.Simons, N. Steinberg et al, 2210.02455

MiniBooNE	$0.2 < \cos \theta_\mu < 0.3$	$0.5 < \cos \theta_\mu < 0.6$	$0.8 < \cos \theta_\mu < 0.9$
GFMC Difference in $d\sigma_{\text{peak}}$ (%)	18.6	17.1	12.2

Study of model dependence in neutrino predictions

T2K results; study of the dependence on the axial form factor:

D.Simons, N. Steinberg, NR, et al arXiv:2210.02455



D.Simons, N. Steinberg et al, 2210.02455

T2K	$0.0 < \cos \theta_\mu < 0.6$	$0.80 < \cos \theta_\mu < 0.85$	$0.94 < \cos \theta_\mu < 0.98$
GFMC difference in $d\sigma_{\text{peak}}$ (%)	15.8	8.0	4.6

Coupled Cluster Method

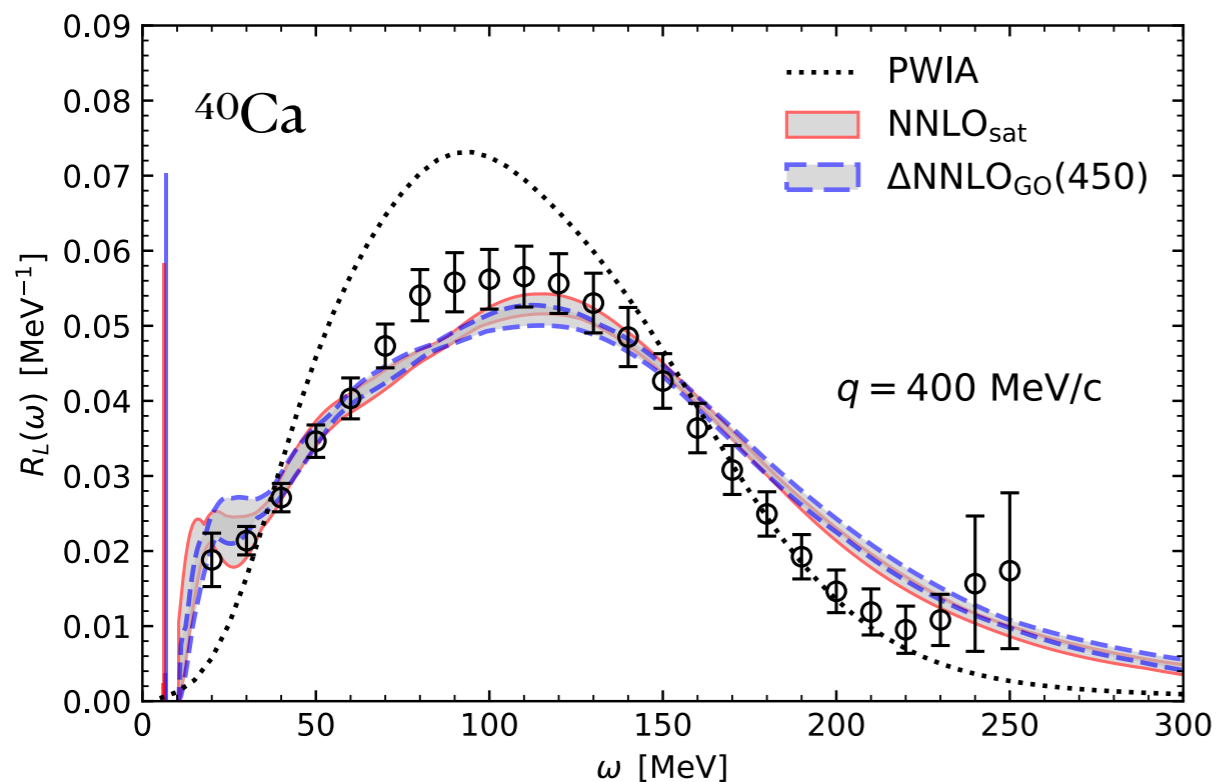
Reference state Hartree Fock: $|\Psi\rangle$

Include correlations through e^T operator

Similarity transformed Hamiltonian $e^{-T} H e^T |\Psi\rangle = \bar{H} |\Psi\rangle = E |\Psi\rangle$

T is an expansion in particle-hole excitations with respect to the reference state $|\Psi\rangle$

$$T = \sum t_a^i a_a^\dagger a_i + \sum t_{ab}^{ij} a_a^\dagger a_b^\dagger a_i a_j + \dots$$



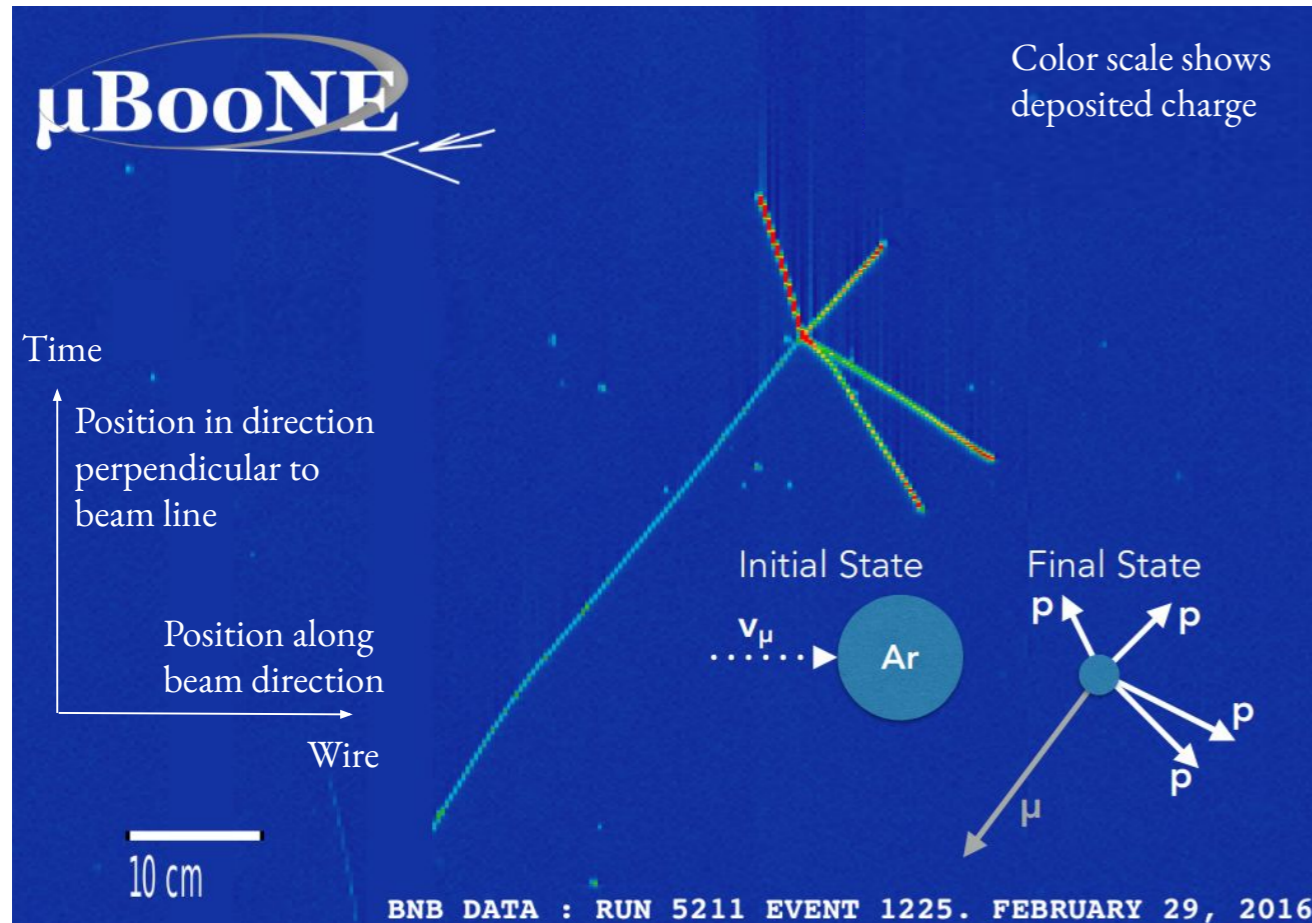
Polynomial scaling with the number of nucleons (predictions for ^{132}Sn and ^{208}Pb)

Electroweak response functions obtained using **LIT**

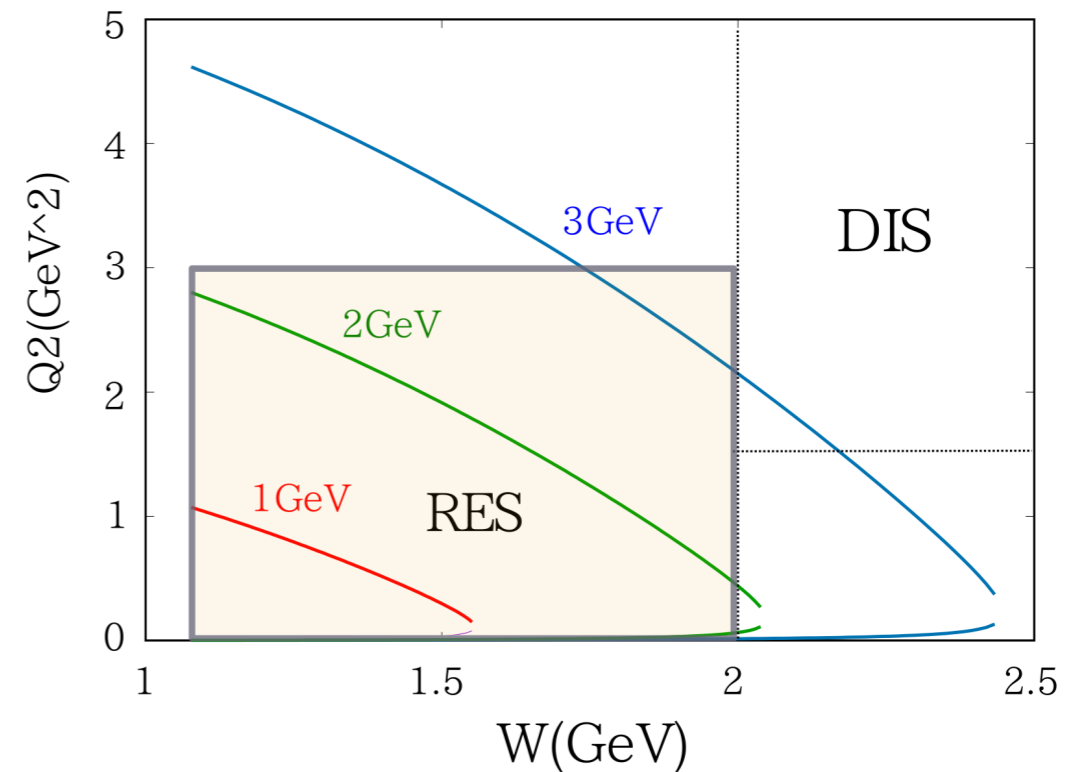
$$K_\Gamma(\omega, \sigma) = \frac{1}{\pi} \frac{\Gamma}{\Gamma^2 + (\omega - \sigma)^2}$$

JES, B. Acharya, S. Bacca, G. Hagen; PRL 127 (2021) 7, 072501, PRC 109 (2024) 2, 025502

Address new experimental capabilities



T.Sato talks @ NuSTEC Workshop on Neutrino-Nucleus Pion Production in the Resonance Region

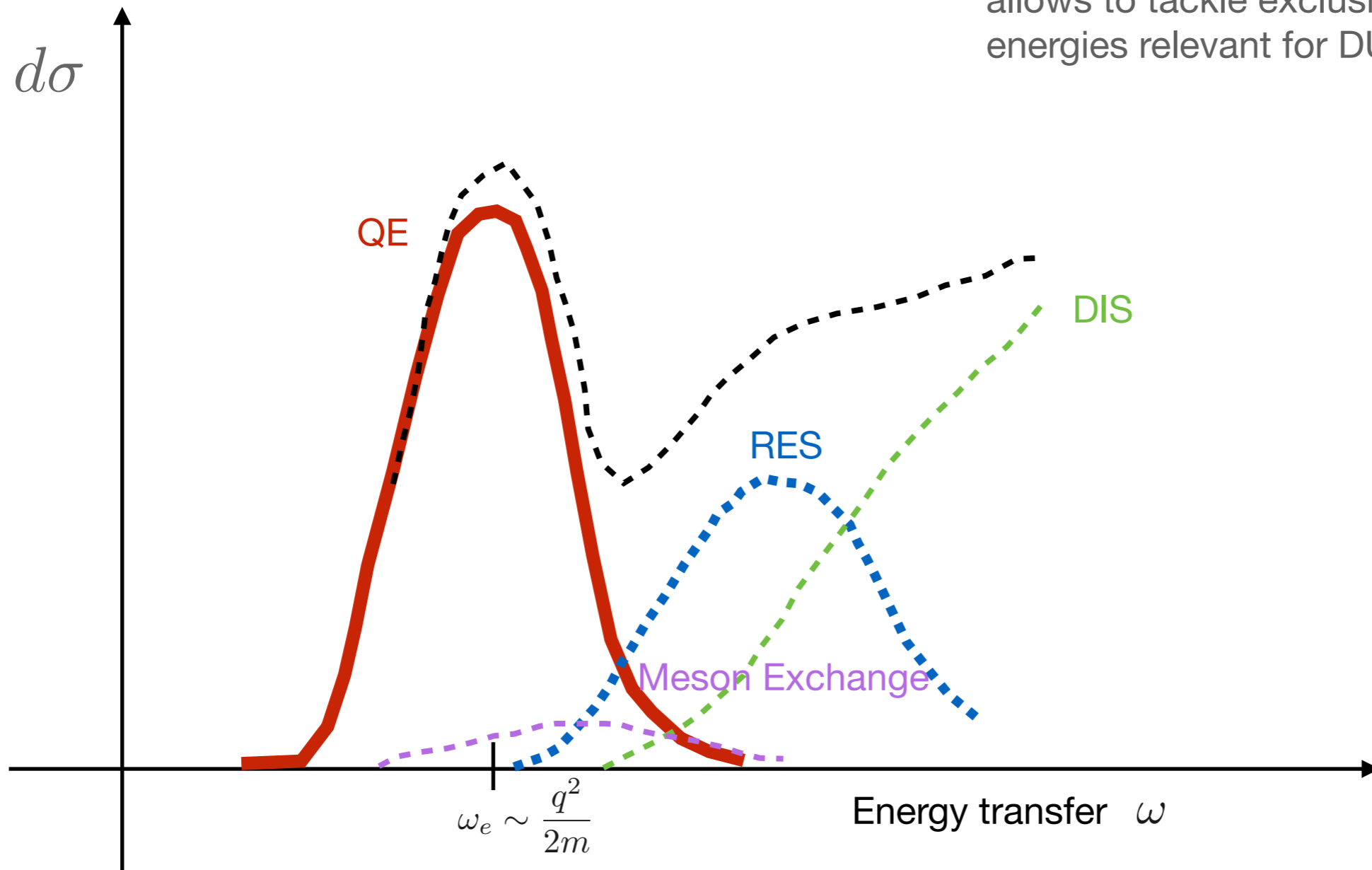


- Excellent spatial resolution
- Precise calorimetric information
- Powerful particle identification

$$W = \sqrt{(p + q)^2}, Q^2 = -q^2 = -(p_\nu - p_l)^2$$

Factorization Based Approaches

Factorization of the hadronic final states:
allows to tackle exclusive channels + higher
energies relevant for DUNE



Short-Time Approximation

Response functions are given by the **scattering from pairs of fully interacting nucleons** that **propagate** into a **correlated pair** of nucleons

The sum over all final states is replaced by a two nucleon propagator

$$R_\alpha(q, \omega) = \int_{-\infty}^{\infty} \frac{dt}{2\pi} e^{i(\omega + E_i)t} \langle \Psi_i | O_\alpha^\dagger(\mathbf{q}) e^{-iHt} O_\alpha(\mathbf{q}) | \Psi_i \rangle$$

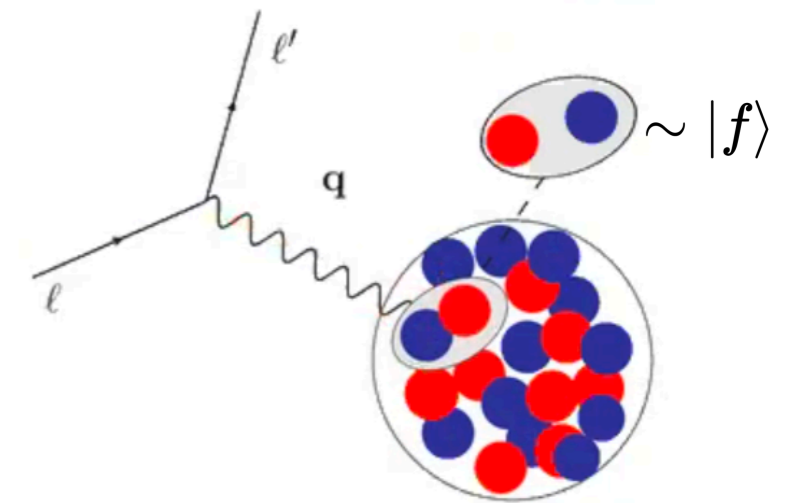
Provides “more” exclusive information in terms of nucleon-pair kinematics via the Response Densities as functions of (E,e)

$$R^{\text{STA}}(q, \omega) \sim \int \delta(\omega + E_0 - E_f) de dE_{cm} \mathcal{D}(e, E_{cm}; q)$$

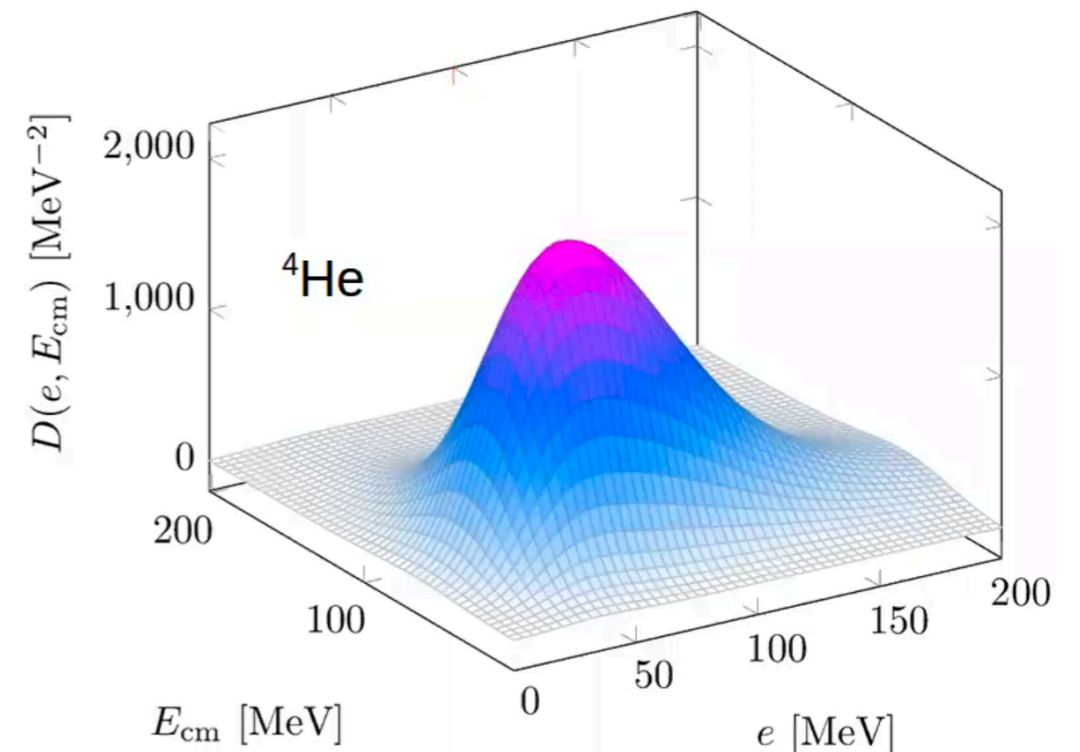
Pastore et al. PRC101(2020)044612

L. Andreoli, NR, et al. PRC 105, 014002 (2022)

[G. King talk this afternoon](#)



Transverse Density $q = 500 \text{ MeV}/c$



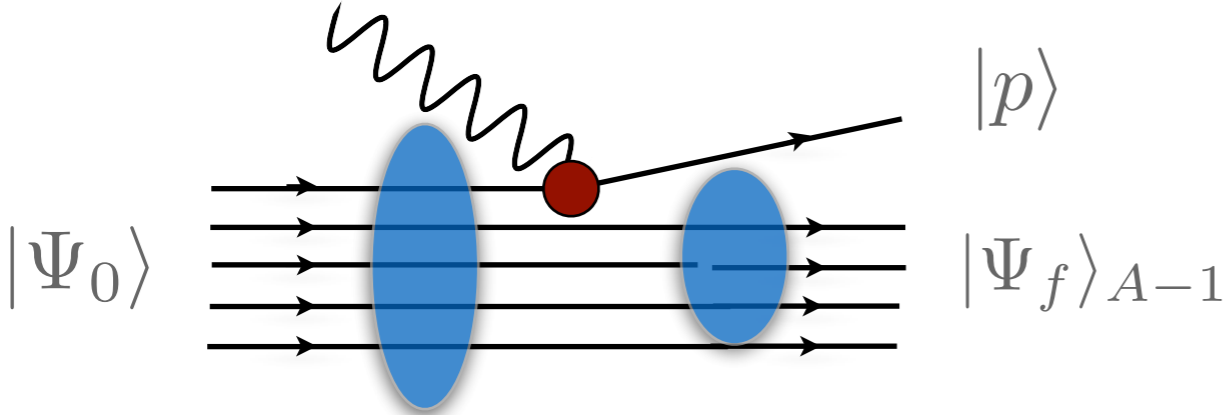
Spectral function approach

At large momentum transfer, the scattering reduces to the sum of individual terms

$$J_\alpha = \sum_i j_\alpha^i \quad |\Psi_f\rangle \rightarrow |p\rangle \otimes |\Psi_f\rangle_{A-1}$$

The incoherent contribution of the one-body response reads

$$R_{\alpha\beta} \simeq \int \frac{d^3k}{(2\pi)^3} dE P_h(\mathbf{k}, E) \sum_i \langle k | j_\alpha^{i\dagger} | k + q \rangle \langle k + q | j_\beta^i | k \rangle \delta(\omega + E - e(\mathbf{k} + \mathbf{q}))$$



The Spectral Function is the imaginary part of the two point Green's Function

Different many-body methods can be adopted to determine it

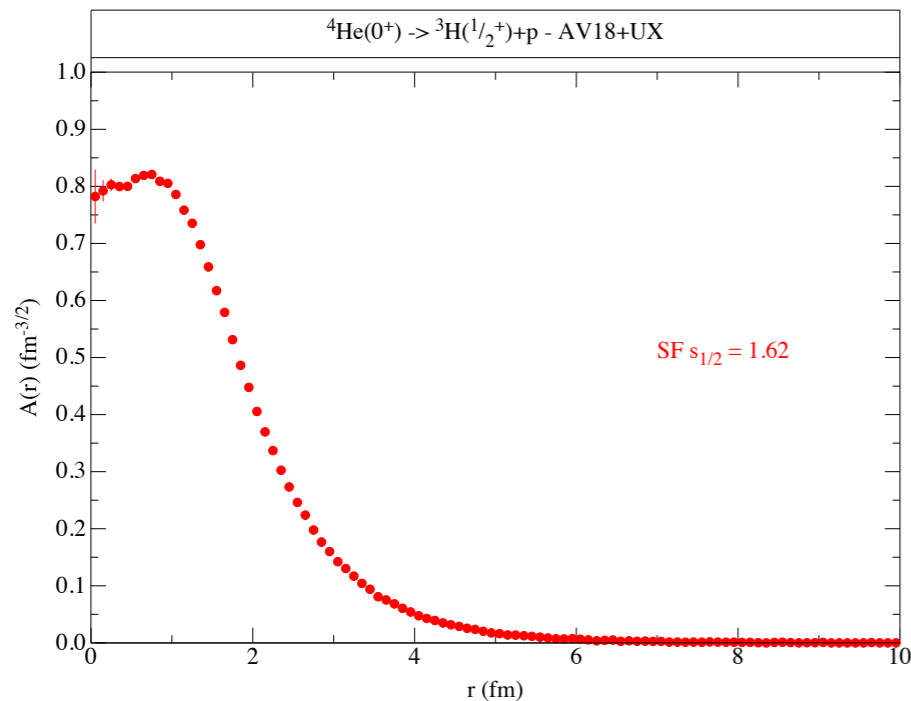
O. Benhar et al, Rev.Mod.Phys. 80 (2008)
 I. Korover, et al Phys.Rev.C 107 (2023) 6, L061301

NR, Frontiers in Phys. 8 (2020) 116
 J.E. Sobczyk et al, PRC 106 (2022) 3
 J.E. Sobczyk et al, PRC 109 (2024)

QMC Spectral function of light nuclei

- Single-nucleon spectral function:

$$P_{p,n}(\mathbf{k}, E) = \sum_n \left| \langle \Psi_0^A | [|k\rangle \otimes | \Psi_n^{A-1} \rangle] \right|^2 \delta(E + E_0^A - E_n^{A-1}) = P^{MF}(\mathbf{k}, E) + P^{\text{corr}}(\mathbf{k}, E)$$

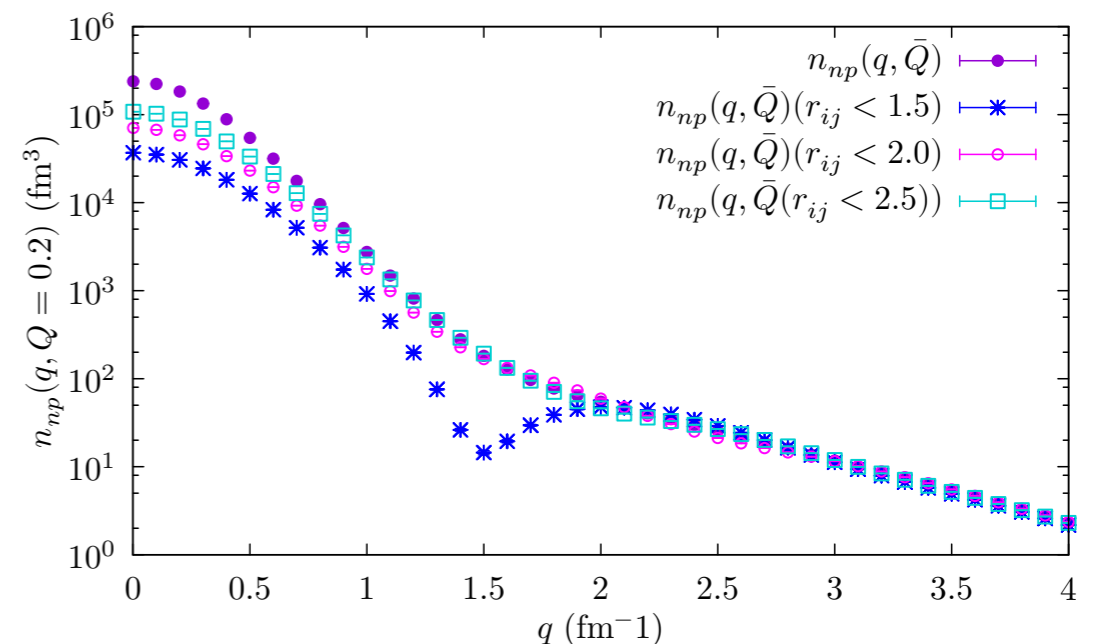


$$P^{MF}(\mathbf{k}, E) = \left| \langle \Psi_0^A | [|k\rangle \otimes | \Psi_n^{A-1} \rangle] \right|^2 \times \delta\left(E - B_A + B_{A-1} - \frac{\mathbf{k}^2}{2m_{A-1}}\right)$$

- The single-nucleon overlap has been computed within VMC (center of mass motion fully accounted for)

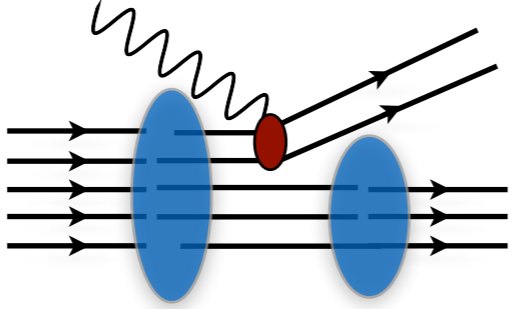
$$P^{\text{corr}}(\mathbf{k}, E) = \int d^3k' \left| \langle \Psi_0^A | [|k\rangle |k'\rangle \otimes | \Psi_n^{A-2} \rangle] \right|^2 \times \delta\left(E - B_A - e(\mathbf{k}') + B_{A-2} - \frac{(\mathbf{k} + \mathbf{k}')^2}{2m_{A-2}}\right)$$

- Written in terms of two-body momentum distribution



Spectral function approach

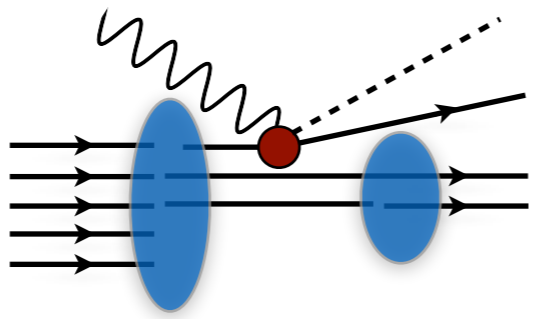
$$|f\rangle \rightarrow |pp'\rangle_a \otimes |f_{A-2}\rangle$$



The hadronic tensor for two-body current factorizes as

$$R_{2b}^{\mu\nu}(\mathbf{q}, \omega) \propto \int dE d^3k d^3k' P_{2b}(\mathbf{k}, \mathbf{k}', E) \times d^3p d^3p' |\langle kk' | j_{2b}^\mu | pp' \rangle|^2$$

$$|f\rangle \rightarrow |p_\pi p\rangle \otimes |f_{A-1}\rangle$$



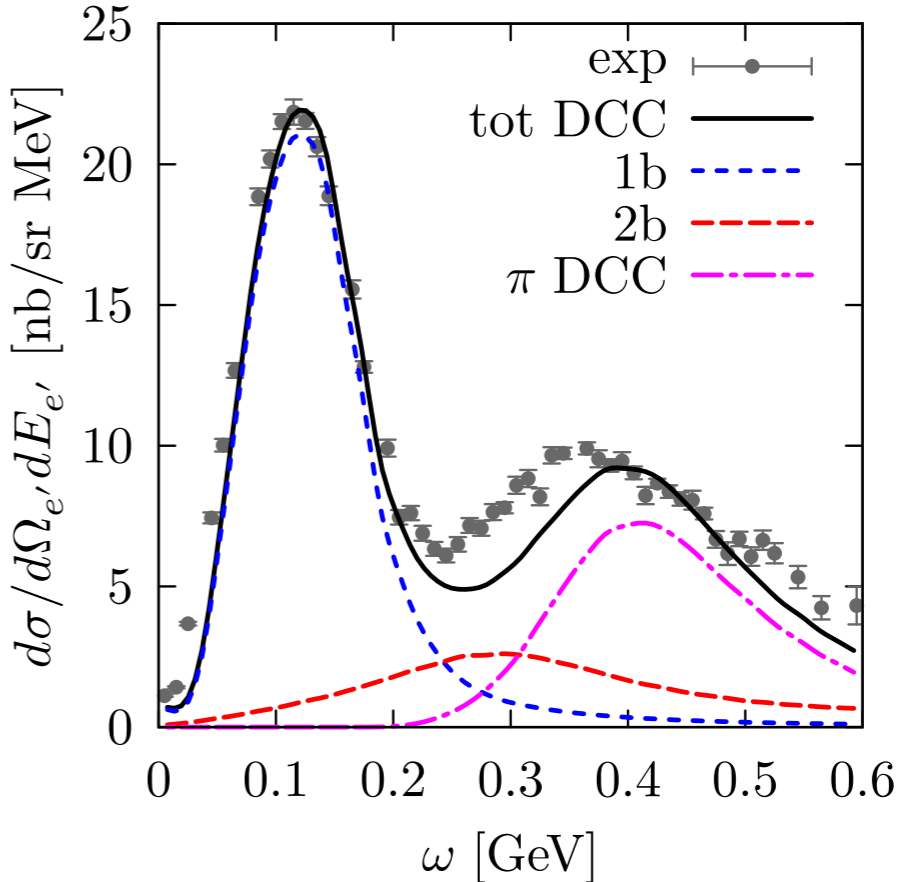
Production of real pi in the final state

$$R_{1b\pi}^{\mu\nu}(\mathbf{q}, \omega) \propto \int dE d^3k P_{1b}(\mathbf{k}, E) \times d^3p d^3k_\pi |\langle k | j^\mu | pk_\pi \rangle|^2$$

* Pion production elementary amplitudes currently derived within the extremely sophisticated **Dynamic Couple Chanel approach**;

S.X.Nakamura, et al PRD92(2015)
T. Sato, et al PRC67(2003)

$E_e = 730 \text{ MeV}, \theta_e = 37.0^\circ$

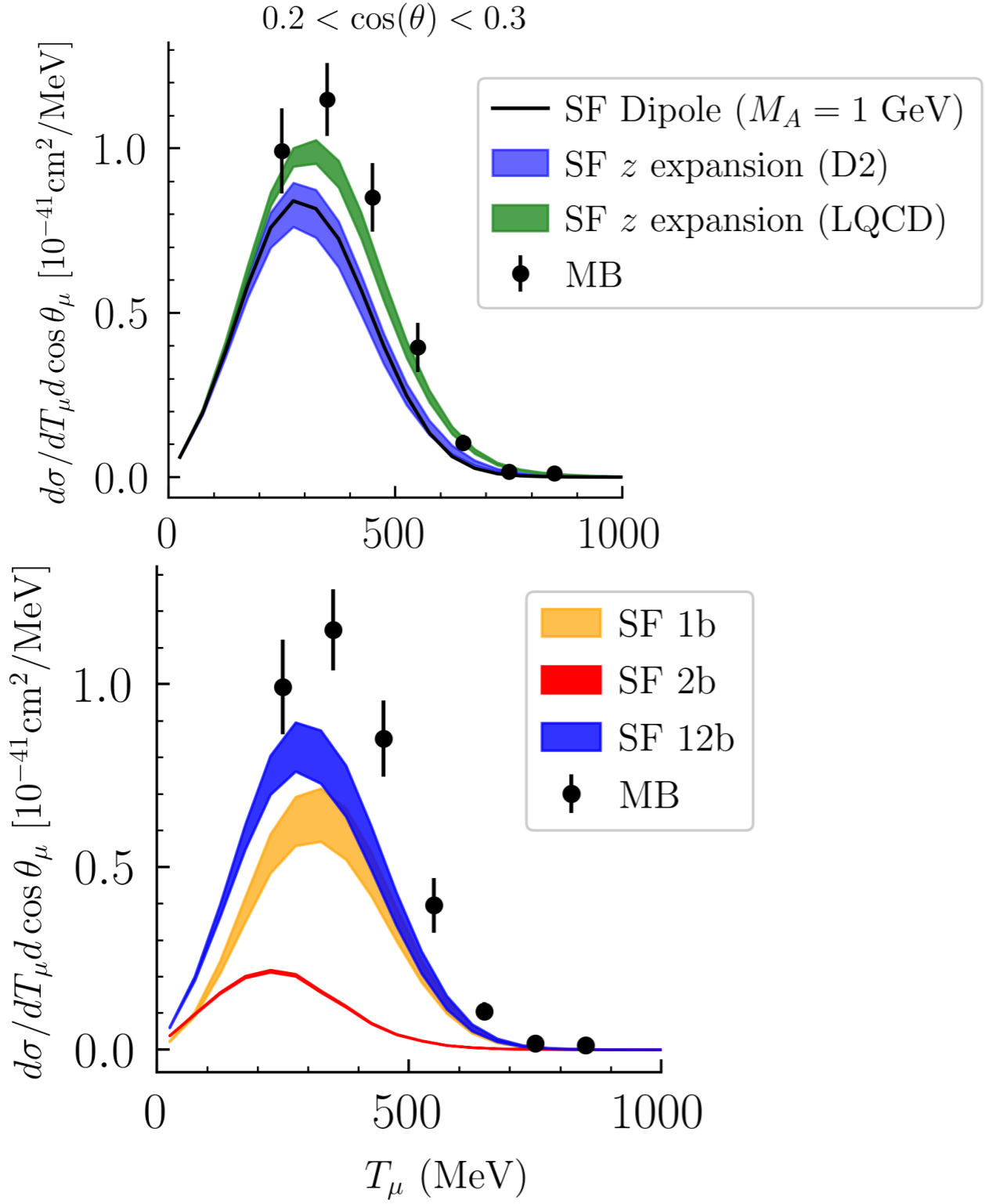


NR, Frontiers in Phys. 8 (2020) 116



Axial Form Factors Uncertainty needs

D.Simons, N. Steinberg et al, 2210.02455



* Axial form factor dependence:

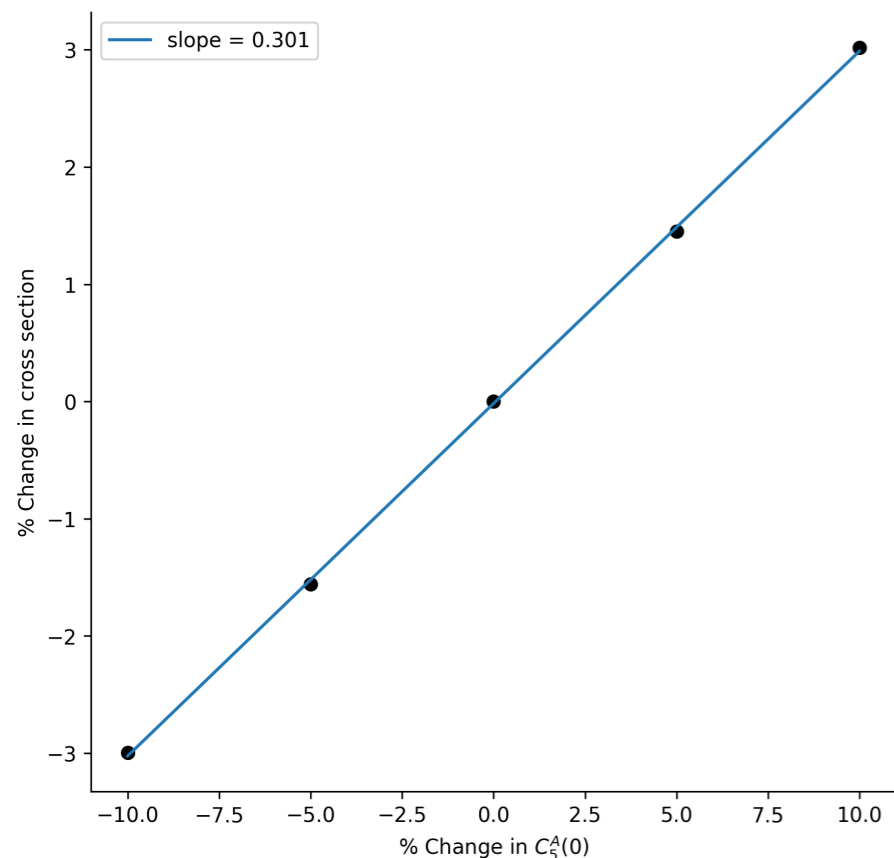
MiniBooNE	$0.2 < \cos\theta_\mu < 0.3$
SF Difference in $d\sigma_{\text{peak}}$ (%)	16.3

* Many-body method dependence:

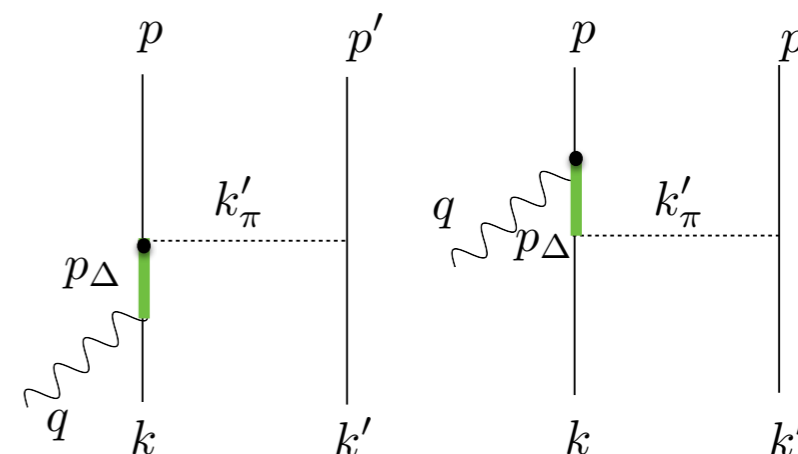
MiniBooNE	$0.2 < \cos\theta_\mu < 0.3$
GFMC/SF difference in $d\sigma_{\text{peak}}$ (%)	22.8

Resonance Uncertainty needs

The largest contributions to two-body currents arise from resonant $N \rightarrow \Delta$ transitions yielding pion production



D.Simons, N. Steinberg et al, 2210.02455



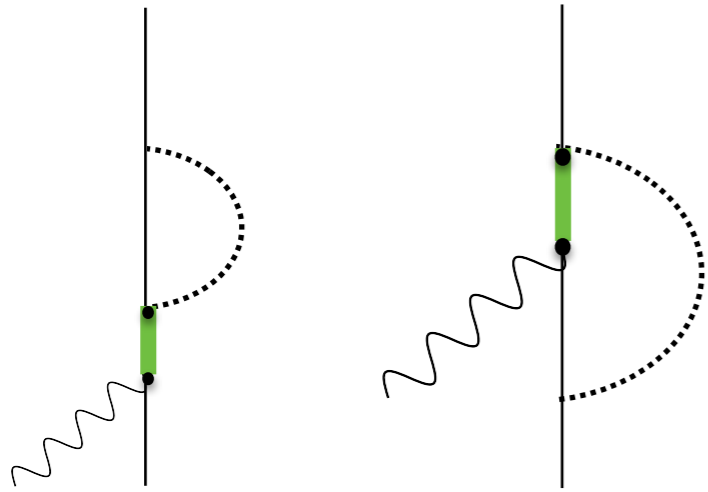
The normalization of the dominant $N \rightarrow \Delta$ transition form factor needs to be known to 3% precision to achieve 1% cross-section precision for MiniBooNE kinematics

State-of-the-art determinations of this form factor from experimental data on pion electroproduction achieve 10-15% precision (under some assumptions)

Hernandez et al, PRD 81 (2010)

Further constraints on $N \rightarrow \Delta$ transition relevant for two-body currents and π production will be necessary to achieve few-percent cross-section precision

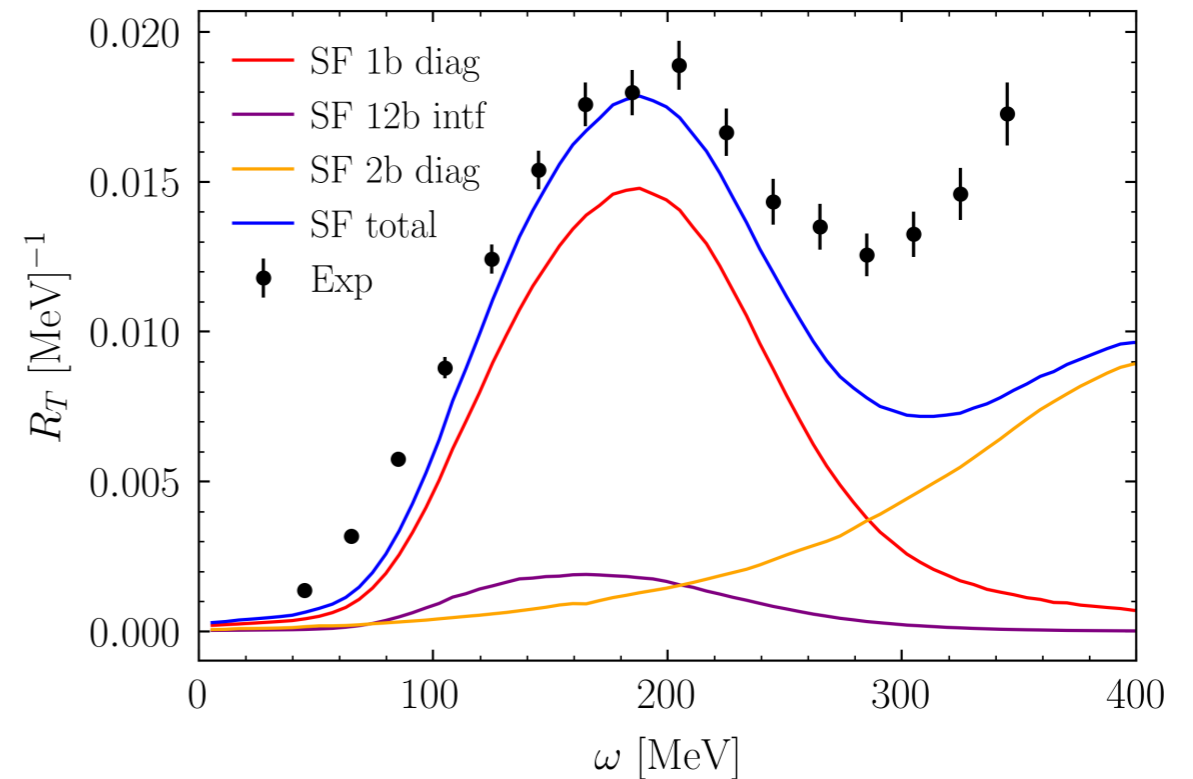
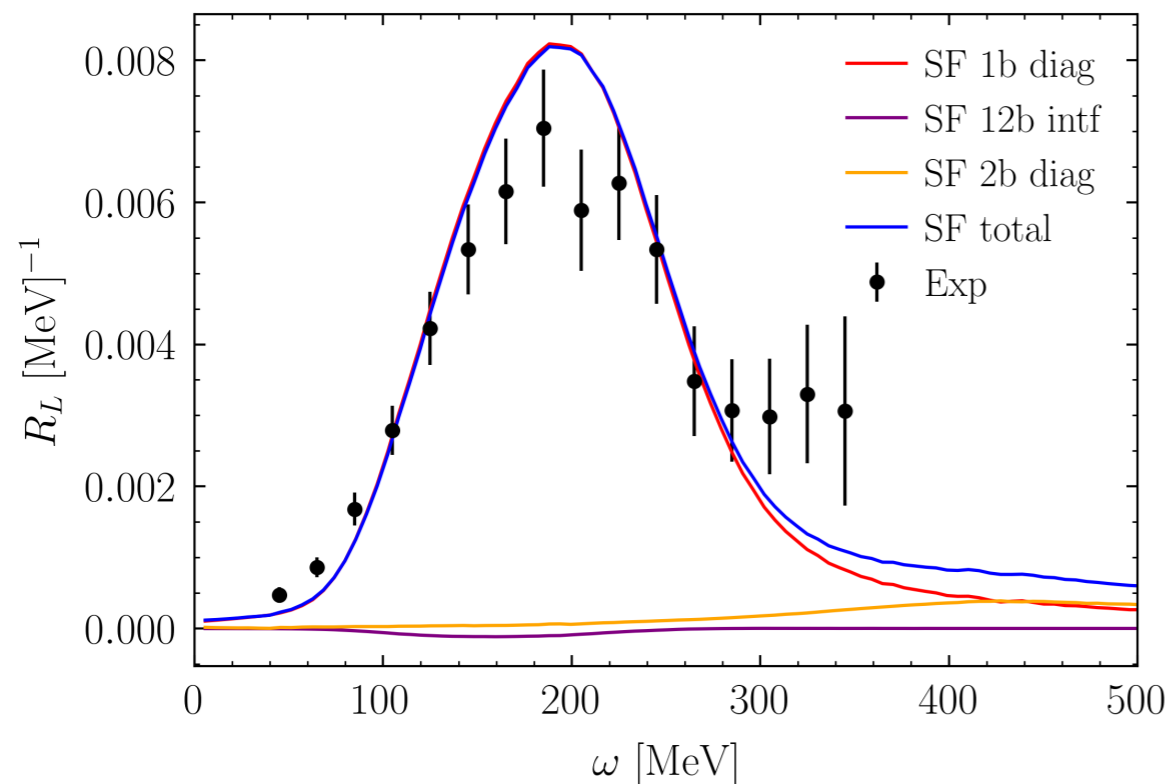
Including the one- and two-body interference



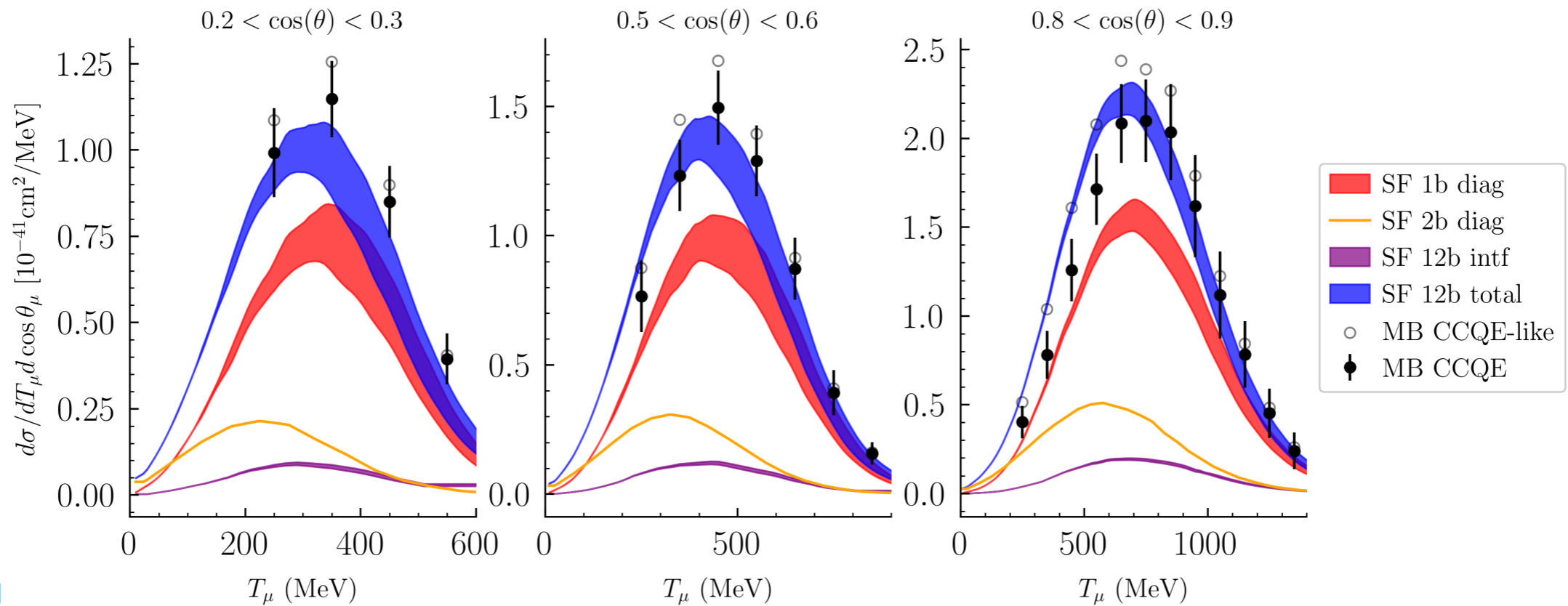
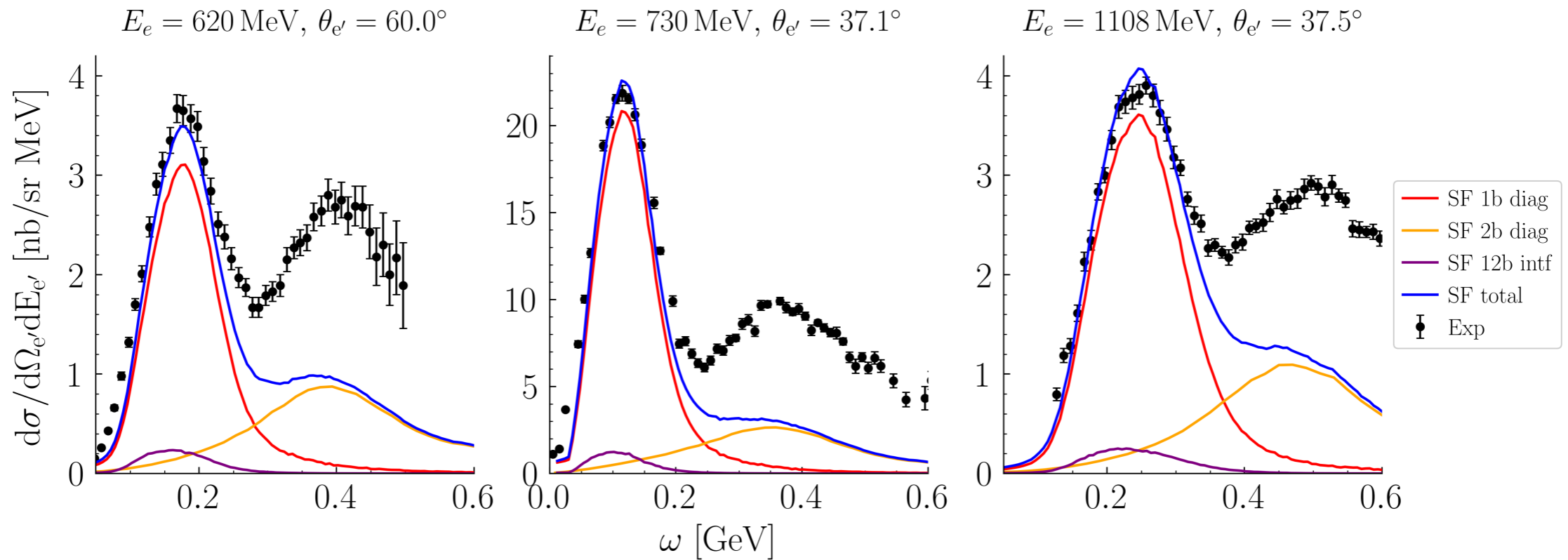
We recently included interference effects between one- and two-body currents yielding single nucleon knock-out

Observe a small quenching in the longitudinal channel and an enhancement in the q.e. peak in the transverse \rightarrow agreement with the GFMC

N. Steinberg, NR, A. Lovato, arXiv: 2312.12545



Including the one- and two-body interference



Using Bayesian ANN for electron-nucleus scattering

J. Sobczyk, NR, A. Lovato, arxiv:2406.06292

The inclusive electron-nucleus cross section can be written in terms of the longitudinal and transverse response function

$$\left(\frac{d^2\sigma}{dE'd\Omega'}\right)_e = \left(\frac{d\sigma}{d\Omega'}\right)_M \left[\frac{q^4}{\mathbf{q}^4} R_L(\mathbf{q}, \omega) + \left(\tan^2 \frac{\theta}{2} - \frac{1}{2} \frac{q^2}{\mathbf{q}^2} \right) R_T(\mathbf{q}, \omega) \right]$$

Traditionally, the **Rosenbluth separation** is adopted to obtain $R_L(\mathbf{q}, \omega)$ and $R_T(\mathbf{q}, \omega)$

$$\Sigma(\mathbf{q}, \omega, \epsilon) = \epsilon \frac{\mathbf{q}^4}{Q^4} \left(\frac{d^2\sigma}{dE'd\Omega'}\right)_e / \left(\frac{d\sigma}{d\Omega'}\right)_M = \epsilon R_L(\mathbf{q}, \omega) + \frac{1}{2} \frac{\mathbf{q}^2}{Q^2} R_T(\mathbf{q}, \omega)$$

Photon polarization

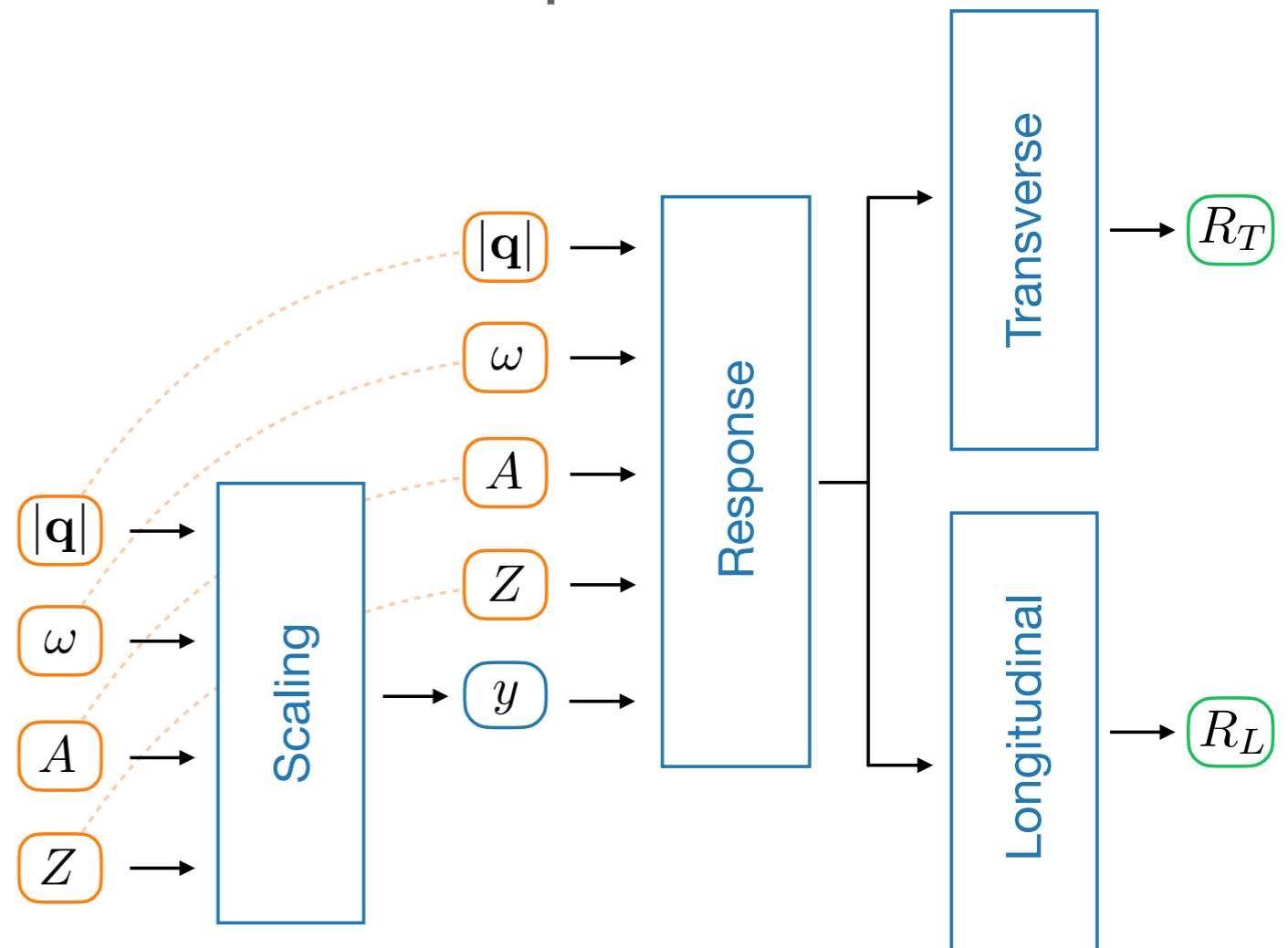
As θ ranges between 180 to 0 degrees, ϵ varies between 0 and 1. Within this approach, R_L is the **slope** while $(\mathbf{q}^2/2Q^2)R_T$ is the **intercept** of the linear fit to data

This definition can only be applied if the Born approximation is valid and if the data have already been corrected to Coulomb distortions of the electron wave function.

Using Bayesian ANN for electron-nucleus scattering

We used ANN architecture to obtain the **longitudinal** and **transverse responses**

- We preprocess the input through a ‘scaling’ net whose output is $y(\mathbf{q}, \omega, A, Z)$.
- We concatenate y with the other inputs to compute the ‘Response’ net which gives a 32-dim output.
- This input is used to build **two completely independent nets**; each provides a single output corresponding to the longitudinal and transverse responses, respectively.



We train our ANN using the quasielastic electron nucleus scattering archive of [arXiv:nucl-ex/0603032](https://arxiv.org/abs/nucl-ex/0603032) considering five different light and medium-mass nuclei, symmetric: ^4He , ^6Li , ^{12}C , ^{16}O and ^{40}Ca .

Using Bayesian ANN for electron-nucleus scattering

We used **Bayesian statistics** to quantify the uncertainty of the ANN. We treat the weights \mathcal{W} as a probability distribution.

The posterior probability of the parameters \mathcal{W} given the measured cross sections Y can be written as

$$P(\mathcal{W} | Y) = \frac{P(Y | \mathcal{W})P(\mathcal{W})}{P(Y)}$$

We assign a normal Gaussian prior for each neural network parameter and assume a **Gaussian distribution for the likelihood** based on a loss function obtained from a **least-squares** fit to the empirical data

$$P(Y | \mathcal{W}) = \exp\left(-\frac{\chi^2}{2}\right) \quad \chi^2 = \sum_{i=1}^N \frac{[y_i - \hat{y}_i(\mathcal{W})]^2}{\sigma_i^2}$$

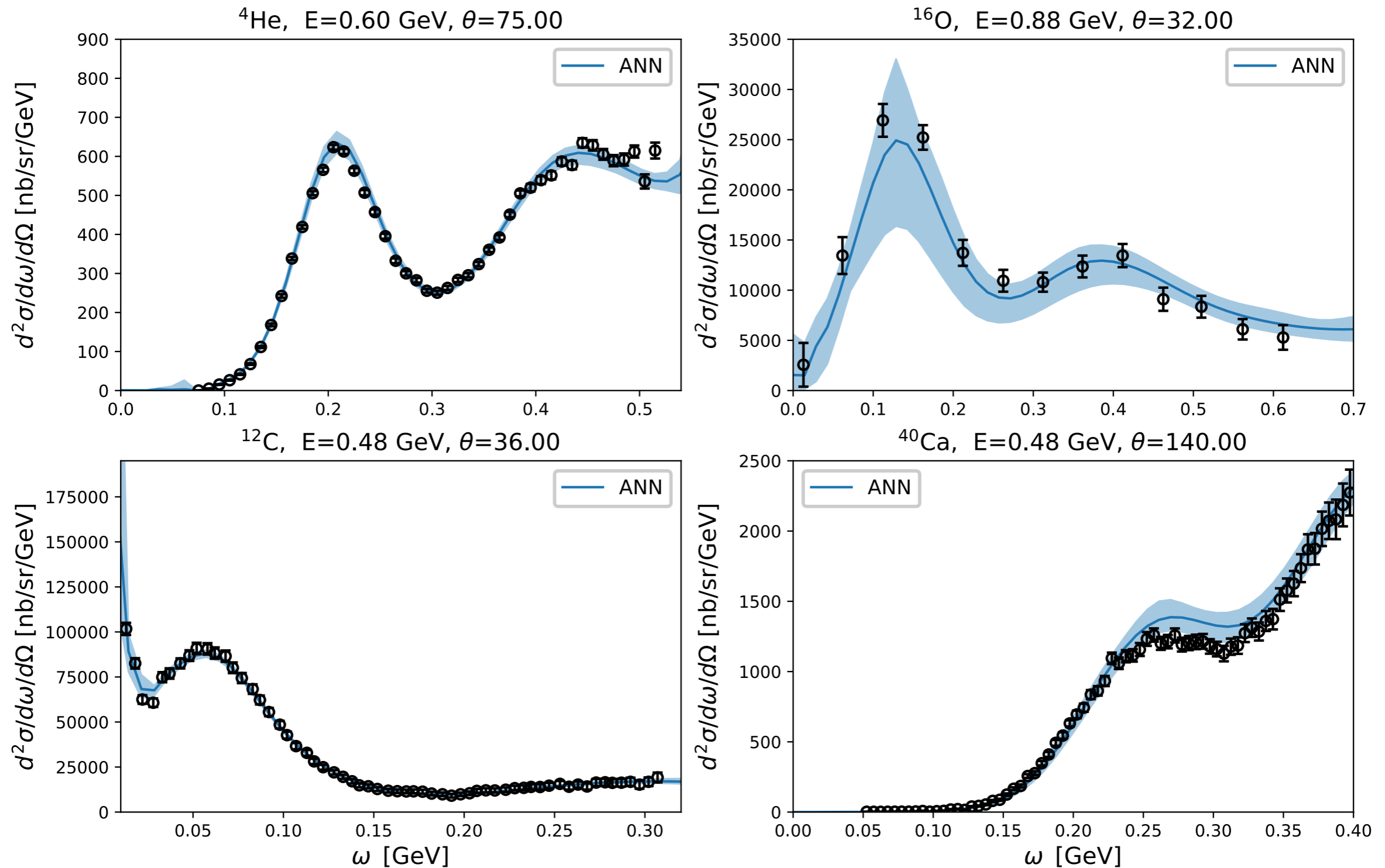
We increase the experimental errors σ_i listed in [arXiv:nucl-ex/0603032](https://arxiv.org/abs/nucl-ex/0603032) including an additional term proportional to the experimental cross section value: $\sigma_i \rightarrow \sigma_i + 0.05y_i$.

The posterior distribution is sampled using the **NumPyro No-U-Turn Sampler** extension of HMC. We also implemented the standard HMC algorithm and validated results.

Using Bayesian ANN for electron-nucleus scattering

Results: Cross sections for different nuclei

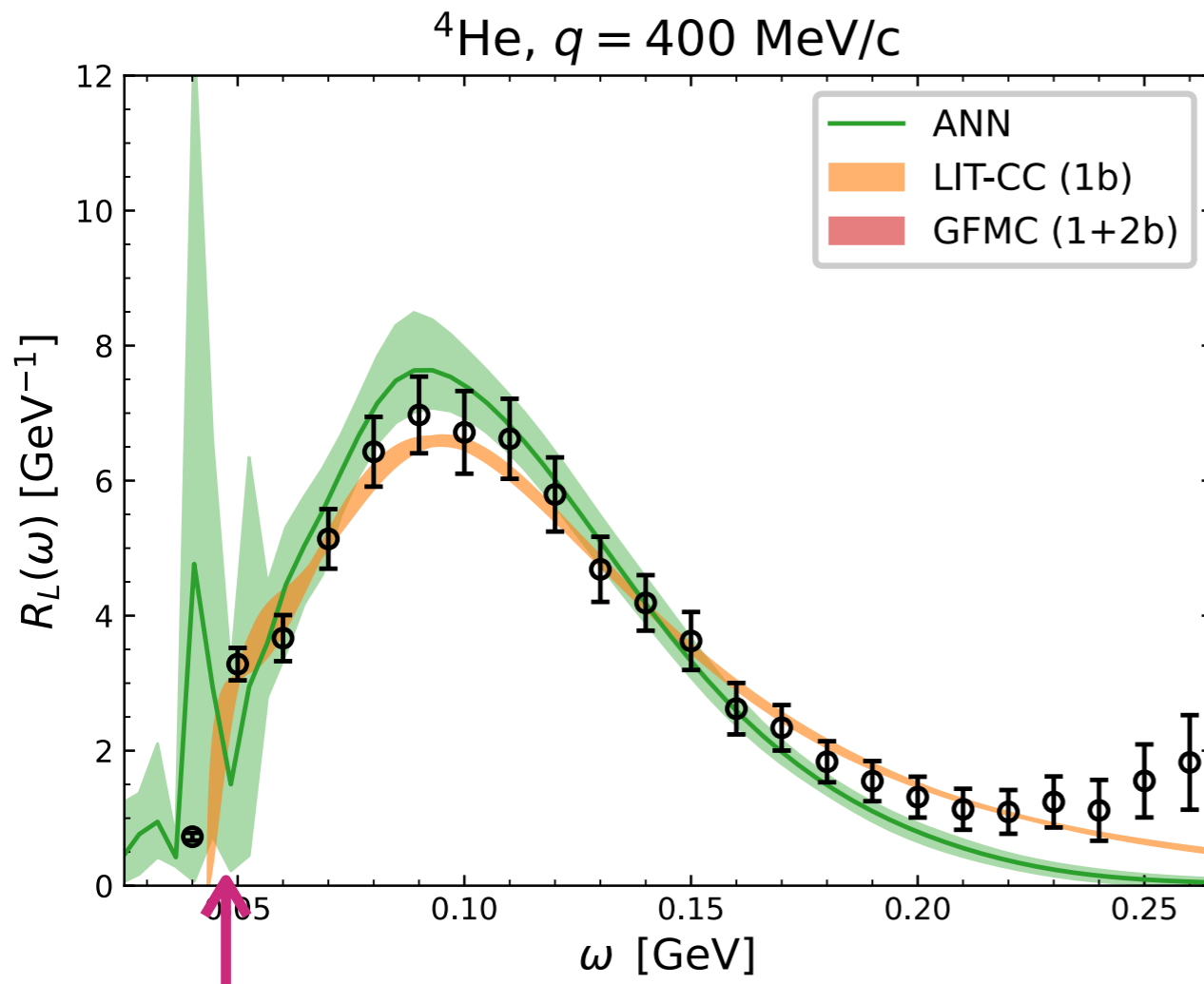
J. Sobczyk, NR, A. Lovato, arxiv:2406.06292



Using Bayesian ANN for electron-nucleus scattering

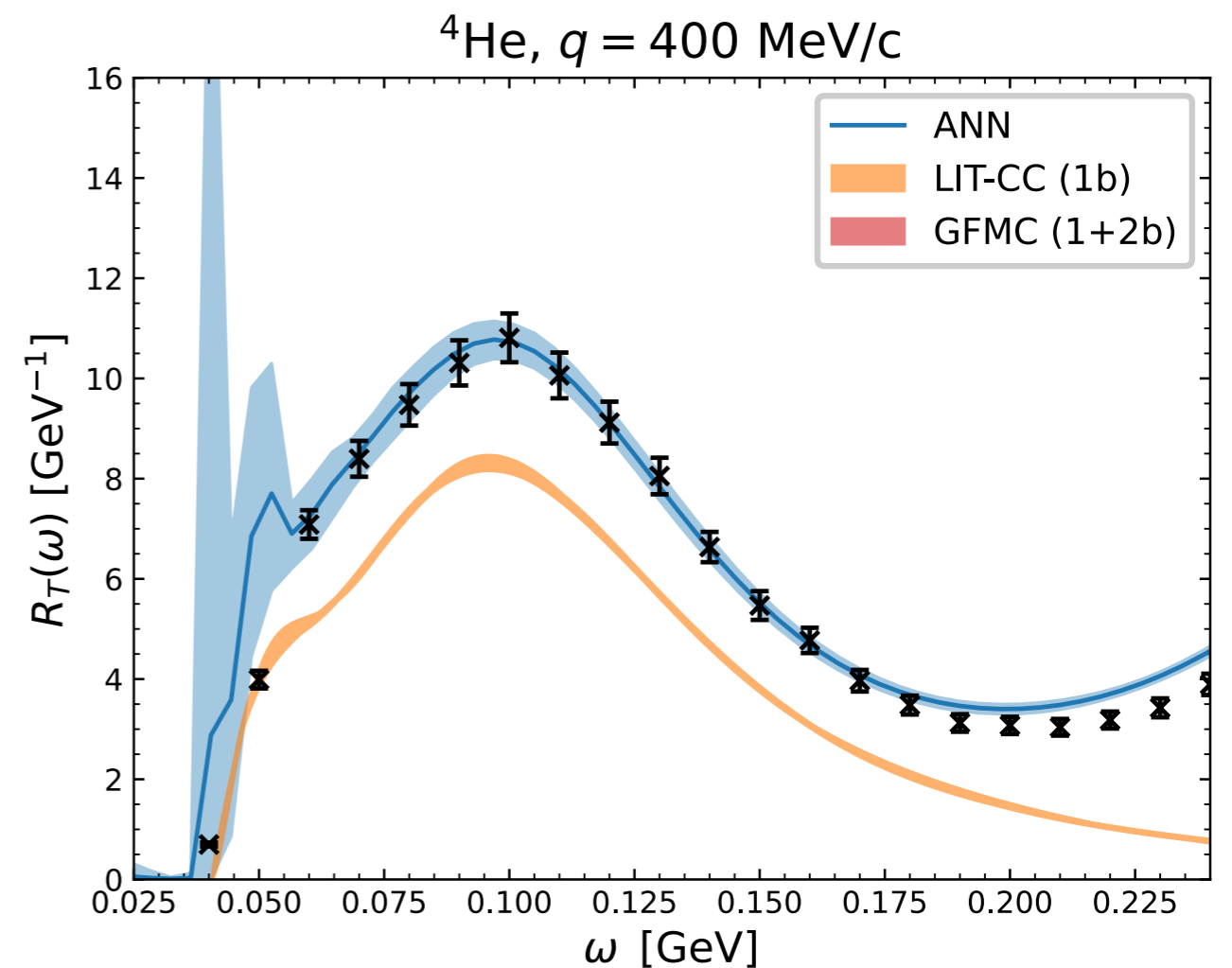
J. Sobczyk, NR, A. Lovato, [arxiv:2406.06292](https://arxiv.org/abs/2406.06292)

Results: Electromagnetic responses



Low lying nuclear states

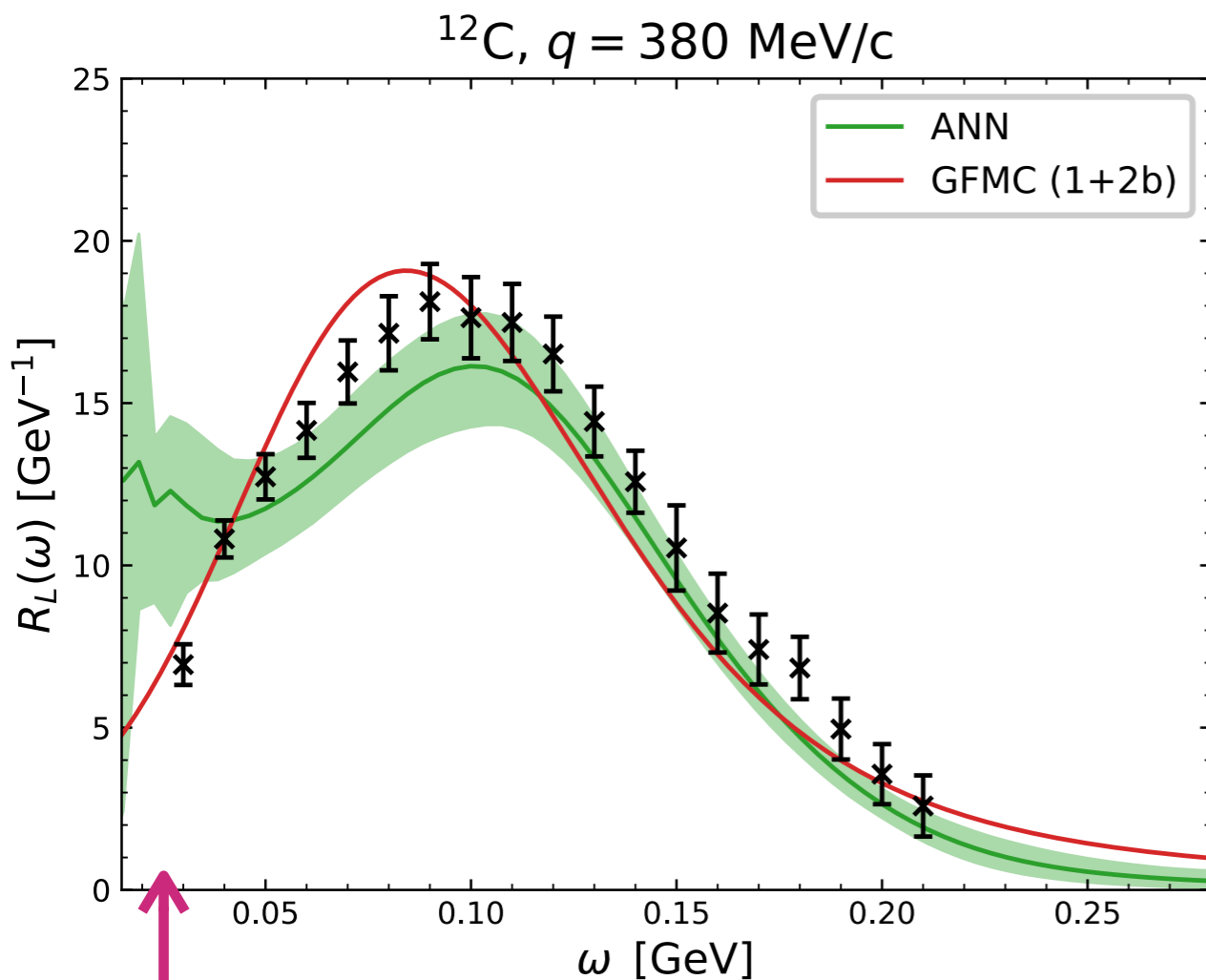
Contributions from elastic and low-lying inelastic transitions are explicitly removed from the GFMC responses and the Rosenbluth analysis, while they are present in the ANN curves



Using Bayesian ANN for electron-nucleus scattering

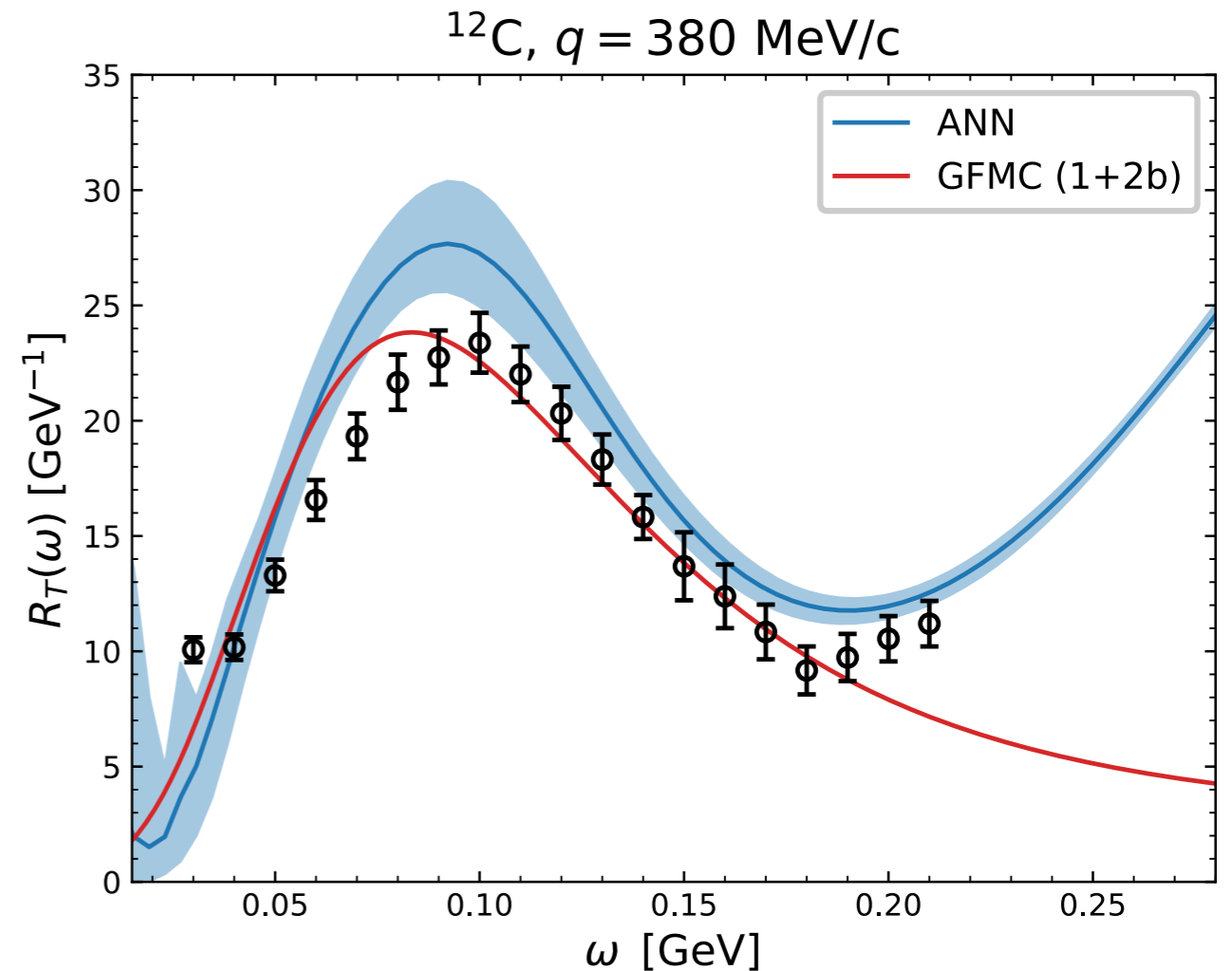
J. Sobczyk, NR, A. Lovato, arxiv:2406.06292

Results: Electromagnetic responses



Low lying nuclear states

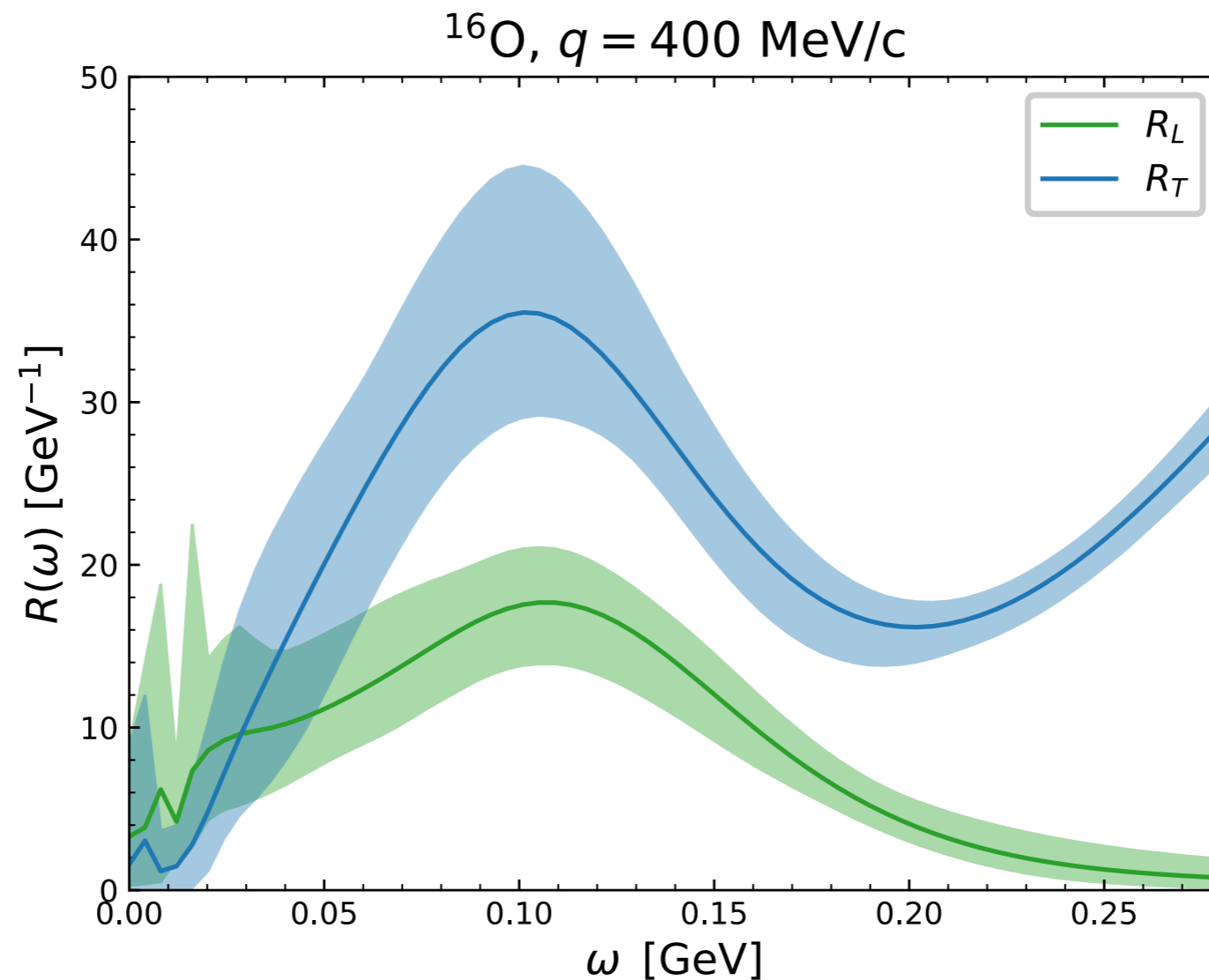
Contributions from elastic and low-lying inelastic transitions are explicitly removed from the GFMC responses and the Rosenbluth analysis, while they are present in the ANN curves



Using Bayesian ANN for electron-nucleus scattering

J. Sobczyk, NR, A. Lovato, arxiv:2406.06292

Results: Electromagnetic responses

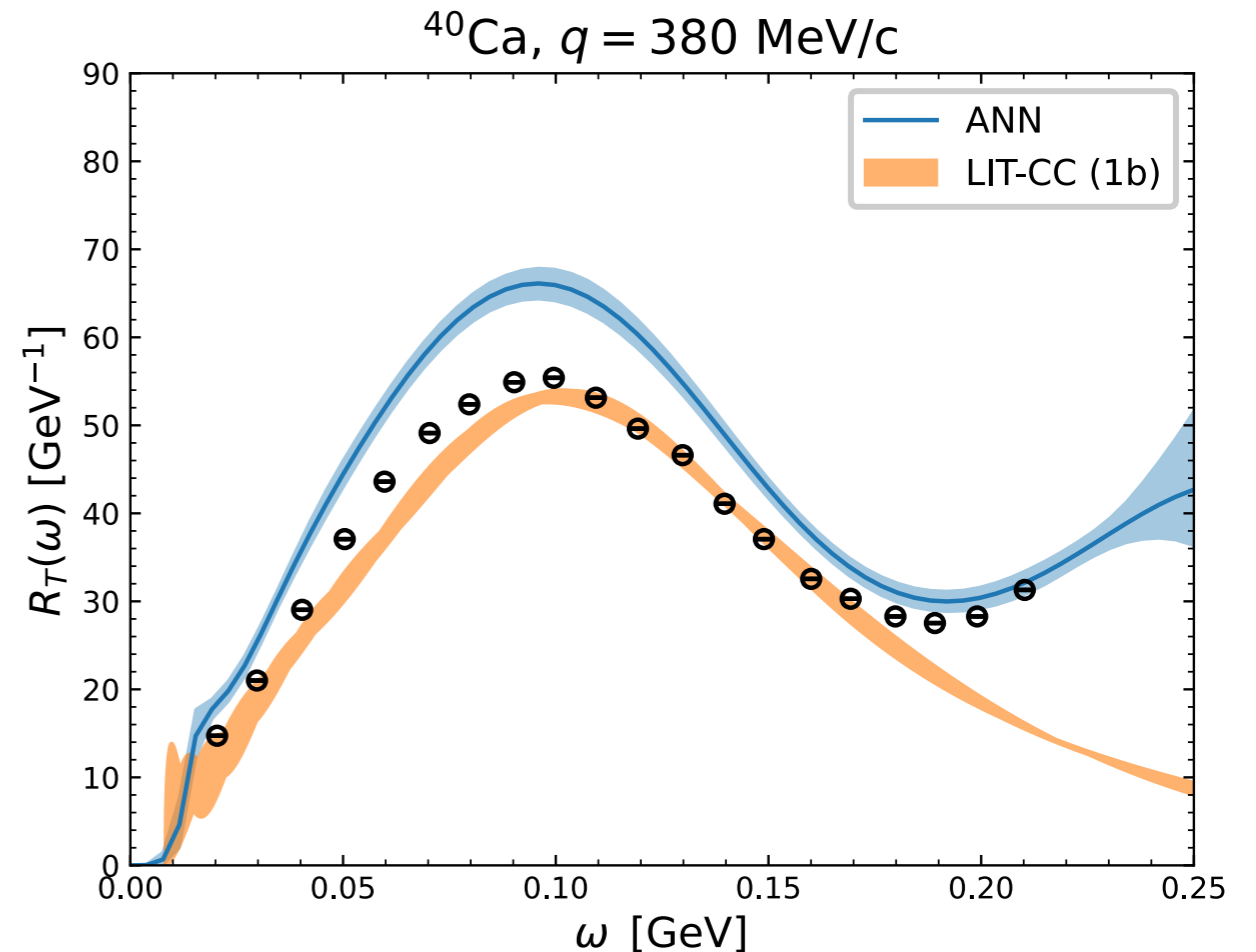
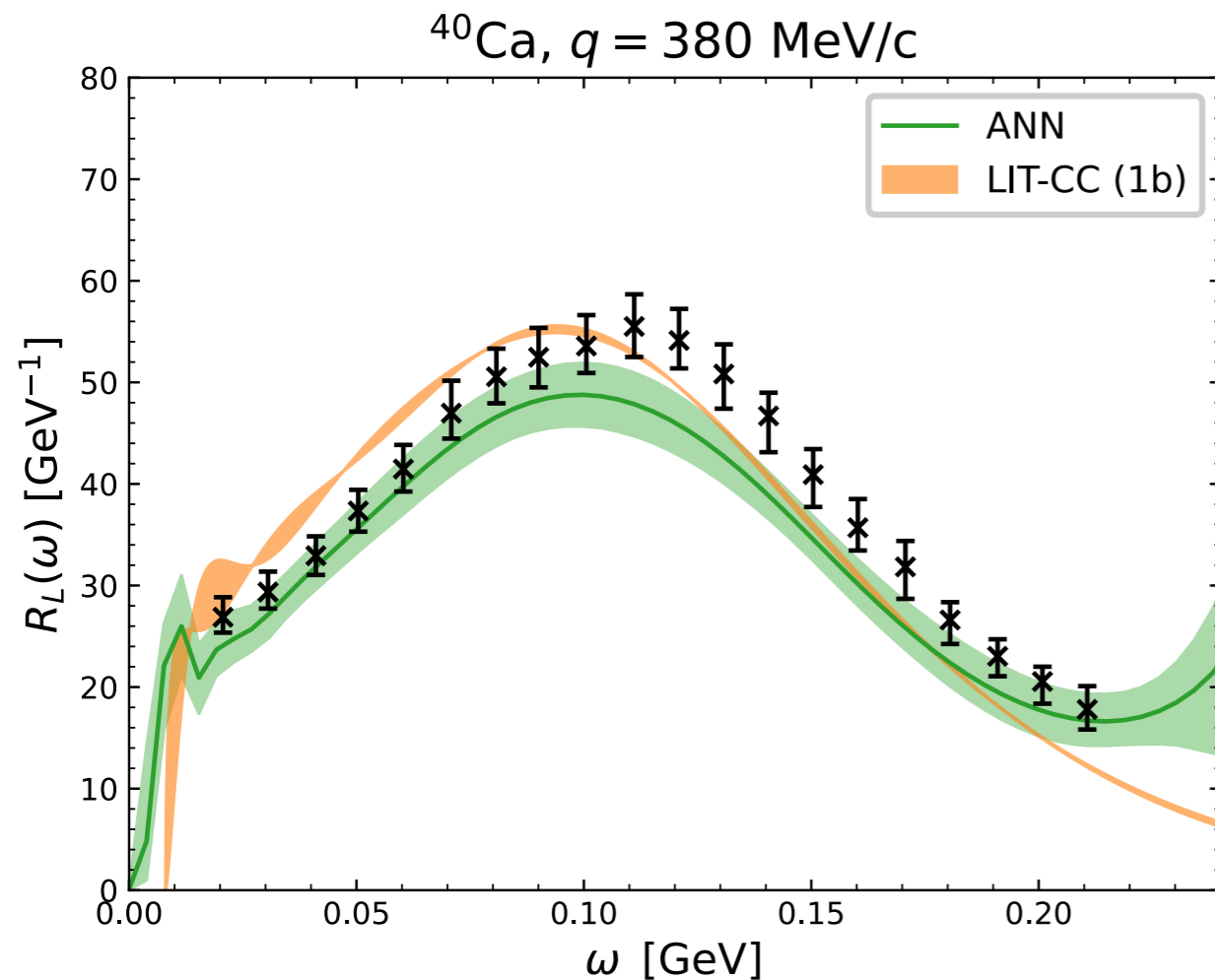


First separation of the longitudinal and transverse responses of ^{16}O . Large uncertainty bands reflect the **scarcity of inclusive cross section data**.

Using Bayesian ANN for electron-nucleus scattering

J. Sobczyk, NR, A. Lovato, [arxiv:2406.06292](https://arxiv.org/abs/2406.06292)

Results: Electromagnetic responses



Note increasing error bars for large ω reflecting the scarcity of data for ^{40}Ca in the high energy-momentum region. The net is learning from other nuclei in this region.

Dedicated discussion on the Rosenbluth separation carried out using two different experiments.

Conclusions

- * Neutrino oscillation experiments are entering a new precision era

- * To match these precision goals accurate predictions of neutrino cross sections are crucial

 - Ab initio methods: almost exact results but limited in energy, fully inclusive

 - Approaches based on factorization schemes are being further developed

- * Uncertainty associated with the theory prediction of the hard interaction vertex needs to be assessed. Initial work has been carried out in this direction studying the dependence on:

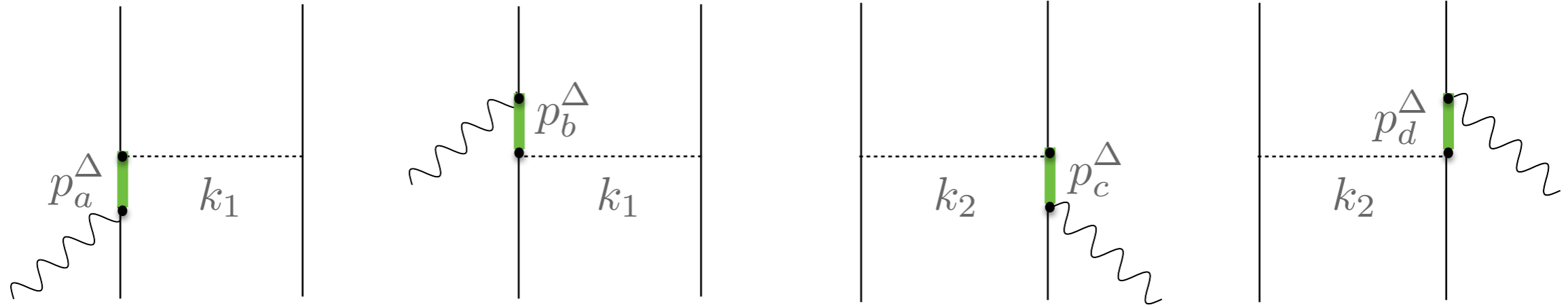
 - Form factors: one- and two-body currents, resonance/ π production

 - Error of factorizing the hard interaction vertex / using a non relativistic approach

- * Study of ANN to extract and predict electromagnetic responses in scenarios where traditional methods fail due to the lack of data. Extend this framework to neutrino-nucleus scattering using near detector data

Thank you for your attention!

Two-body currents - Delta contribution



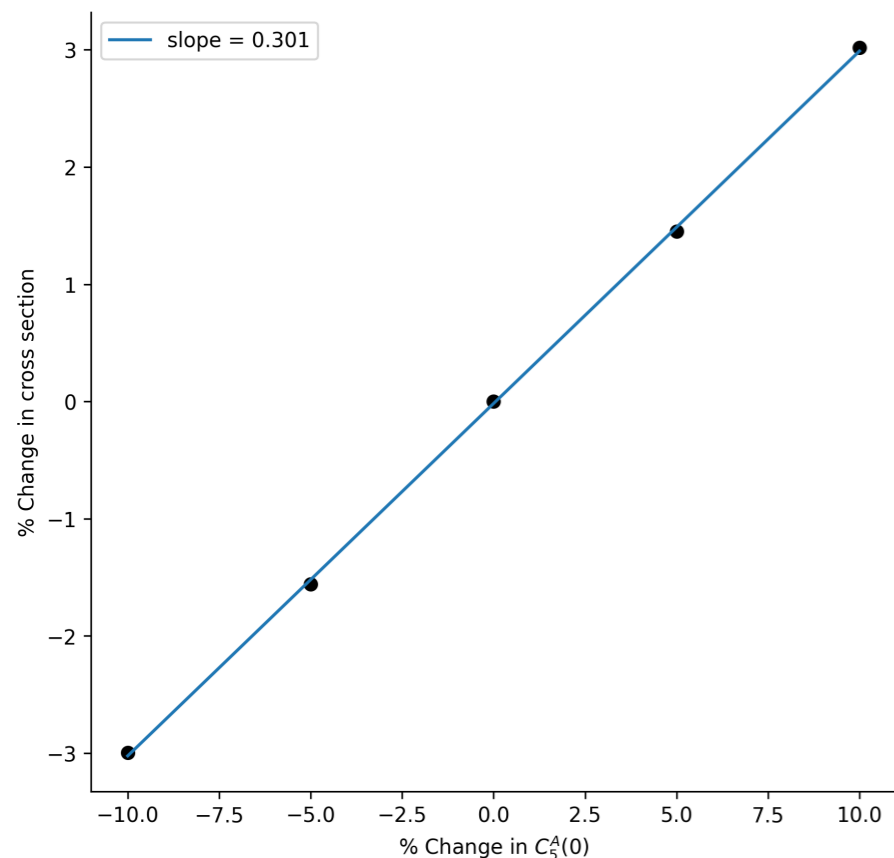
$$j_{\Delta}^{\mu} = \frac{3}{2} \frac{f_{\pi NN} f^{*}}{m_{\pi}^2} \left\{ \Pi(k_2)_{(2)} \left[\left(-\frac{2}{3} \tau^{(2)} + \frac{I_V}{3} \right)_z F_{\pi NN}(k_2) F_{\pi N\Delta}(k_2) (J_a^{\mu})_{(1)} \right. \right. \\ \left. \left. - \left(\frac{2}{3} \tau^{(2)} + \frac{I_V}{3} \right)_z F_{\pi NN}(k_2) F_{\pi N\Delta}(k_2) (J_b^{\mu})_{(1)} \right] + (1 \leftrightarrow 2) \right\}$$

where Rarita Schwinger propagator

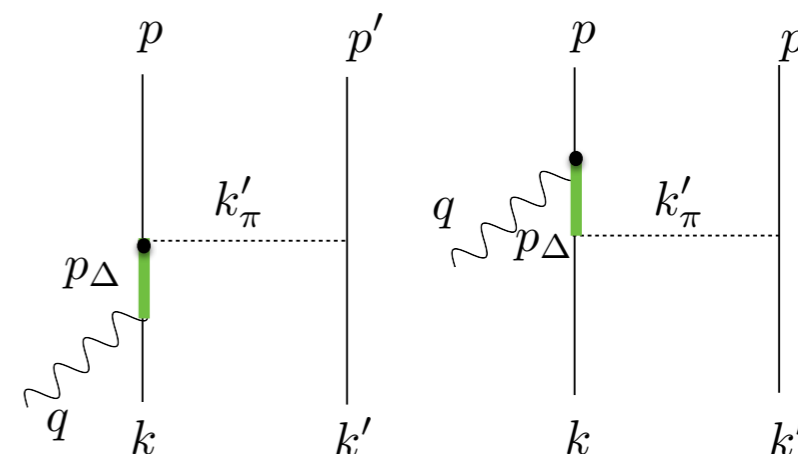
$$(j_a^{\mu})_V = (k'_{\pi})^{\alpha} G_{\alpha\beta}(p_{\Delta}) \left[\frac{C_3^V}{m_N} (g^{\beta\mu} \not{q} - q^{\beta} \gamma^{\mu}) \gamma_5 \right] \quad (j_a^{\mu})_A = (k'_{\pi})^{\alpha} G_{\alpha\beta}(p_{\Delta}) C_5^A g^{\beta\mu}$$

Resonance Uncertainty needs

The largest contributions to two-body currents arise from resonant $N \rightarrow \Delta$ transitions yielding pion production



D.Simons, N. Steinberg et al, 2210.02455



The normalization of the dominant $N \rightarrow \Delta$ transition form factor needs to be known to 3% precision to achieve 1% cross-section precision for MiniBooNE kinematics

State-of-the-art determinations of this form factor from experimental data on pion electroproduction achieve 10-15% precision (under some assumptions)

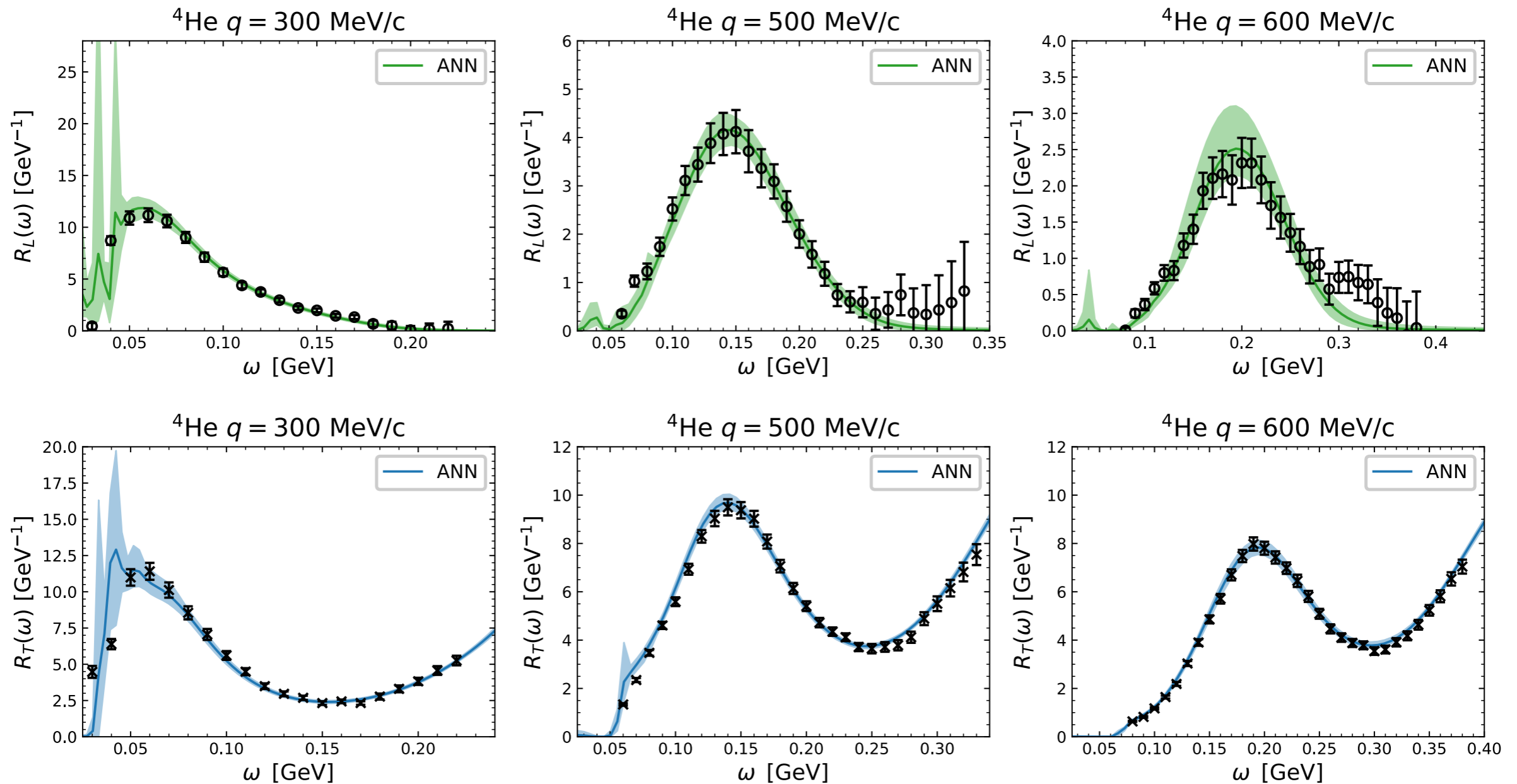
Hernandez et al, PRD 81 (2010)

Further constraints on $N \rightarrow \Delta$ transition relevant for two-body currents and π production will be necessary to achieve few-percent cross-section precision

Using Bayesian ANN for electron-nucleus scattering

J. Sobczyk, NR, A. Lovato, arxiv:2406.06292

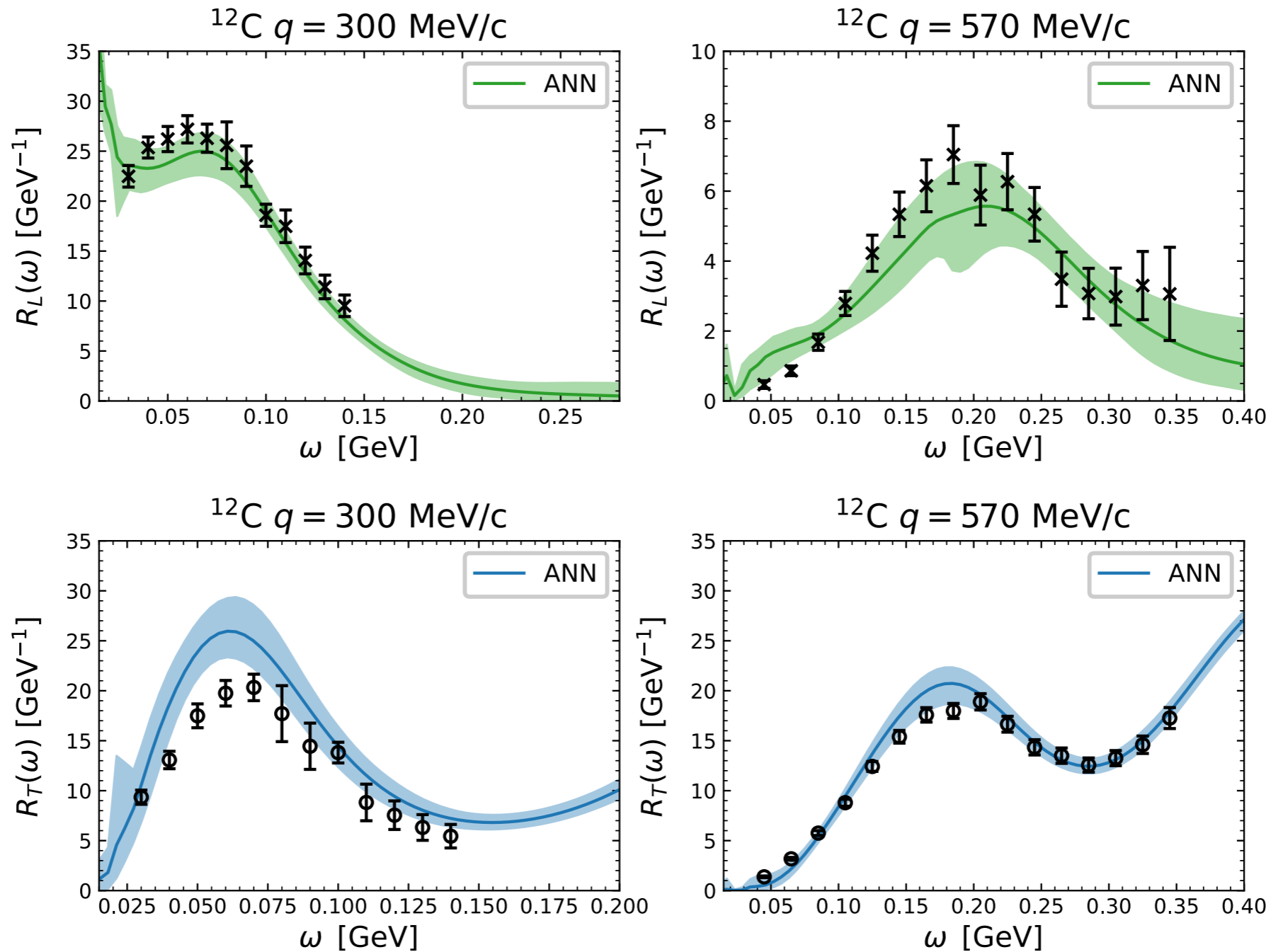
Results: Electromagnetic responses



Using Bayesian ANN for electron-nucleus scattering

J. Sobczyk, NR, A. Lovato, arxiv:2406.06292

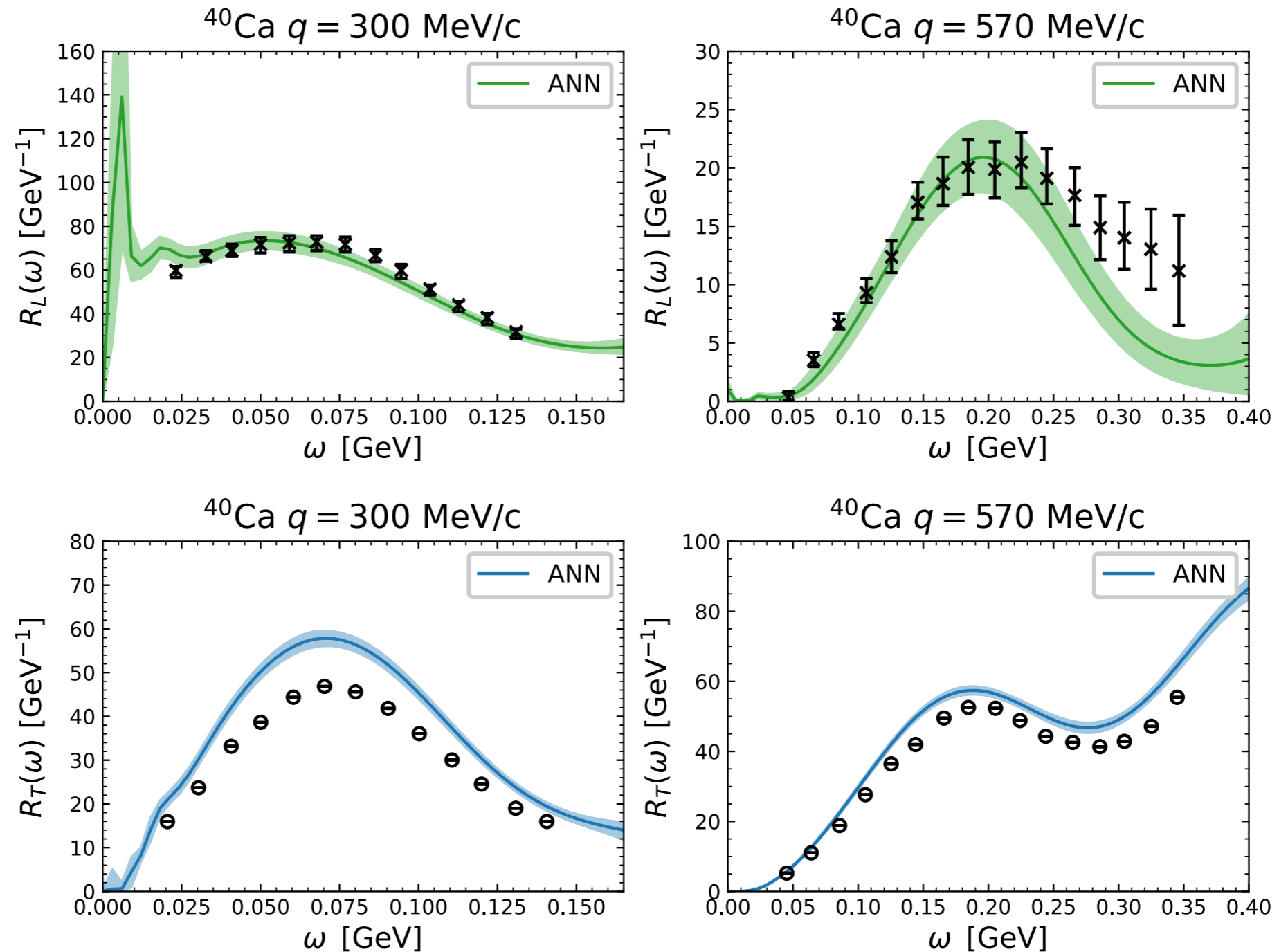
Results: Electromagnetic responses



Using Bayesian ANN for electron-nucleus scattering

J. Sobczyk, NR, A. Lovato, arxiv:2406.06292

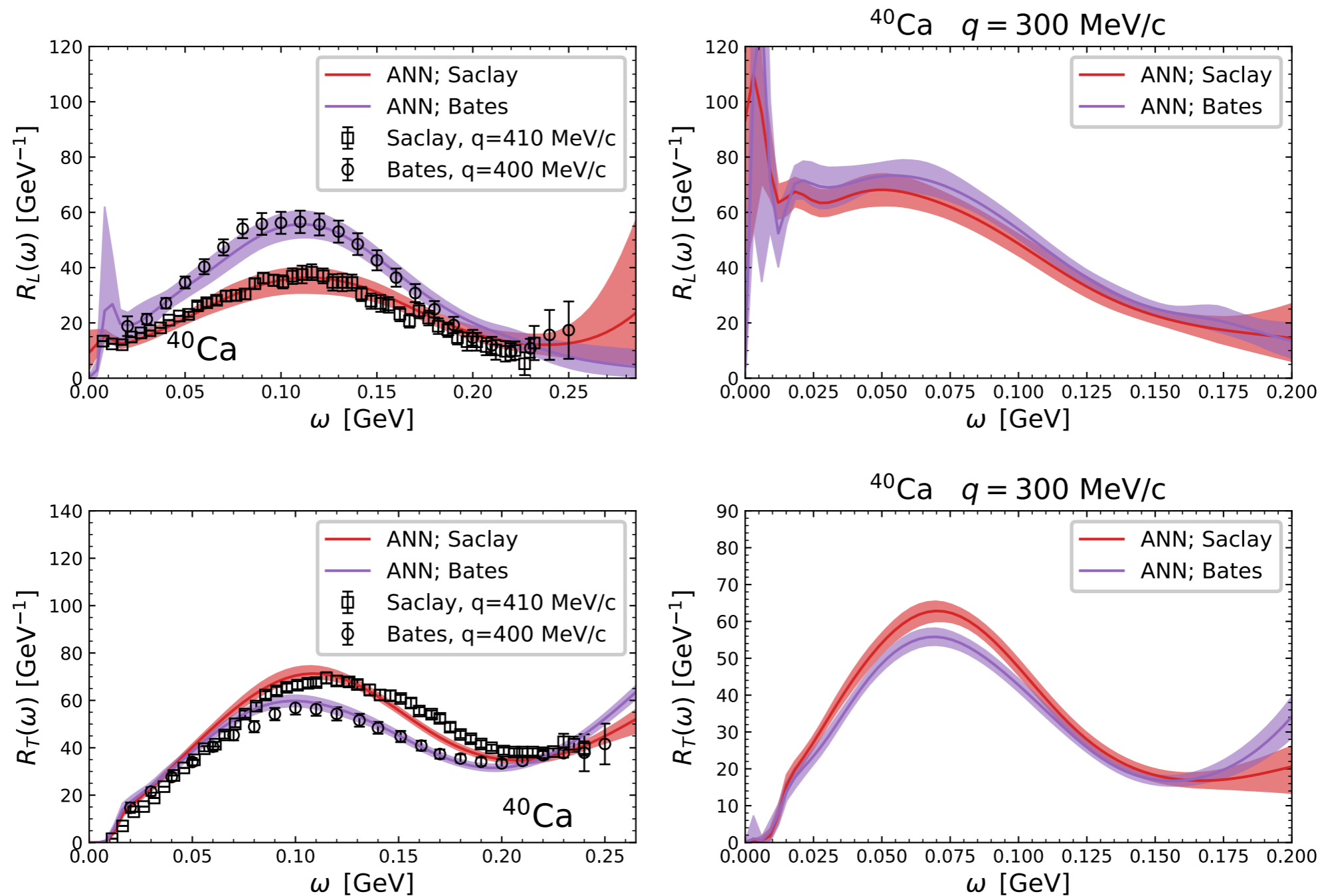
Results: Electromagnetic responses



Using Bayesian ANN for electron-nucleus scattering

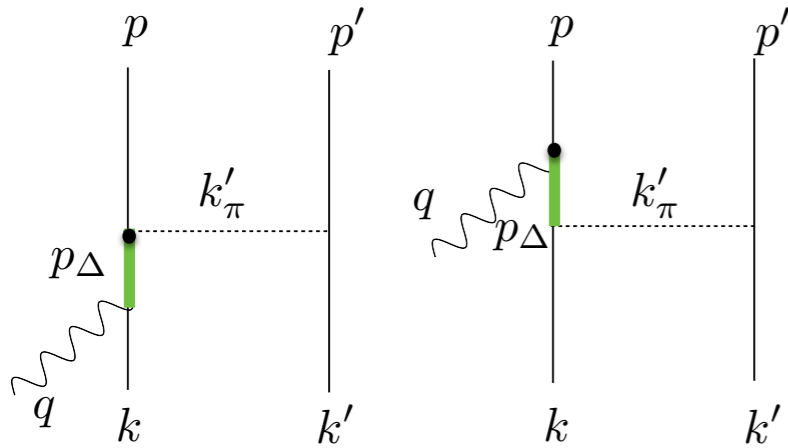
J. Sobczyk, NR, A. Lovato, arxiv:2406.06292

Results: Electromagnetic responses



Delta contribution to MEC

Diagrams including the Delta current depend on many parameters.



$$\begin{aligned}
 (j_a^\mu)_A &= (k'_\pi)^\alpha G_{\alpha\beta}(p_\Delta) \left[\frac{C_3^A}{m_N} (g^{\beta\mu} \not{q} - q^\beta \gamma^\mu) \right. \\
 &+ \frac{C_4^A}{m_N^2} (g^{\beta\mu} q \cdot p_\Delta - q^\beta p_\Delta^\mu) \\
 &\left. + C_5^A g^{\beta\mu} + \frac{C_6^A}{m_N^2} q^\mu q^\alpha \right],
 \end{aligned}$$

Parametrization chosen for the vector ff:

$$C_5^A = \frac{1.2}{(1 - q^2/M_{A\Delta})^2} \times \frac{1}{1 - q^2/(3M_{A\Delta})^2},$$

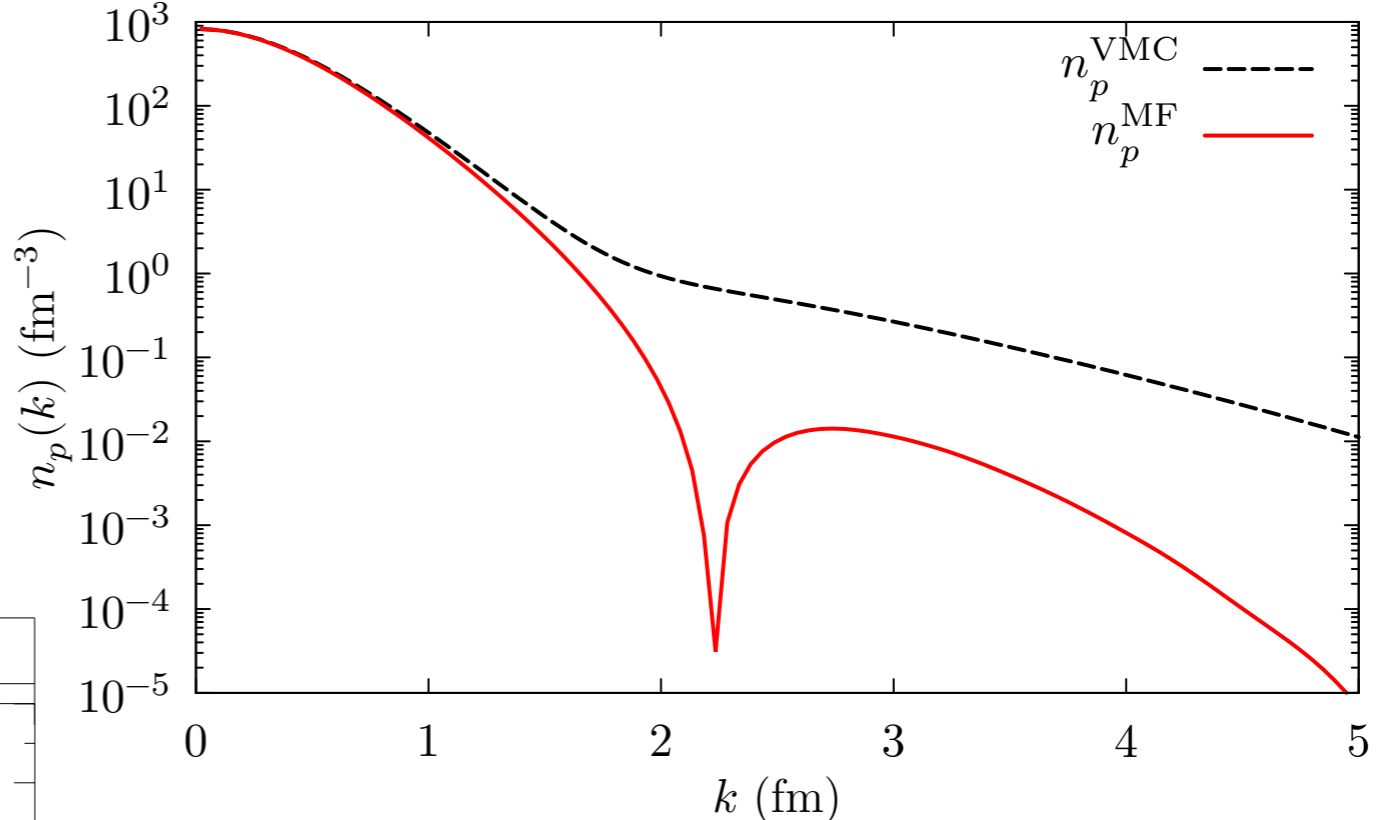
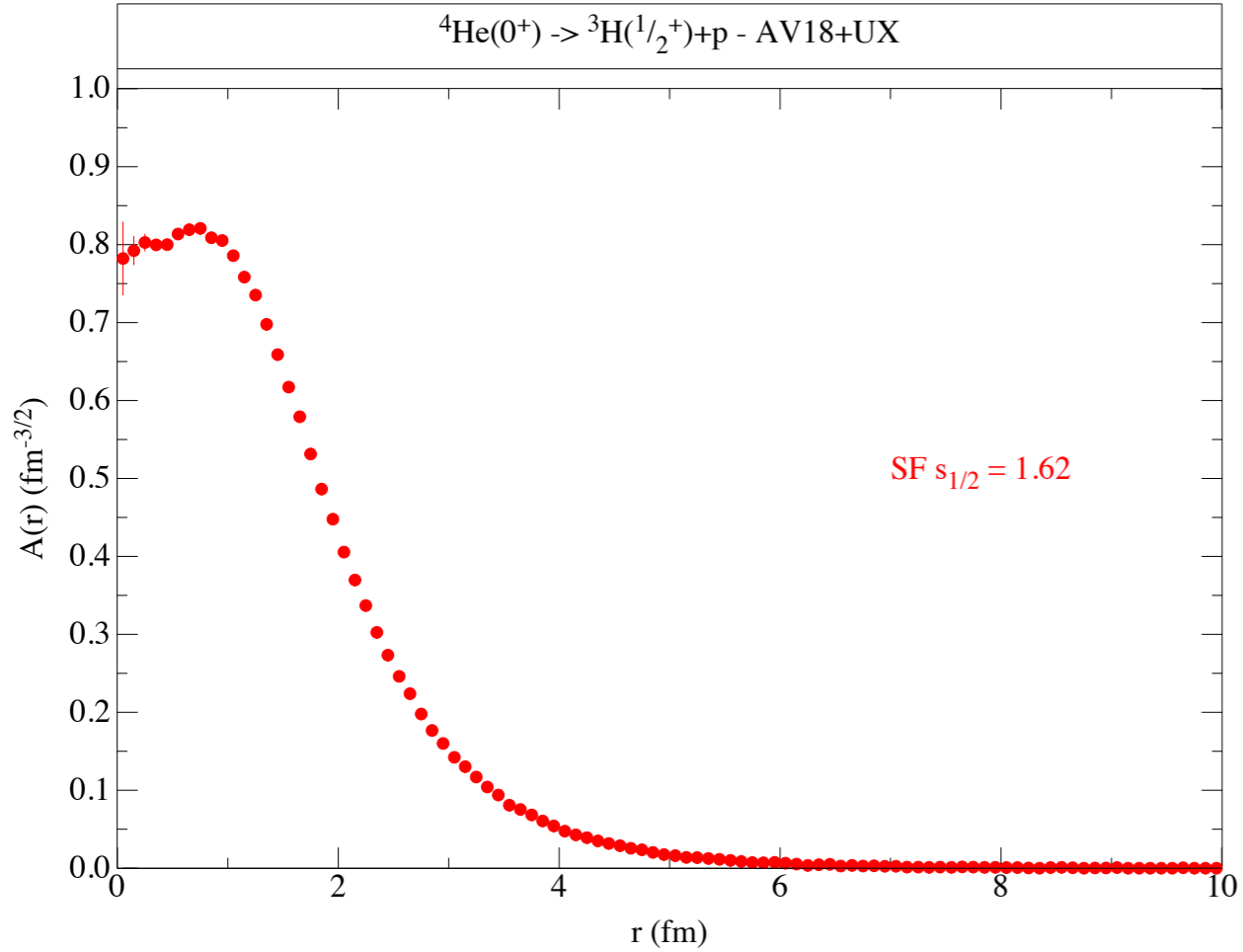
Current extractions of $C_5^A(0)$ rely on single pion production data from deuterium bubble chamber experiments; estimated uncertainty $\sim 15\%$

$$\text{Delta decay width: } \Gamma(p_\Delta) = \frac{(4f_{\pi N\Delta})^2}{12\pi m_\pi^2} \frac{|\mathbf{d}|^3}{\sqrt{s}} (m_N + E_d) R(\mathbf{r}^2) \quad R(\mathbf{r}^2) = \left(\frac{\Lambda_R^2}{\Lambda_R^2 - \mathbf{r}^2} \right)$$

QMC Spectral function of light nuclei

- Single-nucleon spectral function:

$$\begin{aligned}
 P_{p,n}(\mathbf{k}, E) &= \sum_n \left| \langle \Psi_0^A | [|k\rangle | \Psi_n^{A-1} \rangle] \right|^2 \\
 &\quad \times \delta(E + E_0^A - E_n^{A-1}) \\
 &= P^{MF}(\mathbf{k}, E) + P^{corr}(\mathbf{k}, E)
 \end{aligned}$$



$$P_p^{MF}(\mathbf{k}, E) = n_p^{MF}(\mathbf{k}) \delta\left(E - B_{{}^4\text{He}} + B_{{}^3\text{H}} - \frac{k^2}{2m_{{}^3\text{H}}}\right)$$

$$\left| \langle \Psi_0^{{}^4\text{He}} | [|k\rangle \otimes | \Psi_0^{{}^3\text{H}} \rangle] \right|^2$$

- The single-nucleon overlap has been computed within VMC (center of mass motion fully accounted for)



Spectral function approach

$$P_p^{\text{corr}}(\mathbf{k}, E) = \sum_n \int \frac{d^3 k'}{(2\pi)^3} |\langle \Psi_0^A || [k] |k'\rangle | \Psi_n^{A-2} \rangle |^2 \delta(E + E_0^A - e(\mathbf{k}') - E_n^{A-2})$$

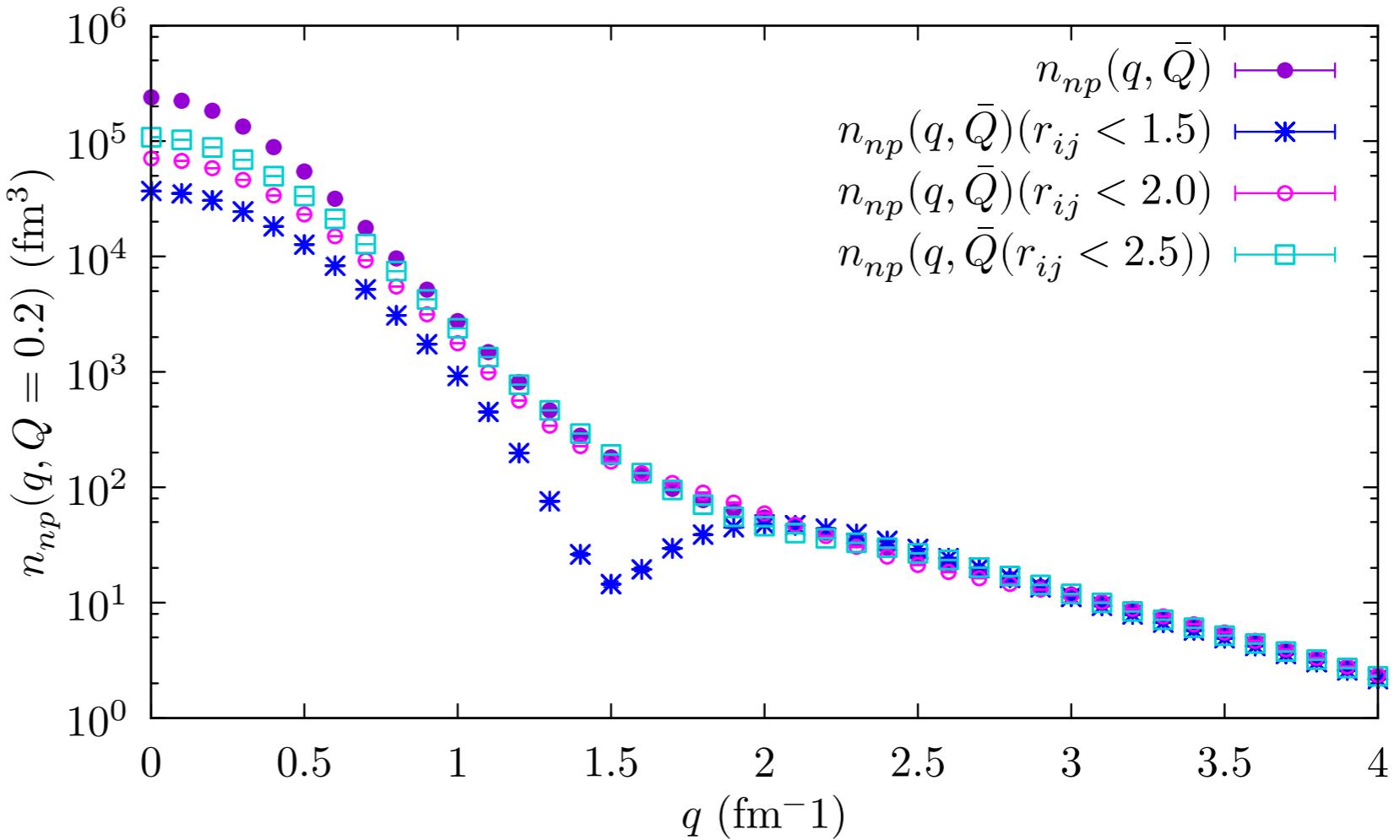


Using QMC techniques

$$\sum_{\tau_{k'}=p,n} n_{p,\tau_{k'}}(\mathbf{k}, \mathbf{k}') \delta\left(E - B_A - e(\mathbf{k}') + B_{A-2} - \frac{(\mathbf{k} + \mathbf{k}')^2}{2m_{A-2}}\right)$$

Only SRC pairs should be considered: $|\Psi_0^{A-1}\rangle$ and $|k'\rangle|\psi_n^{A-2}\rangle$ be orthogonalized

One can introduce **cuts** on the **relative distance** between the particles in the two-body momentum distribution



QMC Spectral Function of ^{12}C

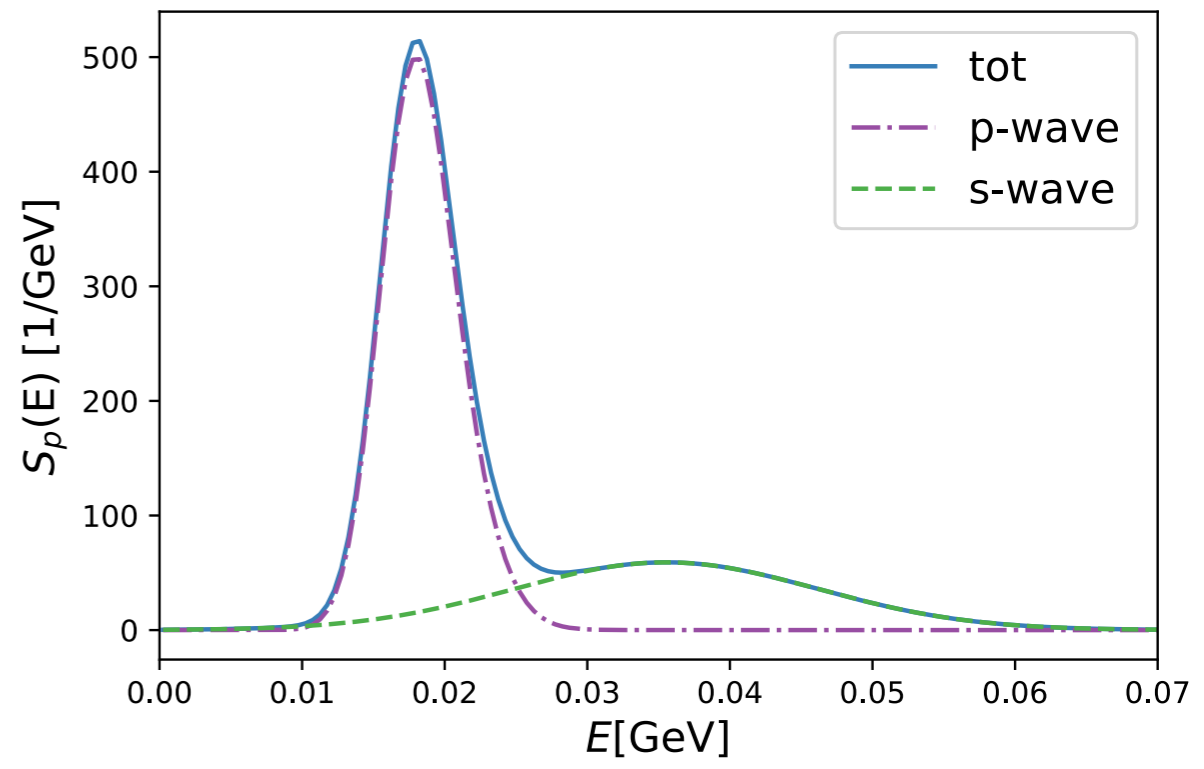
- The p-shell contribution has been obtained by FT the radial overlaps:

$$^{12}\text{C}(0^+) \rightarrow ^{11}\text{B}(3/2^-) + p$$

$$^{12}\text{C}(0^+) \rightarrow ^{11}\text{B}(1/2^-) + p$$

$$^{12}\text{C}(0^+) \rightarrow ^{11}\text{B}(3/2^-)^* + p.$$

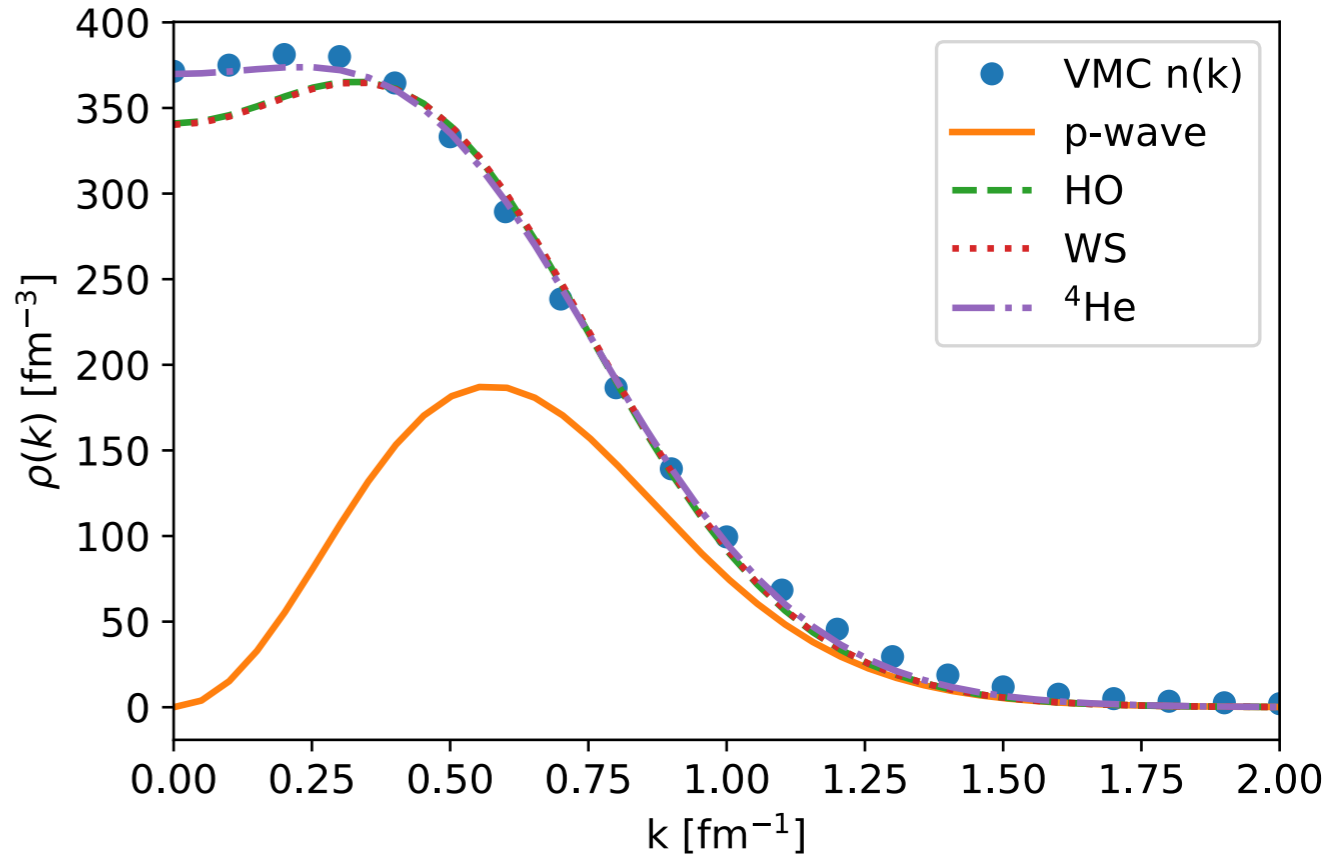
R. Crespo, et al, Phys.Lett.B 803 (2020) 135355



- The quenching of the spectroscopic factors automatically emerges from the VMC calculations

Computing the s-shell contribution is non trivial within VMC. We explored different alternatives:

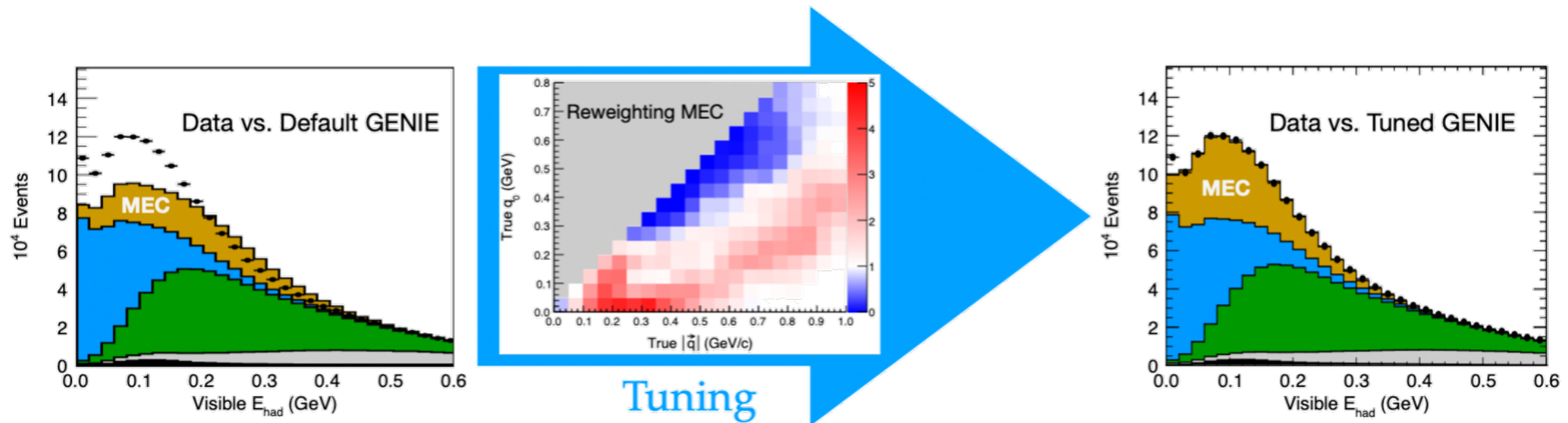
- Quenched Harmonic Oscillator
- Quenched Wood Saxon
- VMC overlap associated for the $^4\text{He}(0^+) \rightarrow ^3\text{H}(1/2^+) + p$ transition



Korover, et al, CLAS collaboration PRC 107 (2023) 6, L061301

Tuning

Discrepancies between generators and data often corrected by tuning an empirical model of the least well known mechanism: MEC (“meson exchange”/two-body currents)



Coyle, Li, and Machado, JHEP 12, 166 (2022)

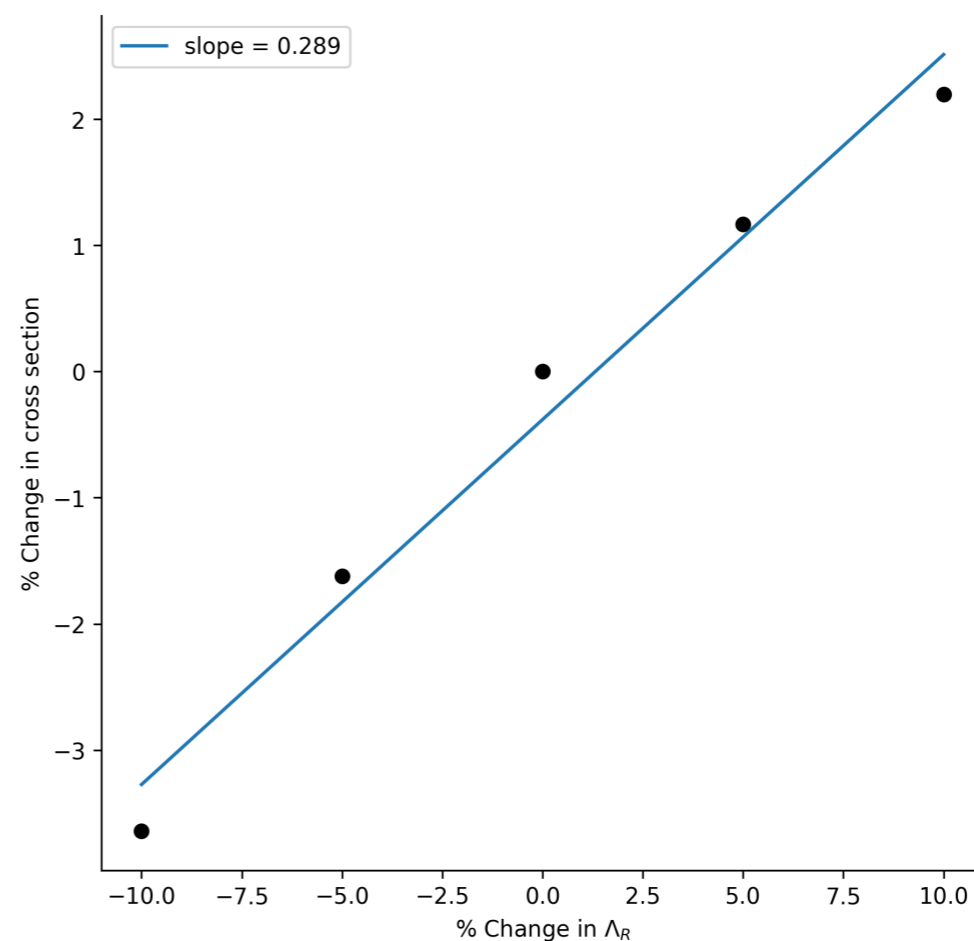
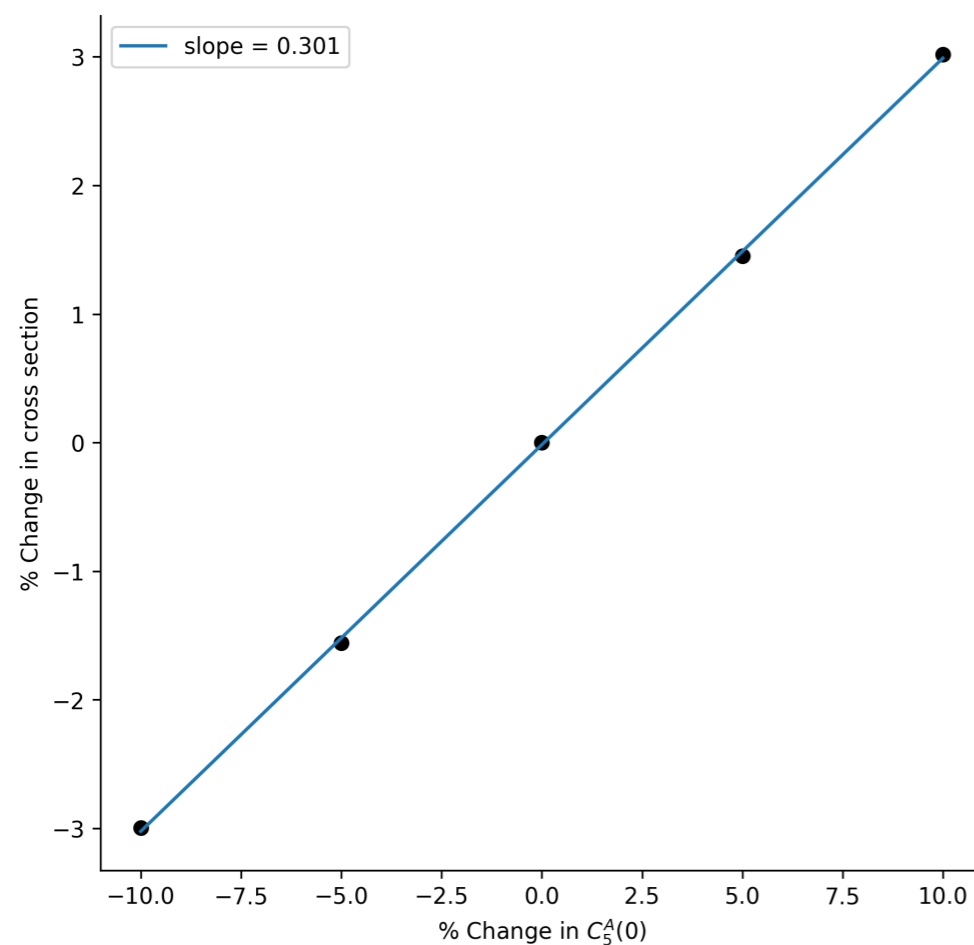
Mis-modeling can distort signals of new physics, **biasing** measurement of **new physics parameters**

Studies on the impact of different neutrino interactions and nuclear models on determining neutrino oscillation parameters are critical. These enable us to assess the level of precision we aim at.

Coloma, et al, Phys.Rev.D 89 (2014) 7, 073015

Study of model dependence in neutrino predictions

Percent change in the MiniBooNE cross section versus the percent change in the two-body current parameters for $0.5 < \cos \theta_\mu < 0.6$, $T_\mu = 325$ MeV

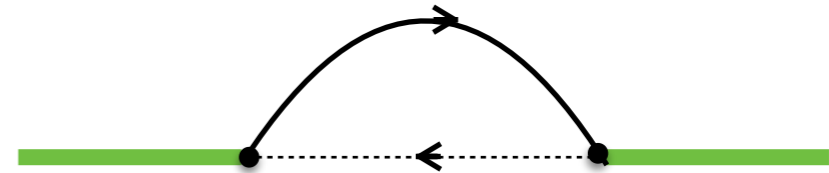


A 15% variation in either $C_5^A(0)$ or Λ_R changes the flux-averaged cross section by roughly 5%

Two-body currents - Delta contribution

Rarita-Schwinger propagator

$$G^{\alpha\beta}(p_\Delta) = \frac{P^{\alpha\beta}(p_\Delta)}{p_\Delta^2 - M_\Delta^2}$$



The spin 3/2 projection operator reads

$$P^{\alpha\beta}(p_\Delta) = (\not{p}_\Delta + M_\Delta) \left[g^{\alpha\beta} - \frac{1}{3} \gamma^\alpha \gamma^\beta - \frac{2}{3} \frac{p_\Delta^\alpha p_\Delta^\beta}{M_\Delta^2} + \frac{1}{3} \frac{p_\Delta^\alpha \gamma^\beta - p_\Delta^\beta \gamma^\alpha}{M_\Delta} \right].$$

To account for the resonant behavior of the Δ : $M_\Delta \rightarrow M_\Delta - i\Gamma(p_\Delta)/2$

$$\Gamma(p_\Delta) = -2\text{Im}\Sigma_{\pi N}(s) = \frac{(4f_{\pi N\Delta})^2}{12\pi m_\pi^2} \frac{|\mathbf{d}|^3}{\sqrt{s}} (m_N + E_d) R(\mathbf{r}^2)$$

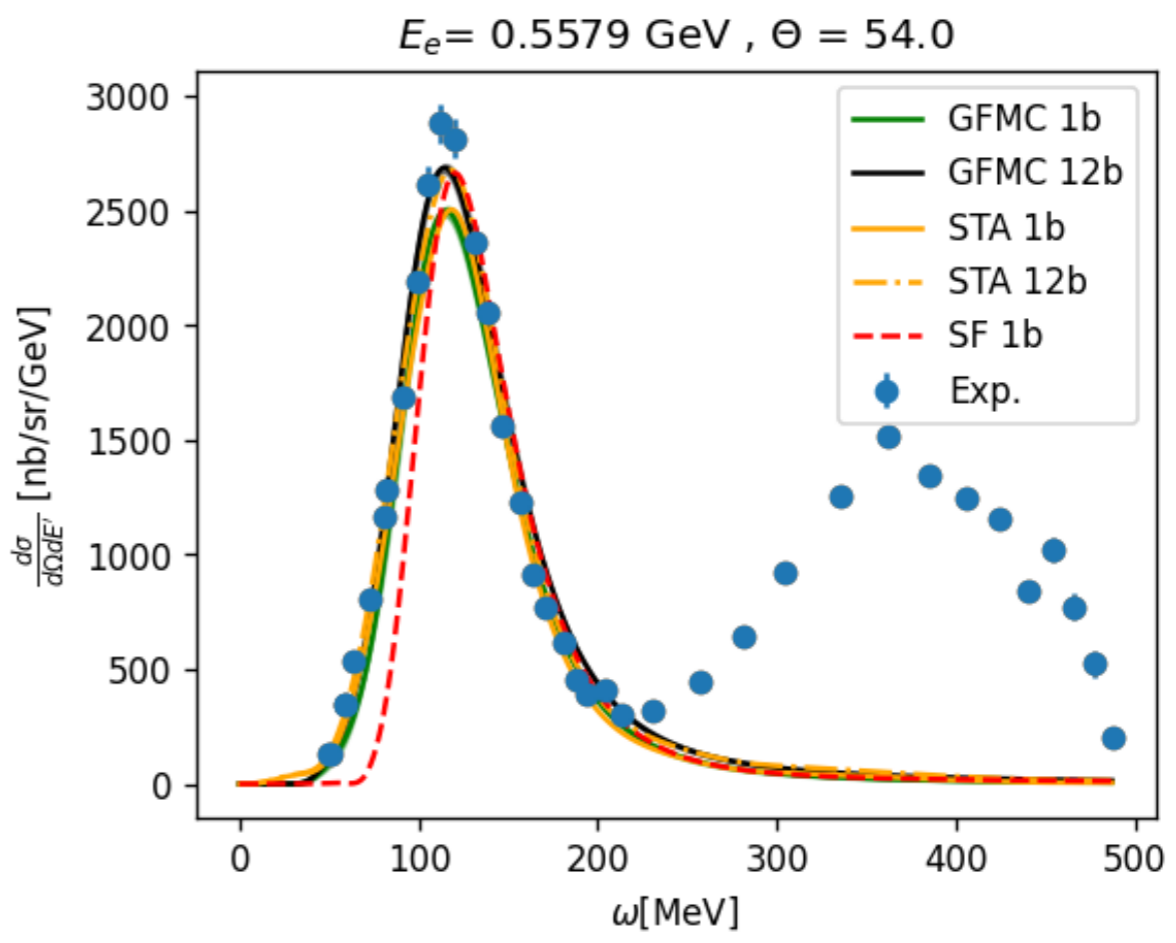
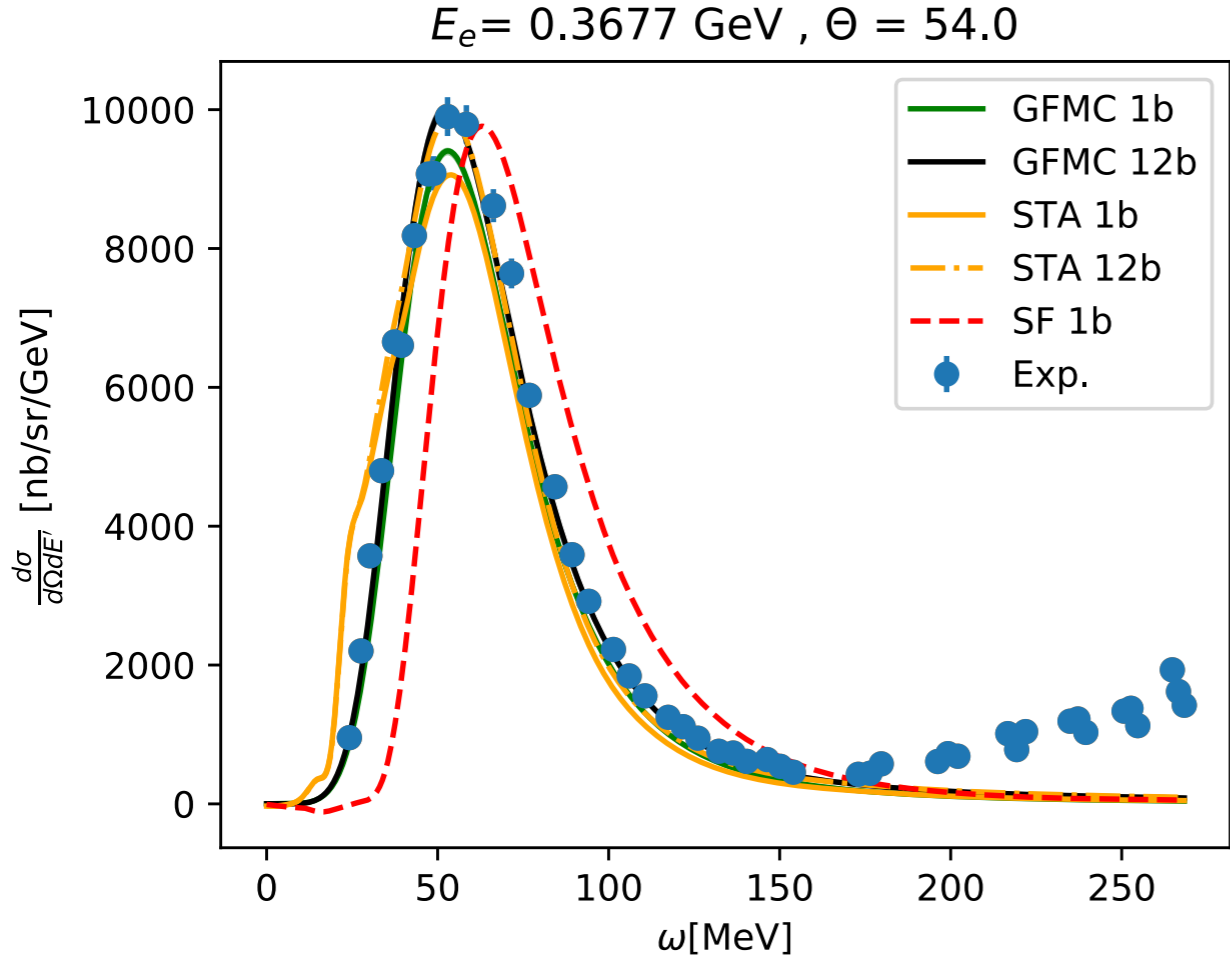
\mathbf{d} is the decay three-momentum in the πN center of mass frame

In medium effects of the Δ $\Gamma_\Delta(p_\Delta) \rightarrow \Gamma_\Delta(p_\Delta) - 2\text{Im}[U_\Delta(p_\Delta, \rho = \rho_0)]$

Comparing different many-body methods

L. Andreoli, NR, et al, PRC 105 (2022) 1, 014002

- e^- - ^3H : inclusive cross section



- Comparisons among QMC, SF, and STA approaches: first step to precisely **quantify the uncertainties** inherent to the factorization of the final state.
- Gauge the role of **relativistic effects** in the energy region relevant for neutrino experiments.

Green's Function Monte Carlo

Any trial wave function can be expanded in the complete set of eigenstates of the the Hamiltonian according to

$$|\Psi_V\rangle = \sum_n c_n |\Psi_n\rangle \quad H|\Psi_n\rangle = E_n |\Psi_n\rangle$$

GFMC uses a projection technique to **enhance the true ground-state component** of a starting wave function.

$$\lim_{\tau \rightarrow \infty} e^{-(H-E_0)\tau} |\Psi_T\rangle = \lim_{\tau \rightarrow \infty} \sum_n c_n e^{-(E_n-E_0)\tau} |\Psi_n\rangle = c_0 |\Psi_0\rangle$$

The direct calculation of the imaginary-time propagator for strongly-interacting systems involves prohibitive difficulties

J. Carlson , et al. Rev. Mod. Phys. 87 (2015) 1067

The imaginary-time evolution is broken into N small imaginary-time steps, and complete sets of states are inserted

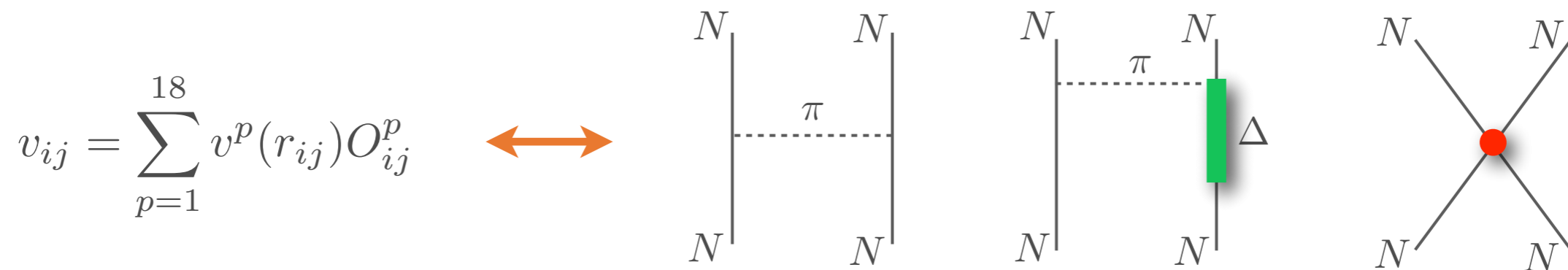
$$e^{-(H-E_0)\tau} |\Psi_V\rangle = \int dR_1 \dots dR_N |R_N\rangle \langle R_N | e^{-(H-E_0)\Delta\tau} |R_{N-1}\rangle \dots \langle R_2 | e^{-(H-E_0)\Delta\tau} |R_1\rangle \Psi_V(R_1)$$

Short Time Propagator

Phenomenological potential: av18 + IL7

Phenomenological potentials explicitly include the **long-range one-pion exchange interaction** and a set of **intermediate- and short-range phenomenological terms**

- **Argonne v₁₈** is a finite, local, configuration-space potential controlled by ~4300 np and pp scattering data below 350 MeV of the Nijmegen database



- Phenomenological three-nucleon interactions, like the **Illinois 7**, effectively include the lowest nucleon excitation, the $\Delta(1232)$ resonance, and other nuclear effects



The parameters of the AV18 + IL7 are fit to properties of **exactly solvable light nuclear systems**.

Axial form factor determination

- The axial form-factor has been fit to the dipole form

$$F_A(q^2) = \frac{g_A}{(1 - q^2/m_A^2)^2}$$

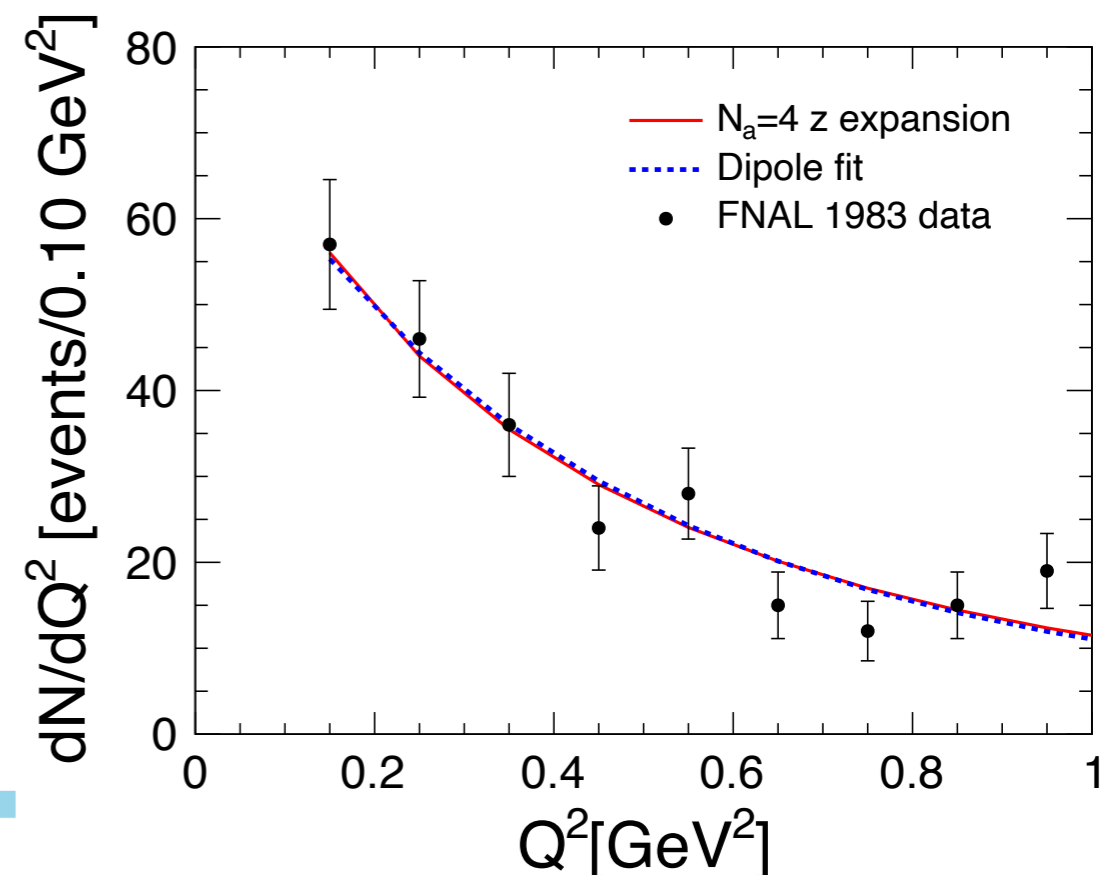
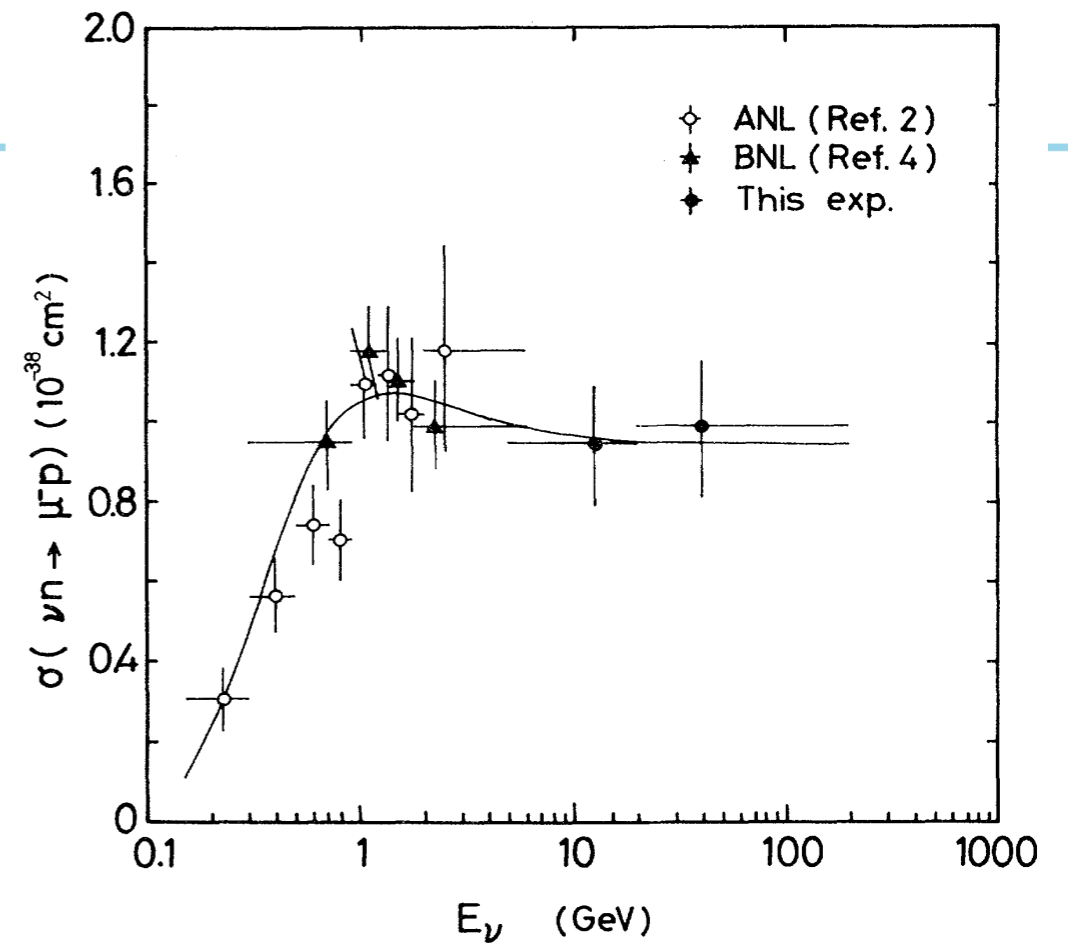
- The intercept $g_A = -1.2723$ is known from neutron β decay
- Different values of m_A from experiments
 - $m_A = 1.02$ GeV q.e. scattering from deuterium
 - $m_A = 1.35$ GeV @ MiniBooNE
- Alternative derivation based on **z-expansion**
 - model independent parametrization

$$F_A(q^2) = \sum_{k=0}^{k_{\max}} a_k z(q^2)^k,$$

↑ known functions
↑ free parameters

Bhattacharya, Hill, and Paz PRD 84 (2011) 073006

A.S.Meyer et al, Phys.Rev.D 93 (2016) 11, 113015



Why relativity is important

$$R_{\alpha\beta}(\omega, \mathbf{q}) = \sum_f \langle 0 | J_\alpha^\dagger(\mathbf{q}) | f \rangle \langle f | J_\beta(\mathbf{q}) | 0 \rangle \delta(\omega - E_f + E_0) \rightarrow \text{Kinematics}$$

\downarrow
Currents

Covariant expression of the e.m. current:

$$j_{\gamma,S}^\mu = \bar{u}(\mathbf{p}') \left[\frac{G_E^S + \tau G_M^S}{2(1 + \tau)} \gamma^\mu + i \frac{\sigma^{\mu\nu} q_\nu}{4m_N} \frac{G_M^S - G_E^S}{1 + \tau} \right] u(\mathbf{p})$$

Nonrelativistic expansion in powers of \mathbf{p}/m_N

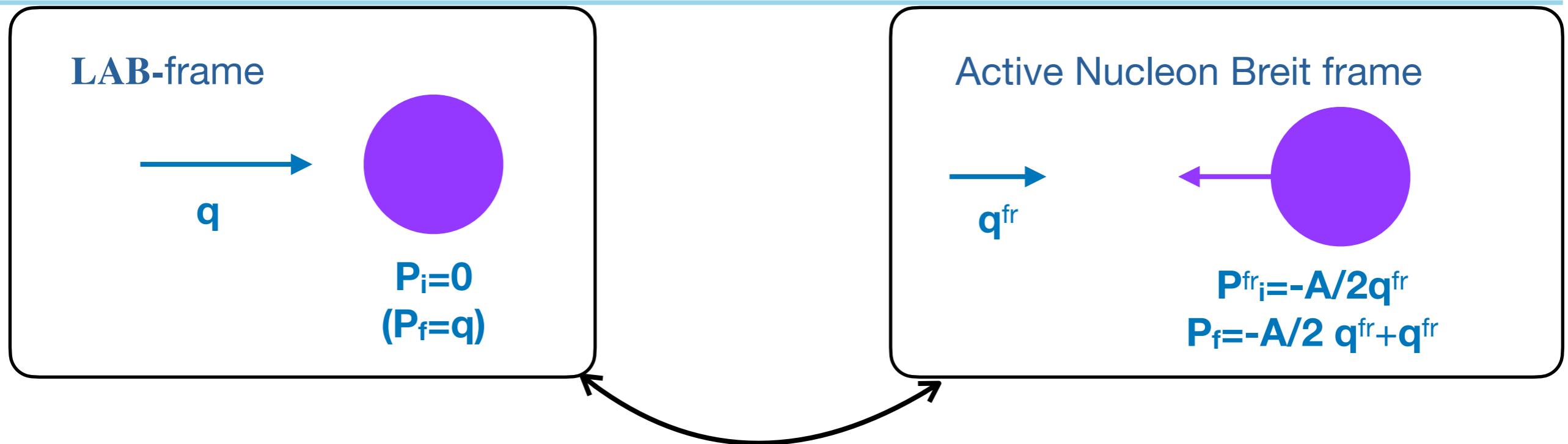
$$j_{\gamma,S}^0 = \frac{G_E^S}{2\sqrt{1 + Q^2/4m_N^2}} - i \frac{2G_M^S - G_E^S}{8m_N^2} \mathbf{q} \cdot (\boldsymbol{\sigma} \times \mathbf{p})$$

Energy transfer at the quasi-elastic peak:

$$w_{QE} = \sqrt{\mathbf{q}^2 + m_N^2} - m_N$$

$$w_{QE}^{nr} = \mathbf{q}^2 / (2m_N)$$

Frame dependence



Lorentz Boost connects the two frames:

$$R_{LAB}^{\mu\nu}(\omega, q) = B^\mu_\alpha[\beta] B^\nu_\beta[\beta] R_{fr}^{\alpha\beta}(\omega^{fr}, \mathbf{q}^{fr})$$

- ANB @ the single nucleon level:

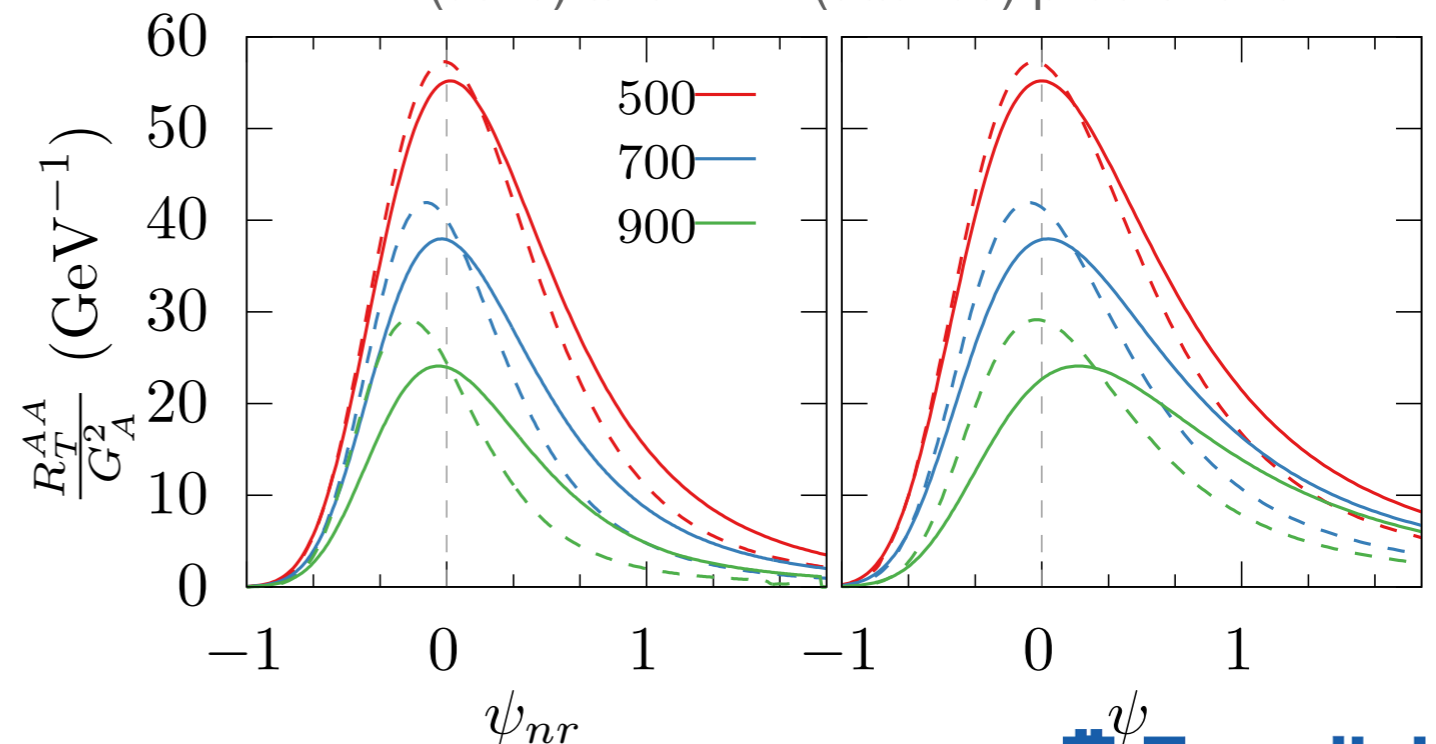
$$\mathbf{p}^{fr_i} \simeq -\mathbf{q}^{fr}/2$$

$$\mathbf{p}^{fr_f} \simeq \mathbf{q}^{fr}/2$$

- Same position of the quasielastic peak

$$\omega_{QE} = \omega_{QE}^{nr} = 0$$

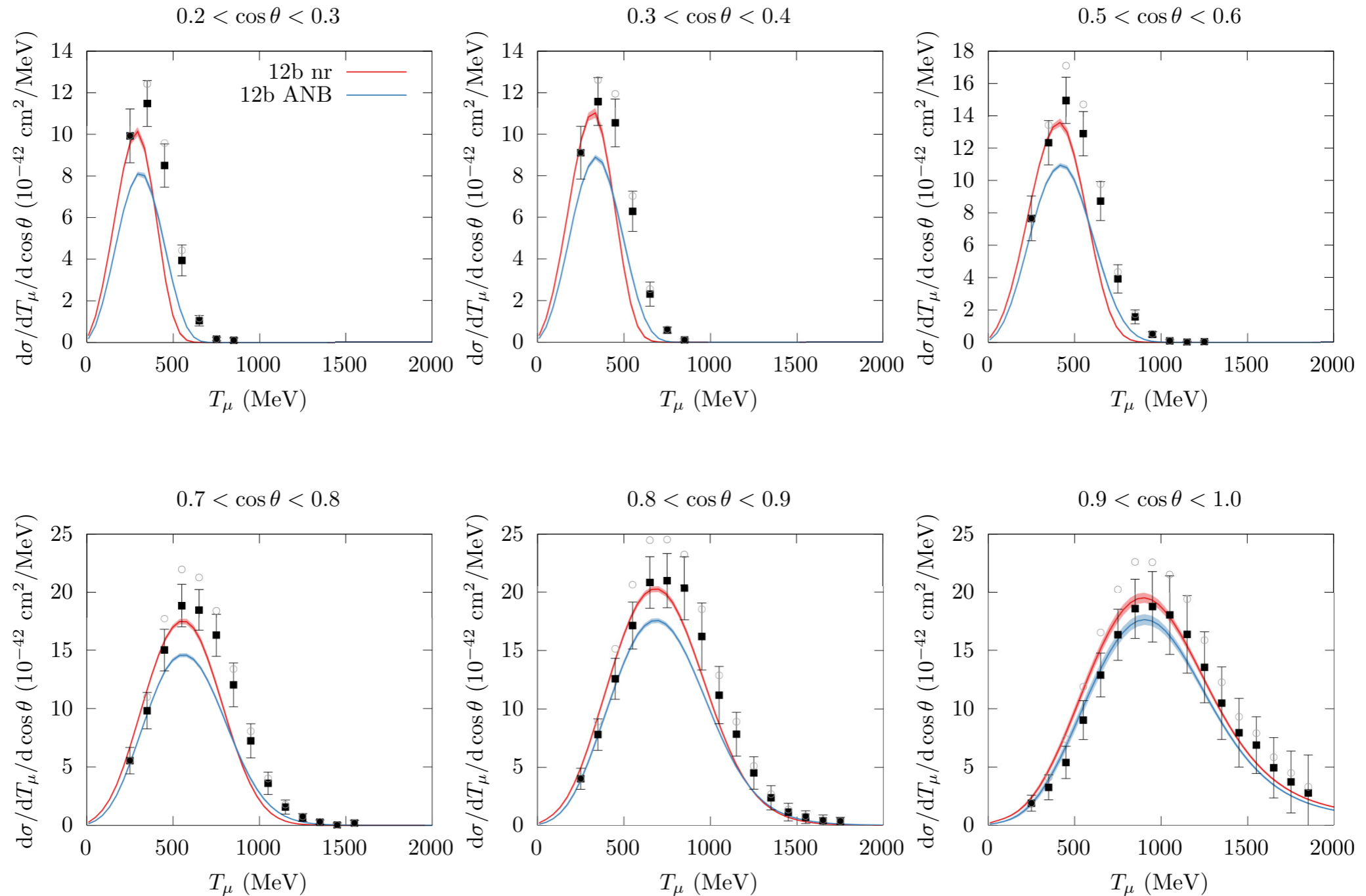
- LAB (solid) and ANB (dashed) predictions



Cross sections: Green's Function Monte Carlo

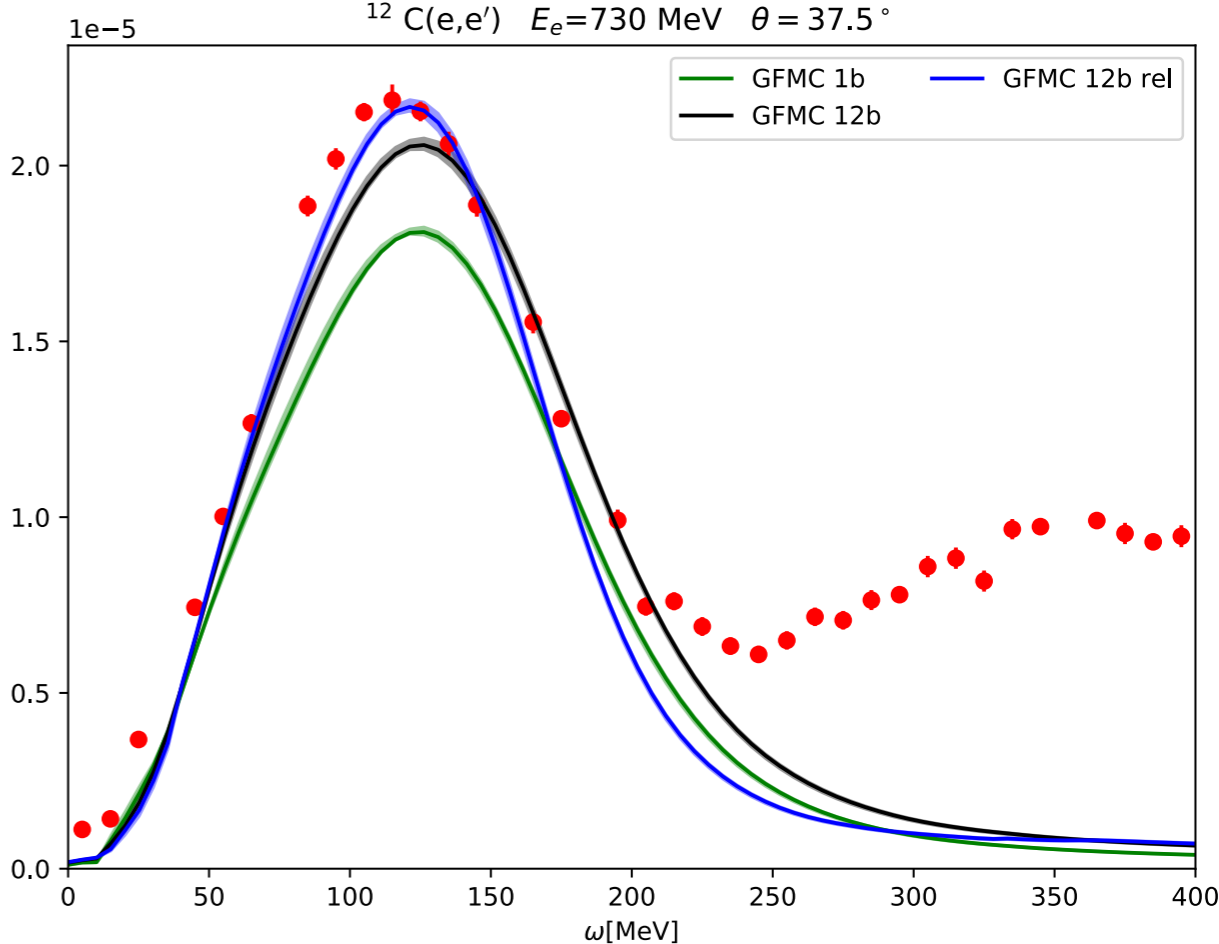
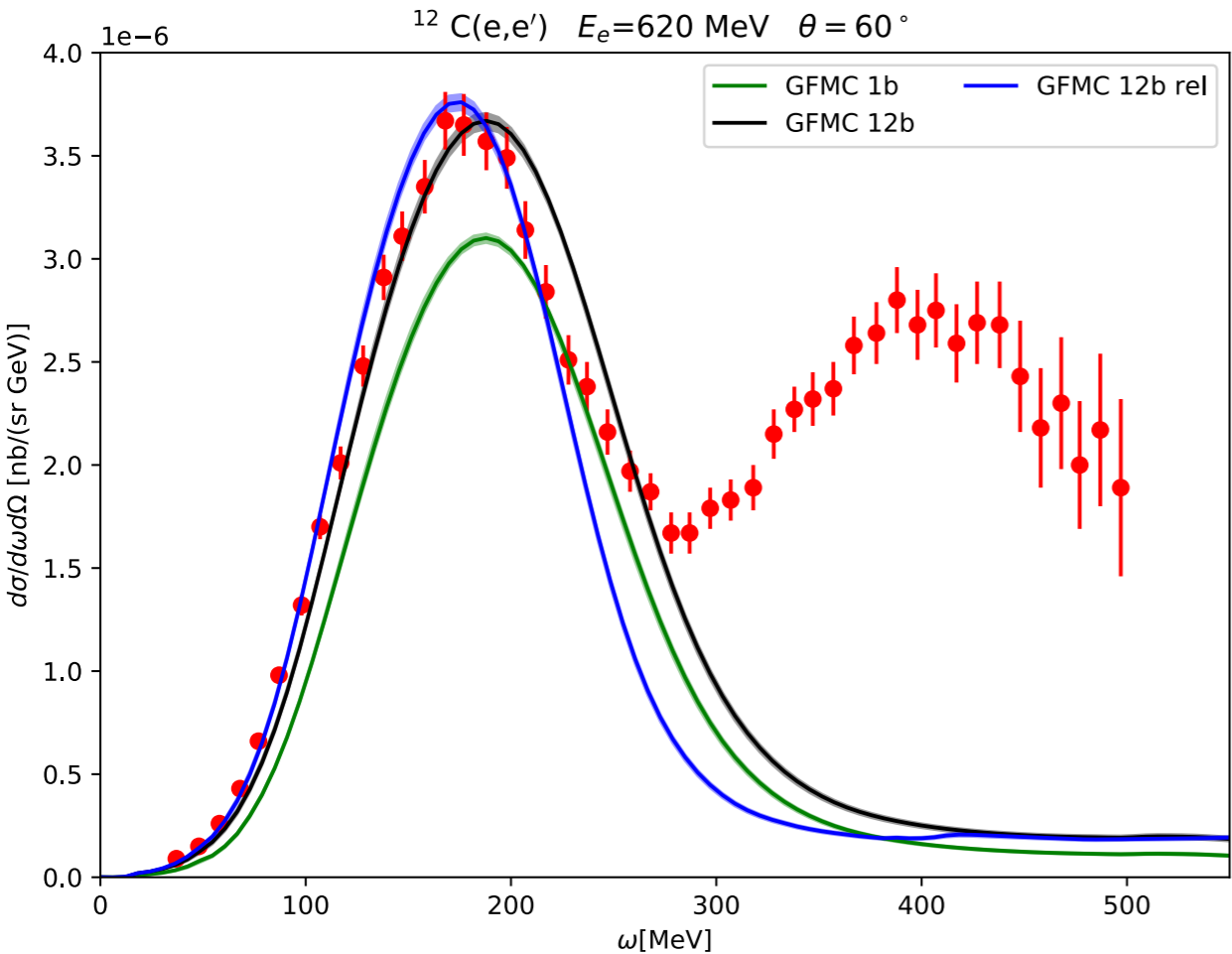
MiniBooNE results including relativistic corrections

A.Nikolakopoulos, A.Lovato, NR, PRC 109 (2024) 1, 014623



Cross sections: Green's Function Monte Carlo

Electron scattering results including relativistic corrections for some kinematics covered by the calculated responses



A.Lovato, A.Nikolakopoulos, NR, N. Steinberg, Universe 9 (2023) 8, 36

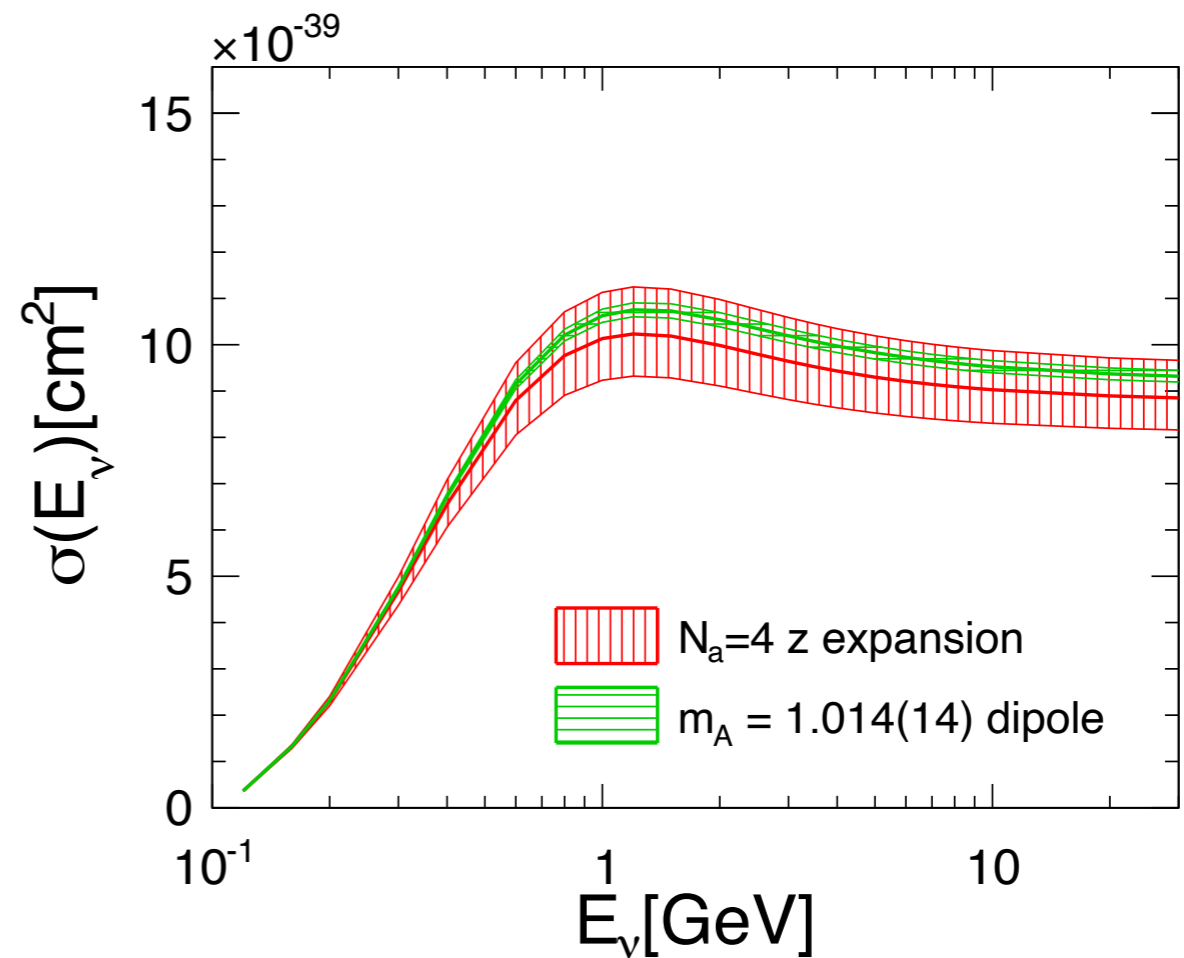
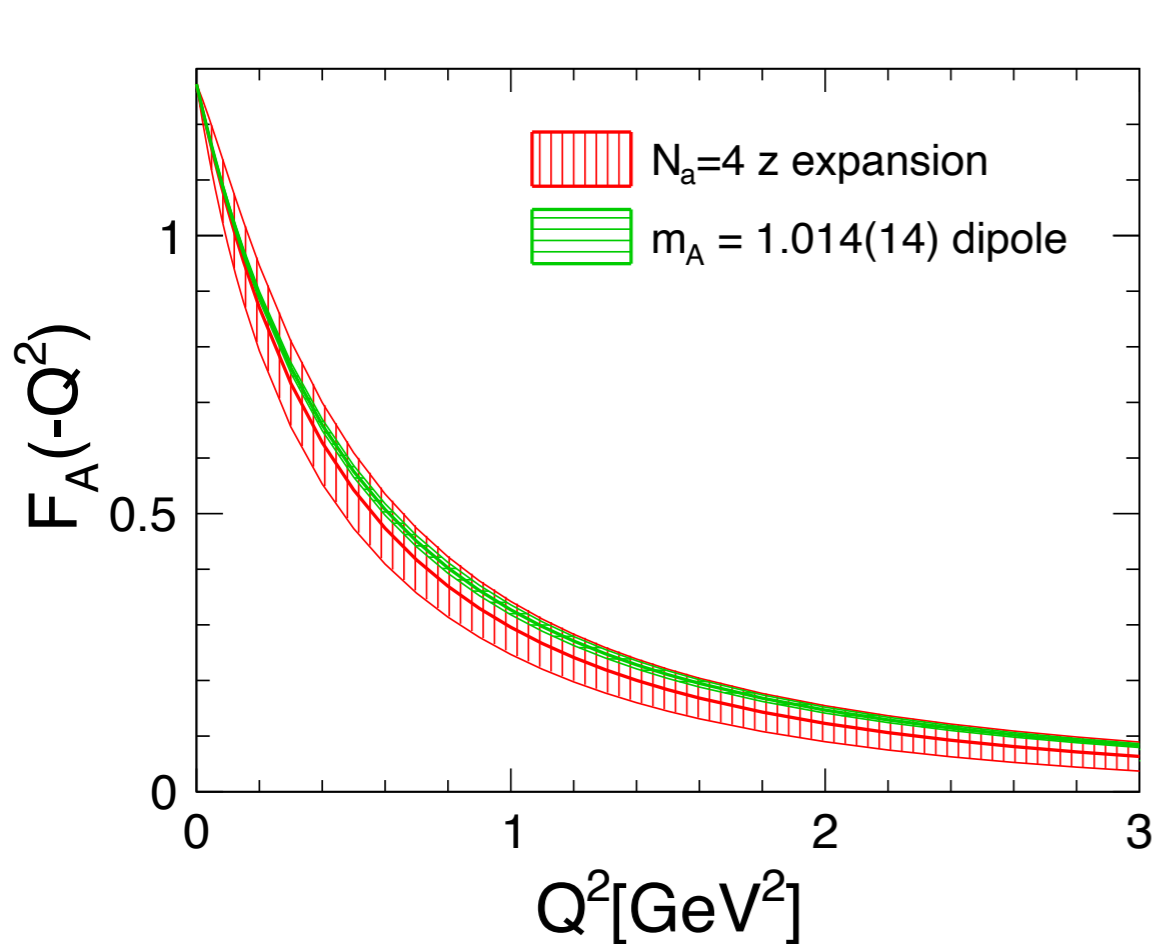


Neutrino-Nucleon scattering

- Sum rule can be enforced ensuring that the form factor falls smoothly to zero at large Q^2

$$\sum_{k=n}^{\infty} k(k-1)\cdots(k-n+1)a_k = 0, \quad n = 0, 1, 2, 3$$

Fit deuteron data replacing dipole axial form factor with z-expansion, enforce the sum rule constraints



A.S.Meyer, Phys.Rev.D 93 (2016) 11, 113015